Doctoral Thesis

Mechanisms by which Bacterial and Viral Pathogens cause Ovarian dysfunction

Adedeji Olufemi Adetunji

Graduate School of Biosphere Science

Hiroshima University

September 2021

Doctoral Thesis

Mechanisms by which Bacterial and Viral Pathogens cause Ovarian dysfunction

Adedeji Olufemi Adetunji

Department of Bioresource Science

Graduate School of Biosphere Science

Hiroshima University

September 2021

ACKNOWLEDGEMENTS

I am very grateful to Jehovah, the Almighty God who gave me life. He has sustained and protected me until this very moment.

I specially thank my research supervisory committee members, Professor Masayuki Shimada, and Dr. Takashi Umehara (Assistant Professor), Laboratory of Animal Production, Graduate School of Biosphere Science, Hiroshima University for their innovative suggestions and guidance throughout my doctoral study and dissertation writing. I also would love to express my appreciation to Professor Naoki Isobe and Professor Hiroyuki Horiuchi for their kind effort and constructive comments during the preparation of my doctoral dissertation.

It is my pleasure to express sincere gratitude to the biosphere science student support team, especially Himiko Koi for her diligence and support during my study.

I am also grateful to my wife, Ebunoluwa Adetunji, I thank you for your sacrifices and selflessness; my parents, Mr. and Mrs. R.A. Adetunji, and entire family, Adetutu, Adeola and Tejumade for their united and untiring love and support from the onset until this moment. I appreciate their kind gesture. I cannot also forget to thank my aunt, Olayinka Oluwunmi and all my friends especially Ogunsina sola, Adesina Adedayo and Saliu Tolulope, for their words of encouragement and for providing moral support throughout the course of my doctoral research.

To Prof. Teruo Maeda (Ret.) and Dr. Tomoko Kawai, I say it has been wonderful having you as a tutor and guide throughout my doctoral journey and I would cherish all the moment spent in the laboratory with you. To chizuka san, Yuki san, Zhu san, Tawara san, Hibi san, Islam san and other laboratory members, I say thank you for your support and guidance. May Jehovah bless you all.

List of Contents

Topics			Page No
Chapter 1: General Introduction			
1.1	The Ovary		1
1.2	Folliculogenesis		1
	1.2.1	Primordial follicle formation and recruitment	2
	1.2.2	Development of primary, preantral, antral, and preovulatory follicles	2
1.3	Luteinizing hormone/choriogonadotropin receptor (*LHCGR*)		4
	1.3.1	Mechanism of cumulus expansion, ovulation, and luteinization	4
1.4	Innate immune system and Toll-like receptors		6
	1.4.1	Toll-like receptor 4 and LPS	7
	1.4.2	Toll-like receptor 7 and 8 roles in Viral infection	7
	1.4.3	Endogenous Ligands	8
1.5	Pelvic Inflammatory Diseases and other diseases caused by Bacteria and Viral infections		8
	1.5.1	Follicular Cyst	9
	1.5.2	Polycystic Ovarian Cyst	9
1.6	Aim of this study		10

Topics		Page No.
Chapter 2: Experiment 1		
Study on the effect of LPS on overall ovarian health and Epigenetic dynamics of the *Lhcgr* and *Cyp19a1* gene promoter region		
2.1	Introduction	13
2.2	Materials and Methods	16
2.3	Results	26
2.4	Discussion	29
	Abstract	33
Chapter 3: Experiment 2		
Study on the role of Toll-like receptor 7/8 on mouse ovary		
3.1	Introduction	46
3.2	Materials and Methods	47
3.3	Results	53
3.4	Discussion	57
	Abstract	60
Chapter 4: General Discussion		74
Chapter 5: Summary		80
References		84

List of Tables

	Title of Tables	Page No.
Table 1	PCR primers used for profiling the expression of genes markers for GC function	34
Table 2	PCR primers used for profiling the expression of TLR7/8 and genes markers for ovarian function	61

List of Figures

	Title of the figures	Page No.
Figure 1	Structure of lipopolysaccharide (LPS). LPS is found on the cell wall of gram-negative bacteria, such as *Escherichia coli*. The lipid A region, depicted in red, elicits the immune response.	12
Figure 2	Expression of TLR4 (A) in granulosa cells of mice ovary at 15, 23 days and 24 and 48 hr after eCG, (B) Immunohistochemistry staining of the ovary during the immature and follicle development phase (eCG 48 hr).	36
Figure 3	Ovarian morphology and follicular health (A) Hematoxylin-eosin staining during the follicular development and ovulation phase. (B) The number of primary, secondary, and antral follicles in mice ovary at 48 hr after eCG and/or LPS injection and hematoxylin-eosin staining.	37
Figure 4	Follicular atresia and cell proliferation in ovarian follicles resulting from LPS action. (A) TUNEL staining of the ovary during the follicular development phase. (B) Immunofluorescence staining of the ovary from mice injected with eCG with or without LPS at 48 hr the immature.	38
Figure 5	Ovarian morphology and follicular health (A) Hematoxylin-eosin staining of ovaries during the ovulation phase. (B) The average number of ovulated oocyte (C, 0.1, 1 μg/kg LPS). (C) the maturation rate (D) the average number of follicular cysts	39
Figure 6A	The expression of *Cyp19a1, Ccnd2, Fshr, Lhcgr genes* and Inhibin hormone related to cell proliferation, differentiation, and ovulation in granulosa cells of mice during the follicular development phase *in vivo*.	40
Figure 6B	The expression of *Lhcgr, Cyp19a1 and Ccnd2* genes related to cell proliferation, differentiation, and ovulation in granulosa cells of mice during the follicular development phase cultured *in vitro.*	41

	Title of the Figures	Page No.
Figure 7A	The effect of LPS on the expression of EGF-like factors, progesterone receptor (PGR)-dependent events and other targets of the LH-LH receptor (LHR)-dependent pathway (*Snap25* and *Star*) in granulosa cells of mice.	42
Figure 7B	The effect of LPS on the expression of EGF-like factors, progesterone receptor (PGR)-dependent events and other targets of the LH-LH receptor (LHR)-dependent pathway (*Ptgs2, Nrg1, Cyp11a1 and Areg*) in granulosa cells of mice.	43
Figure 8	The effect of LPS on the expression of chemokines and cytokines (Chemokine ligand 5 and Interlukin-6) in the granulosa cells of mice.	44
Figure 9	The expression of *Dnmt1* gene implicated in DNA methylation in **(A)** granulosa cells *in vivo* (B) cultured granulosa cells.	45
Figure 10	Kinetic changes of cytosine methylation in the (A) *Lhcgr* promoter region, and (B) *Cyp19a1* promoter region of granulosa cells of mouse ovaries.	46
Figure 11	TLR7 expression in the ovary at different time points (A) Expression of TLR7 through western blotting, where β-actin was used as control. (B) Quantitative expression of TLR7 over β-actin in the ovary.	64
Figure 12	Immunofluorescence staining of the ovary during the immature, follicle development and ovulation phase using anti-TLR7 antibody.	65
Figure 13	TLR7 and TLR8 expression in the ovary at different time points (A) Quantitative expression in the cumulus cells. (B) Quantitative expression in the granulosa cells.	66
Figure 14	The expression of inflammation-associated genes (Chemokine ligand 5, Interferon-gamma and Interlukin-6*)* in the spleen of mice.	67

	Title of the Figures	Page No.
Figure 15	Effect of Resiquimod (R848) on ovarian morphology and follicular health (A) Hematoxylin-eosin staining of ovaries during the ovulation phase. (B) The average number of ovulated oocytes. (C) the maturation rate (D) fertilization rate.	68
Figure 16A	The effect of LPS on the expression of EGF-like factors, progesterone receptor (PGR)-dependent events and other targets of the LH-LH receptor (LHR)-dependent pathway (*Ptgs2, Cyp11a1, Star* and *Nrg1*) in granulosa cells of mice.	69
Figure 16B	The effect of LPS on the expression of EGF-like factors, progesterone receptor (PGR)-dependent events and other targets of the LH-LH receptor (LHR)-dependent pathway (*Snap25, Pgr, Ereg* and *Areg*) in granulosa cells of mice.	70
Figure 16C	Dose-dependent expression of *Snap25, Ptgs2, Cyp11a1, Star, Adamts1* and *HSD3B1* in granulosa cells cultured *in vitro.*	71
Figure 17	The expression of inflammation-associated genes (Chemokine ligand 5 and Interlukin-6*)* in granulosa cells of mice ovaries.	72
Figure 18	Ovarian morphology and follicular health (A) The average number of ovulated oocyte (eCG+hCG and eCG+R848 0.1 µg/kg). (B) The average number of ovulated oocyte (eCG+hCG+GnRH antagonist and eCG+R848 (0.1 µg/kg) +GnRH antagonist) (C) Hematoxylin-eosin staining of ovaries during the ovulation phase. (D) Level of progesterone	73
Figure 19	ACE2 receptor expression in the ovary at different time points	74

Chapter 1

General Introduction

Contents

Topics			Page No
1.1	The Ovary		1
1.2	Folliculogenesis		1
	1.2.1	Primordial follicle formation and recruitment	2
	1.2.2	Development of primary, preantral, antral, and preovulatory follicles	2
1.3	Luteinizing hormone/choriogonadotropin receptor (*LHCGR*)		4
	1.3.1	Mechanism of cumulus expansion, ovulation, and luteinization	4
1.4	Innate immune system and Toll-like receptors		6
	1.4.1	Toll-like receptor 4 and LPS	7
	1.4.2	Toll-like receptor 7 and 8 roles in Viral infection	7
	1.4.3	Endogenous Ligands	8
1.5	Pelvic Inflammatory Diseases and other diseases caused by Bacteria and Viral infections		8
	1.5.1	Follicular Cyst	9
	1.5.2	Polycystic Ovarian Cyst	9
1.6	Aim of this study		10

1.0 Introduction

1.1 The Ovary

The ovary is the female reproductive organ that influences so many activities such as the development of secondary sex characteristics, regulation of the hypothalamic-pituitary-ovarian axis as well as the production of growth factors, peptides, and steroids to mention a few (Edson *et al.,* 2009). The ovary has two fundamental functions, and they include the production of developmentally competent oocytes and the secretion of steroid hormones which play a role in fertilization and embryo implantation (Palermo, 2007). The somatic cells and germ cells which consist of oocytes and cumulus, granulosa, theca, and stroma cells respectively are the main components of the ovary.

1.2 Folliculogenesis

The first step leading to the ovulatory stage is referred to as folliculogenesis and this describes the process through which a follicle is formed. A mammalian follicle comprises an oocyte that is surrounded by somatic cells such as cumulus and granulosa cells. The granulosa cells act as a source of energy and nutrient supply. Likewise, the theca cells which are somatic cells produce steroids such as androgen which is later converted into estrogen by the granulosa cells, a steroid that is vital for follicle development and reproductive health (Balla *et al.,* 2003 and Tingen *et al.,* 2009). It is the interaction of somatic and germ cells that leads to ovarian follicle maturation and the process of maturation occurs in a stepwise manner. The process includes initiation, growth selection, ovulation, and luteinization (Richards and Pangas, 2010).

1.2.1 Primordial follicle formation and recruitment

During the early stage of fetal development, the ovaries contain a large pool of oogonia that develops into the oocyte by entering the first meiotic division after which they are arrested at the prophase stage (resting phase). In mice, the formation of primordial follicles containing an oocyte in the first prophase of meiosis with a single layer of granulosa cells occurs within the first few days after parturition (Hirshfield, 1991). However, from this large pool, there is continuous recruitment of primordial follicles into the growing pool but only a few develop to become preovulatory follicles and undergo ovulation while the majority of the follicles undergo atresia (Matsuda *et al.,* 2012 and Hsueh *et al.,* 1994).

1.2.2 Development of primary, preantral, antral, and preovulatory follicles

Following the initial activation of primordial follicles and the cyclic recruitment or selection of a few follicles from the pool of primordial follicles for dominance and subsequent ovulation. There is a transition from primordial to primary follicle stage which is markedly recognized histologically by a change in a squamous morphology or shape of the granulosa cells to cuboidal and they begin to express proliferating cell nuclear antigen (PCNA) (Fortune *et al.,* 2000 and McGee and Hsueh, 2000). During the preantral stage, follicles acquire an additional somatic cell layer called the theca cells and undergo granulosa cell proliferation and a further increase in the size of the oocyte. The secondary follicle contains oocytes in mid-growth stages, and it is surrounded by two or more layers of granulosa cells. Overall, the growth of the preantral follicles is dependent on paracrine, autocrine regulatory factors, and the action of gonadotropin which produces follicle-stimulating hormone (FSH) (Cattanach *et al.,* 1977). Also, the bidirectional interaction between the oocyte and the somatic structures of the follicle using growth factors such as inhibin/activin, insulin-like growth factor and bone morphogenetic systems (BMP) also affect

the growth of preantral follicles (Webb et al., 1999, Knight and Glister 2001, Eppig *et al.,* 2002). In addition, the oocyte secretes numerous factors that mediate follicle development and ovarian function, which include GDF9 and BMP15 (Dong *et al.,* 1996 and Aaltonen *et al.,* 2000). These oocyte secreted factors play a crucial role in granulosa cell proliferation, theca cell development, and steroid regulation (Carabatsos *et al.,* 1998). The formation of the antrum which is marked by fluid-filled spaces that graduate from small spaces to form a single antral cavity signifies the emergence of antral follicles. In mice, it takes around 15 days postpartum from the activation of primordial follicles to the formation of antral follicles (Hirshfield, 1991). In the matured Graafian follicle, two functionally different granulosa cell populations can be seen, the cumulus cells which surround the oocyte, and the mural granulosa cells which lines the wall of the follicle. The cumulus cells play a role in oocyte growth and developmental competence while the mural granulosa cells are implicated in steroid production and ovulation (Balla *et al.,* 2003). It is during the antral stage that FSH and LH act on the granulosa and theca cells to synthesis both androgens and oestrogen. Moreover, the ovary also produces other growth factors such as activins and inhibin to modulate the action of FSH, hereby regulating the follicle development process when necessary (Bernard and Woodruff, 2001). To enter the preovulatory follicle stage, follicles with higher FSHR expression survive the reduction of FSH level in the serum. These follicles which express *Lhcgr* and *Cyp19a1* in granulosa cells are termed dominant follicle. The high expression of *Cyp19a1* induces estrogen production in preovulatory follicles, which impacts the induction of LH surge. The transient secretion of LH from pituitary grand acts on LH receptors expressed in granulosa cells of preovulatory follicles to undergo the ovulation process.

1.3 Luteinizing hormone/choriogonadotropin receptor (*LHCGR*)

LHCGR is a member of the G-protein coupling receptor family and it is expressed in the theca cells of actively dividing follicles and in mural granulosa cells of preovulatory follicles (Minegishi *et al.,* 1990; Eppig *et al.,* 1997). Therefore, the expression of LHR in preovulatory follicles can be said to be a marker of the mural granulosa cell phenotype in the follicles. Also, the activation of *Lhcgr* is necessary for ovulation and progesterone production (Richards, 1994). *Lhcgr* in theca cells stimulates the production of androgen which serves as a substrate for conversion of androgen to estradiol through the action of FSH-induced aromatase in granulosa cells. To ensure the initiation and completion of these processes, *Lhcgr* activates the Protein Kinase A and ERK1/2 pathways (Breen et al., 2013). In addition, PKA promotes the activation TCF3 and SF1 site/region found in the *Lhcgr* promoter by increasing the phosphorylation of β-catenin that interacts with both transcriptional factors to enhance *Lhcgr* transcriptional activity (Law *et al.,* 2013). Likewise, the *Lhcgr* promoter region has the SP1 binding sites whose activities not only influence the expression of *Lhcgr* in both granulosa and theca cells but also serve as the main regulator of *Lhcgr* gene expression (Law *et al.,* 2013). The expression and silencing of genes are regulated by epigenetic mechanisms. Therefore, epigenetic changes in the *Lhcgr* promoter region can prevent *Lhcgr* transcriptional factor Sp1 from gaining access and binding to its target sequence, hereby resulting in gene suppression (Genhard *et al.,* 2010).

1.3.1 Mechanism of cumulus expansion, ovulation, and luteinization

LH directly induces follicle rupture and luteinization processes via the expression of genes in granulosa cells. LH induces and activates progesterone production and progesterone receptor (PGR) lead to an increase in *Adamts1,* a downstream target that mediates follicle rupture and release of oocyte (Palanisamy *et al.,* 2006). The progesterone was produced by the induction of

several proteins such as *Star* and *Cyp11a1* are induced in the ovary. However, ovulation has been described as an inflammatory-like process because of the occurrence of follicular hyperemia, an increase in the production of prostaglandins, implicating the activation of collagenase and other protease cascades. During ovulation, LH induces plasminogen activators of the urokinase-type in the preovulatory follicles of mouse ovary which play a huge role in activating collagenase an enzyme that is involved in tissue remodeling (Espey and Lipner, 1994). Together, these genes support the follicle rupture and ovulation processes.

However, due to the low level of LH receptor in cumulus cells surrounding the oocyte, the process of cumulus expansion and oocyte maturation is indirectly induced by LH through EGF network (Fu et al., 2007; Fan et al., 2009). The binding of LH to LHR in mural granulosa cells leads to the accumulation of cAMP and increased expression of secondary factors such as amphiregulin (AREG) and epiregulin (EREG) which in turn activates the ERK1/2 cascade in the cumulus cells of preovulatory follicles (Conti *et al.,* 2012; Park *et al.,* 2004). This kinase acts as a mediator that stimulates the expansion of cumulus cells and oocyte maturation due to the expression of *Ptgs2, Tnfaip6, Has2, and Ptx3*. With Has2 producing hyaluronan which plays a role as the backbone of the matrix, TNFaip6 catalyzing the formation of covalent crosslinks between the chains of serum-derived inter-alpha -trypsin inhibitor and hyaluronan, Pentraxin (Ptx3) functions in stabilizing the interaction between the cumulus matrix and serum-derived inter-alpha -trypsin inhibitor and Ptgs2 synthesizing prostaglandins required for supporting the activity of TNFaip6 (Hernandez-Gonzalez *et al.,* 2006). With the induction of cumulus expansion, these genes including members of the innate surveillance system (PRRs) from the TLR family, *Myd88* and *Cd34*, and *Cd36* are expressed in cumulus cells. This shows that just as it is seen during bacterial invasion-immune cell

stimulation, under ovulatory circumstances cumulus cells also prompt TLR2&4 and CD14 and other immune-related genes (Hernandez-Gonzalez et al., 2006; Shimada et al., 2008).

1.4 Innate immune system and Toll-like receptors

The first responders to external invasion or infection in the host are the immune components of the innate immune system and they include cytokines, natural killer cells, macrophages, and neutrophils. In posing an inflammatory response, the host recruits immune cells to the site of tissue damage or microbial invasion (Tizard, 2018). This process is initiated when pattern-recognition receptors (PRRs) on the surface or within host cells recognize or bind to pathogen-associated molecular patterns (PAMPs) released from damaged cells or microbial components in a distinct and specific manner (Akira *et al.,* 2006). Toll-like receptors which are a notable example of PRRs are of 10 different types (TLR 1-10 inclusive) (Akira *et al.,* 2001) and their signaling pathway is activated from the cytoplasmic Toll-interleukin-1 receptor (TIR) domains. In this domain, an adaptor named MyD88 which contains the TIR domain in the C-terminal portion and a death domain in the N-terminal portion plays a huge role in signaling for all toll-like receptors (Horng *et al.,* 2001). When MyD88 is stimulated it recruits IL-1 receptor-associated kinase (IRAK) to TLRs by the interaction of the death domains of both molecules. This leads to the activation of a serine/threonine kinase (IRAK) associated with the IL-1 receptor which contains the TIR domain by phosphorylation. It is the interaction between IRAK and TRAF6, a member of the tumor necrosis factor receptor-associated factor family that leads to the activation of two distinct MyD88 signaling pathways and the resultant activation of JNK and Nuclear factor-κB (*NF-κB*) (Fitzgerald, 2001). Thereafter, *NF-κB* translocates into the nucleus to activate the expression of genes associated with proinflammatory cytokines (Takeuchi and Akira et al., 2010).

1.4.1 Toll-like receptor 4 and LPS

LPS is a complex glycolipid containing a hydrophilic polysaccharide and hydrophobic domain. It is found in the outer membrane component of Gram-negative bacteria. Its hydrophobic domain which is referred to as Lipid A is responsible for its biological activity. When a bacterial infection occurs in a host, LPS binding proteins (LBP) detect the presence of LPS and initiates signals through the membrane or soluble CD14 which are present on immune cells such as monocytes and myeloid cells as well as in the plasma. However, TLR4 and MD-2 have been shown to play a huge role in LPS signaling and have direct interaction with LPS in a manner that is distinct from CD14 (Hoshino, 1999 and Akashi *et al.,* 2003).

1.4.2 Toll-like receptor 7 and 8 roles in Viral infection

The presence of Resiquimod and imidazoquinoline compounds in the host activate immune cells and prompt a response through Myd88-dependent signaling cascade which eventually leads to the production of the transcription factor NF-κB (Akira and Hemimi, 2003). TLR7 has been shown to recognize the presence of Resiquimod and imidazoquinoline by acting as an adjuvant receptor to control innate and adaptive immune responses (Miller *et al.,* 1999). Over time, plasmacytoid DC precursors have been implicated to produce IFN-α and IFN-β in response to viral infections but in recent time, TLR7 and TLR8 ligands like R848 have been recognized as a more potent inducer of IFN-α. Although R837 and R848 both illicit immune response from immune cells, it has been discovered that R848 is about 100 times more potent than its counterpart (Ekman, 2011).

1.4.3 Endogenous Ligands

Endogenous molecules are derived from host tissues and cells or cell components and they activate TLR signaling and induce sterile inflammatory responses. Examples of endogenous ligands

include fibronectin, heparan sulfate, biglycan, fibrinogen, oligosaccharides of hyaluronan, and hyaluronan fragments (Chiron et al., 2008; Rifkin et al., 2005). Likewise, heat shock proteins, purified preparations from bacterial, and humans may serve as potent activators of the innate immune system (Tsan and Gao, 2004). Usually, these endogenous ligands and their receptors are localized in different cellular compartments and are unable to interact physiologically. In most cases, endogenous ligands are released from injured or dying cells through a non-conventional lysosomal route (Pollanen et al., 2009). Likewise, endogenous TLR ligands are also referred to as alarmins and provide early warning calls to the innate and adaptive immune systems. The innate immune system is not only activated by PAMPs but also by DAMPs released by injured cells and they help the immune system to sense an ongoing infection and in recruiting more immune cells to the predilection site (Seong and Matzinger, 2004; Medzhitov, 2008). More so, endogenous TLR ligands may be involved in the pathogenesis of some autoimmune diseases (Marshak-Rothstein, 2006). Overall, TLR-mediated sterile inflammation triggered by endogenous ligands is involved in many pathological processes.

1.5 Pelvic Inflammatory Disease and other diseases caused by Bacteria and Viral infections

The action of LPS and R848 on the reproductive ability of an organism is disruptive and result in aberrant developments in the structure and function of an organism's reproductive system. Noteworthy is a myriad of pelvic inflammatory diseases that plaque women and female livestock across the world. These diseases occur when pathogenic organisms enter the vagina or cervix and ascend to other structures of the upper female reproductive tract. A Pelvic inflammatory disease refers to a clinical syndrome of a broad range of infectious diseases that cause inflammation and affect the upper genital tract of a female (Brunham *et al.,* 2015). Some of such conditions caused by PID include pelvic pain, follicular cyst, polycystic ovarian syndrome (PCOS), endometritis,

salpingitis, tubal-ovarian abscess, perihepatitis, reduced pregnancy rate, and most devastatingly sub-infertility and outright infertility (Verweij *et al.,* 2016 and Brunham *et al.,* 2015). Other diseases caused by bacterial and viral infections are brucellosis, leptospirosis, urethritis, and vaginitis as well as genital herpes, virus diarrhea (BVD), Bovine leukemia virus, and porcine reproductive and respiratory syndrome respectively.

1.5.1 Follicular cyst

Follicular cyst refers to the failure of one or multiple secondary follicles to ovulate. These cysts are formed in most cases by the blockage of ovulation arising from an inadequate supply of Luteinizing hormone during LH surge and due to excess production of follicle-stimulating hormone (FSH) during ovulation. At its peak, LH prompts the expulsion of the oocyte or follicle rupture but when this does not take place the follicle becomes a cyst.

1.5.2 Polycystic Ovarian cyst

Polycystic Ovarian cyst is an endocrine disorder that affects women in their perimenopausal years. It is characterized by clinical or biochemical hyperandrogenism, amenorrhea, and polycystic ovaries. In young girls, it is marked by an increase in gonadotropin-releasing hormone (GnRH) pulse frequency which leads to over-secretion and an increase in ovarian androgen production (Blank *et al.,* 2006). As a result, ovarian follicles grow too early and antral follicle development is arrested leading to PCOS (Franks *et al.,* 2000). Due to the insulin resistance and obesity that is associated with PCOS, it is regarded not only as a reproductive condition but also metabolic disease.

1.6 Aim of this study

It is known that bacteria or viruses that invade the body elicit an immune response from the host. More so, LPS and ssRNA viral particles have been found in the uterus of cattle and testes of humans where they impact negatively on the normal functioning of the reproductive system including reduction in the synthesis of steroids such as estrogen and progesterone. Apart from disrupting follicle growth and maturation, they also cause an increase in the level of chemokine and cytokine, an occurrence that can be attributed to the inflammatory response posed by the host's innate immune system. Since these pathogenic components of the cell membrane can penetrate through the external and internal barriers of the ovary to reach the granulosa cells, any disruption in the functioning of GC's will affect cumulus expansion, oocyte maturation, and oocyte release during ovulation. In addition, toll-like receptors 4, 7, and 8 prompt an inflammatory response from the host on recognizing bacteria components (LPS) and viral pathogens or agonists (Resiquimod) respectively, leading to a cascade of reactions including the recruitment of immune cells and hormonal imbalances that affect the functioning of the cells at the predilection site. However, the direct mechanism through which bacterial infections cause a reduction in steroid secretion and ovulation of oocytes remains unclear. Likewise, there is no report on the expression of SARS-COV-2, ACE2 receptor or TLR7/8 agonist (R848) on granulosa cells and the impact on ovarian functioning as well as the mechanism by which it causes ovarian dysfunction.

Therefore, this study was undertaken to understand the mechanism by which LPS and ssRNA viruses cause low reproductive performance of the female reproductive system. Likewise, for the first time detecting the expression of ACE2 and TLR 7/8 on the granulosa cells of mouse ovary and the mechanism by which ssRNA agonist, Resiquimod (R848) disrupt normal ovarian function. For this, two (2) individual experiments were conducted considering the precise hypothesis.

In Experiment 1, it was hypothesized that the disruptive action of LPS on follicle development, ovulation, and overall ovarian health is a result of the epigenetic regulatory action of LPS which results in the methylation of DNA at the *Lhcgr* and *Cyp19a1* gene promoter region. To clear the hypothesis, the impact of LPS on follicle development and ovulation was studied both *in vivo* and *in vitro* when required. More so, the expression of *Dnmt1* was studied both *in vitro* and *in vivo*, as well DNA methylation analysis of the *Lhcgr* and *Cyp19a1* gene promoter region in mice treated with LPS was compared with that of non-treated mice to understand the epigenetic regulatory action of LPS.

In Experiment 2, it was hypothesized that TLR7 and 8 are expressed in the granulosa cells of mouse ovary and R848 prompts a disruption in the normal functioning of the female reproductive health. To clear this hypothesis, TLR7 and 8 expression level in the mRNA and protein extracts of granulosa cells of mouse ovary was examined. TLR7 immunostaining was carried out to detect if TLR7 positive cells can be detected in the ovary of mice. Likewise, R848 a ligand of TLR7 and 8 was injected into mice and ovarian morphology and fertility parameters were studied using super-ovulated mice.

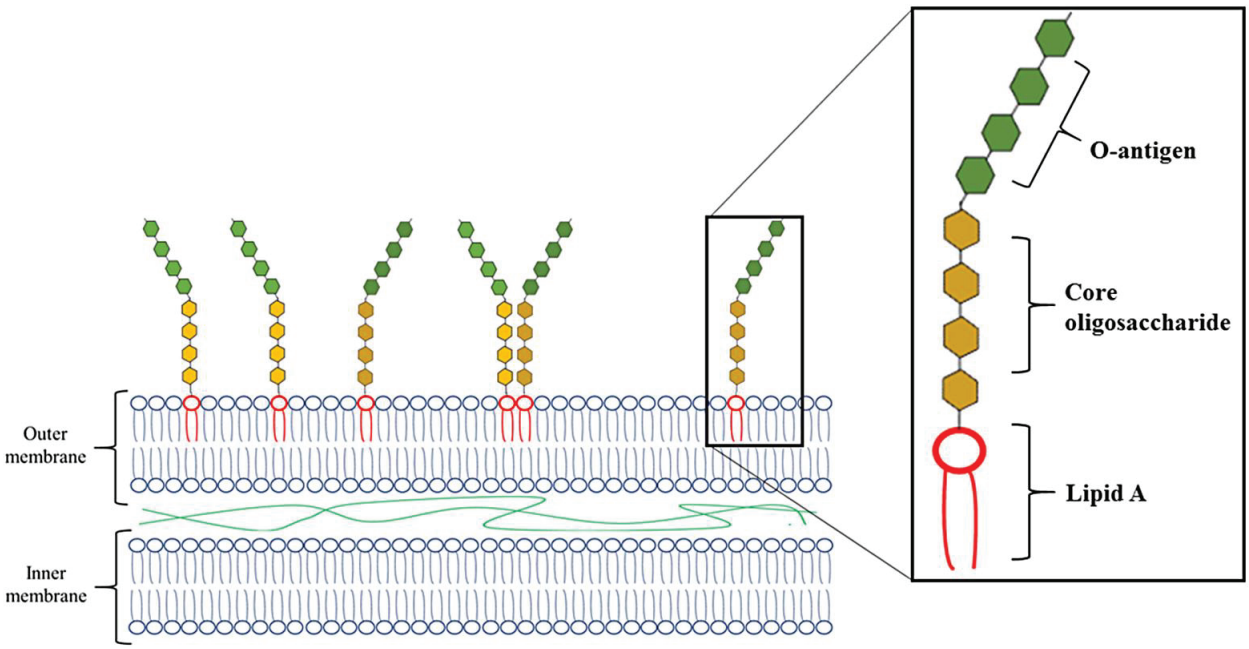

Figure 1: Structure of lipopolysaccharide (LPS). LPS is found on the cell wall of gram-negative bacteria, such as *Escherichia coli*. The lipid A region, depicted in red, elicits the immune response.

Experiment 1

Study on the effect of LPS on overall ovarian health and Epigenetic dynamics of the *Lhcgr* and *Cyp19a1* gene promoter region

Contents

	Topics	Page No
2.1	Introduction	13
2.2	Materials and Methods	16
2.3	Results	26
2.4	Discussion	29
	Abstract	33

2.1 Introduction

Infections of the upper female genital tract result in pelvic inflammatory disease (PID), which causes infertility (Ross, 2002). Gram-negative bacteria, among other factors that can cause PID, have been a menace in countries around the globe (Deb *et al.,* 2004). According to the National Health and Nutrition Examination Survey (NHANES) 2013-2014 cycle, the number of women with a reported lifetime history of PID is estimated to be approximately 5 million, representing 4.4% of sexually experienced women between 18 and 44 years old (Kreisel *et al.,* 2017). Likewise, *Bos taurus* is not exempted from bacterial infection of the genital tract, resulting in low reproductive performance, abnormal estrus cycle, follicular cysts, and low conception rates (Sheldon and Dobson, 2004).

Gram-negative bacteria possess an outer protective cell wall that harbors several pathogen-associated molecular patterns (PAMPs) that trigger inflammation and cause other toxic effects when they infect a host or are lysed by antibiotics (Tuomanen *et al.,* 1985a,b and Rietschel *et al*., 1994). A notable example is the outer membrane component of *Escherichia coli*, lipopolysaccharide (LPS), which has been found and isolated from the genital tract of cows suffering from uterine damage, ovarian dysfunction, and infertility (Sheldon *et al.* 2002; Ross, 2002 and Williams, 2007). When released into circulation, LPS is recognized by its receptor, a transmembrane protein Toll-like receptor (TLR4), which is mainly expressed in immune cells such as neutrophils and macrophages. LPS is also recognized by other coreceptors such as cluster of differentiation 14 (CD14) and myeloid differentiation factor 2 (MD2) (Akira *et al.,* 2006; Bromfield and Sheldon, 2011). The binding of LPS to its receptor (TLR4) then triggers the induction of NF-κB-dependent proinflammatory cytokines such as tumor necrosis factor-α (TNF-α) and prostaglandins (Medzhitov and Kagan, 2006). The production of a type I interferon response

by the host is regulated by Toll-interleukin-1 receptor (TIR) domain-containing adaptor-inducing interferon beta (TRIF) as well as TRIF-related adaptor molecule (TRAM), which are the downstream pathways of TLR4 (Kawai *et al*. 1999; Yamamoto *et al.,* 2003 a,b). TLR4 is also expressed in ovarian granulosa cells and cumulus cells. Endogenous ligands such as hyaluronic acid activate TLR4 in these cells during the ovulation process, which plays a substantial role in achieving successful fertilization (Shimada *et al.,* 2006, 2008). Additionally, *E. coli* infection and LPS have been observed to perturb ovarian follicle growth and to interfere with granulosa cell estradiol production and secretion *in vivo* (Erin *et al.,* 2008).

FSH acts on granulosa cells, and LH stimulates theca cells to induce follicular development with granulosa cell proliferation and expansion of small follicles into larger follicles. In large antral follicles, the gene expression pattern changes in a manner that allows granulosa cells to acquire responsive ability to ovulation stimuli. The transient induction of LH acts on the LH receptor encoded by *Lhcgr* which is expressed in granulosa cells to ensure oocyte maturation and successful ovulation (Barros *et al.,* 2010). The mechanism behind *Lhcgr* expression is a complex process in which β-catenin is reported to activate SF1 and T-cell factor (TCF) 3, which is required for FSH to induce the expression of *Lhcgr* mRNA (Law *et al.,* 2013, and Hunzicker-Dunn *et al.,* 2012). Interestingly, an *in vitro* promoter assay study showed that FSH directly upregulates *Lhcgr* promoter activity; however, the mRNA level of *Lhcgr* is only induced in granulosa cells after more than 24 hrs under both *in vivo* and *in vitro* conditions (Kawai *et al.,* 2012 and Selig *et al.,* 2013).

The late response is explained by epigenetic regulation; in the granulosa cells of small follicles, a high rate of DNA methylation is observed in the *Lhcgr* promoter region, which changes to a demethylated state in larger follicles following the injection of equine chorionic gonadotropin (eCG) (Kawai *et al.,* 2018). However, bacterial infection or LPS, a component of the cell

membrane is capable of inducing changes in histone modifications in cells and altering the host transcriptional framework (Hamon and Cossart, 2008). The lack of binding between the transcriptional factor and the CpG island is due to methylation patterns because when DNA methylation occurs it inhibits the binding of transcriptional factors. At the level of embryonic cell division, *de novo* methyltransferases DNMT3A and DNMT3B, as well as DNMT1, regulates and maintains the methylation and demethylation of genes which explains the silence and expression of some genes at a specific stage of development (Lock *et al.,* 1987, Mutskov and Felsenfeld, 2004 and Okano *et al.,* 1999). While some studies have shown that LPS disrupt steroid production and ovarian function, there is little information about the mechanism of this action. However, LPS has been discovered to influence some epigenetic regulator genes (Matt *et al.,* 2018). Therefore, we hypothesized that the low reproductive performance observed during bacterial infection is as a result of changes in the DNA methylation status of the *Lhcgr and Cyp19a1* promoter region. To this end, we investigated the effect of bacterial infection on ovulation as well as the expression of genes involved in DNA methylation.

2.2 Materials and methods

2.2.1 Materials

Equine chorionic gonadotropin (eCG) and human chorionic gonadotropin (hCG) were obtained from Asuka Seiyaku (Tokyo, Japan). Dulbecco's modified Eagle medium (DMEM)/F12 medium and penicillin-streptomycin were obtained from Invitrogen (Carlsbad, CA), and fetal calf serum (FCS) was obtained from Life Technologies (Grand Island, NY). Oligonucleotide poly-(dT) was obtained from Invitrogen, and avian myeloma virus (AMV) reverse transcription was obtained from Promega Corporation (Madison, WI). Lipopolysaccharide (LPS) (O111: B4 *E. coli* strain) was obtained from Sigma-Aldrich (St. Louis, MO). Additionally, QIAamp DNA Blood Mini, Gel extraction and EpiTect Bisulfite Kits were purchased from Qiagen (Germantown, USA). Routine chemicals and reagent were purchased from Sigma Chemical Co. (St. Louis, MO) and Nakalai Chemical Co. (Osaka, Japan).

2.2.2 Animals

Immature 3-week-old female C57BL/6 mice were obtained from Charles River Laboratories Japan (Yokohama, Japan). The animals were housed at the Experimental Animal Center, Hiroshima University, under a 12-hr light/12-hr dark schedule with food and water provided *ad libitum*. The animals were cared for in adherence to the National Institutes of Health *Guide for the Care and Use of Laboratory Animals*, as approved by Hiroshima University's Animal Care and Use Committee (#C18-34).

2.2.3 Treatment of mice with LPS

Twenty-five-day-old female mice were injected intraperitoneal (IP) with 4 IU of eCG to stimulate follicular growth. Thereafter, they were injected with 5 IU of hCG at 48 hr to stimulate ovulation and subsequent luteinization. LPS was injected intraperitoneal into mice at a dosage of 1 μg/kg BW at 23 days and ovaries were collected at 25 days. Also, LPS was injected intraperitoneal to mice at a dosage of 1 μg/kg BW when animals were 25 days old. At 16 hr after hCG injection following 48 hr after eCG injection, ovulated COCs were collected from the oviducts of three mice.

2.2.4 Collection of ovulated oocyte and in vitro fertilization

Twenty-five-day-old female mice were injected intraperitoneal (IP) with 4 IU of eCG to stimulate follicular growth. Thereafter, they were injected with 5 IU of hCG at 48 hr to stimulate ovulation and subsequent luteinization. LPS was injected intraperitoneal into mice at a dosage of 1 μg/kg BW at 23 days and ovaries were collected at 25 days. Also, LPS was injected IP to mice at a dosage of 1μg/kg BW when animals were 25 days old. At 16 hr after hCG injection following 48 hr after eCG injection, ovulated cumulus-oocyte-complexes (COCs) were collected from the oviducts of three mice that were euthanized and placed in 50 μl of human tubal fluid (HTF) medium. One hr before the collection of the COCs, spermatozoa was collected from the cauda epididymis of an adult male mouse and placed in 500 μl of HTF medium to allow for capacitation in an incubator set at a temperature of 37°C, an atmosphere of 5% CO_2 at maximum humidity. This was done before the sperm was introduced to the HTF medium containing oocyte at a final concentration of 1,000 sperm cells per μl. Thereafter, the sperm-oocyte-containing medium was incubated at 37°C in an atmosphere of 5% CO2 at maximum humidity for 8 hr for fertilization to occur. After washing in HTF medium the oocytes are transferred to KSOM media and placed in the incubator at 37°C

in an atmosphere of 5% CO_2 at maximum humidity for further development. The number of ovulated oocytes was scored.

2.2.5 Preparation of paraffin block and ovarian section staining

To prepare paraffin block for ovarian sectioning, the ovaries collected from three mice were fixed in 4% (w/v) paraformaldehyde (PFA) solution (Nacalai Chemical Co) overnight at 4°C, which was followed by dehydration and embedding in paraffin. The dehydration process involved step-by-step incubation in 70, 80, 90, 95, and 100% ethanol solution for 2 hr each, and the dehydrated ovaries were then incubated twice in xylene with each incubation period lasting for 2 hrs. Lastly, the ovaries were incubated for 2 hr in paraffin liquid before they were appended in paraffin, and blocks were made by solidifying the liquid paraffin containing the ovaries. Thereafter, 5 μm thick sections were cut from the paraffin block by microtome and placed in water warmed up to 42°C before they were mounted on slides and air-dried. Thereafter, the slide containing ovaries was deparaffinized by incubating in xylene twice for a period lasting 2 mins. The ovarian sections on the glass slide were then rehydrated using ethanol following stepwise incubation in 100, 90, 80, and 70% ethanol for a period lasting 1 to 2 mins each. Thereafter, the sections were washed in distilled water and stained with eosin for 1 min followed by washing under running tap water and counterstaining with hematoxylin for 30 secs followed by washing under running tap water. The stained sections in the slides were then dehydrated by incubating step-wisely in 100, 90, 80, and 70% ethanol followed by incubating in xylene twice for a period lasting 2 mins. Thereafter, the ovarian sections were covered by a coverslip using the multi-mount DPX solution. The slides were airdried and visualized by an optical microscope using BZ-II application software (Keyence, Tokyo, Japan).

2.2.6 TUNEL apoptosis detection

Terminal deoxynucleotidyl transferase nick end labeling (TUNEL) assay was carried out with the aid of *In-situ* Cell Death Detection Kit, POD (Roche, Mannheim, Germany) as described in the manufacturer's protocol to detect follicular atresia and apoptosis. Deparaffinization and rehydration of the tissue sections were carried out by washing twice in xylene for 2 mins on both occasions followed by a chronological incubation in gradient concentration ethanol of (100, 95, 90, 80, and 70%) for 2 mins at each concentration. Thereafter, the slides were rinsed in PBS for 5 mins and the tissue sections were incubated in Proteinase K solution containing 2 µl of 50x Proteinase K in 98 µl PBS buffer. Thereafter, the glass slide was washed twice in PBS buffer for 5 minutes each time and incubated with a blocking solution containing 3% (v/v) hydrogen peroxide in methanol for 10minutes at a temperature of 15 to 25^{o}C. Thereafter, the glass slide was washed twice in PBS buffer for 5 mins each time and the area around the tissue was kept dry. After that, 50 µl of TUNEL reaction mixture was added to the tissue sections and incubated at 37^{o}C for 1 hr under wet conditions devoid of light. The glass slide containing tissue sections serving as a negative control was treated with 50 µl of TUNEL label solution only and kept at the same condition as described earlier. Also, the glass slide containing tissue sections serving as a positive control was treated with DNase 1 recombinant grade I (50 IU/ml in 50 mM Tris-HCL, pH 7.5, 10 mMMgCl2 1 mg/ml BSA) for 10 mins at room temperature to induce DNA strand damage before labeling procedures. After incubation, the glass slides were rinsed in PBS twice for 5 mins on both occasions followed by incubation with a secondary antibody for 1hr 30minutes at 37^{o}C under wet conditions devoid of light. Thereafter, the glass slides were rinsed in PBS in preparation for immunohistochemistry. For this process, 50 to 100 µl of DAB substrate (DAB substrate comprises 5 µl of 20x DAB buffer and 20 µl 30% hydrogen peroxide) was added to the tissue sections and

incubated for 20 secs. The glass slides were transferred to water to stop the reaction and in preparation for counterstaining with hematoxylin and the stained sections were then dehydrated by incubating step-wisely in 100, 90, 80, and 70% ethanol followed by incubating in xylene twice for a period lasting 2 mins. Thereafter, the ovarian sections were covered by a coverslip using the multi-mount DPX solution. The slides were airdried and visualized by an optical microscope using BZ-II application software (Keyence, Tokyo, Japan).

2.2.7 RNA extraction and reverse transcription

Total RNA was obtained from the granulosa cells of mouse ovaries or cultured GCs using an RNAeasy mini kit (Qiagen, Germantown, MD, USA) based on the manufacturer's instructions. For RNA extraction, the cultured or collected granulosa cells were placed in a tube and subjected to homogenization and lysed using cell lysate solution containing RLT Buffer and 2-mercaptoethanol. Thereafter, 70% ethanol was added to the cell lysate mixture and mixed properly by pipetting. After that, the entire mixture was transferred to a Rneasy Mini spin column and centrifuged at a speed of 8000 × g, washed with RW1 buffer followed by DNase (DNase stock 5 µl + 35 µl) treatment for 15 mins at room temperature to disintegrate the DNA in the cells. Thereafter, repeated washing with RW1 and RPE was done, and RNA was extracted from the column using RNA-free water. The concentration of RNA was calculated at an optical density of 260 nm with the assumption that an OD260 unit is equivalent to 40 ng/ml RNA. The purity of the RNA extract was determined by measuring the absorbance ratio at 260/280 nm. Total RNA was then reverse-transcribed using 500 ng poly-Dt (deoxythymidine) and 0.25 IU of avian myeloblastosis virus reverse transcriptase (AMVRT) (Promega) at 42ºC for 75 min and 95ºC for 5 mins. The reverse transcriptase (RT) reaction mixture consisted of 7.25 µl of 50 ng mRNA + RNase free water, 0.5µl oligo DT (Primers of mRNA with poly A tail), 0.8 µl dNTP (Base, ATGC),

7.2 µl RNase free water, 4µl RT Buffer and 0.25µl RT Enzyme. cDNA products collected were resolved on 2% (w/v) concentration of agarose gel.

2.2.8 Real-Time PCR

Complementary DNA (cDNA) and primers of interest were added to Power SYBR Green PCR Master Mix (Applied Biosystems, Foster City, CA). Thereafter, PCR was carried out with the aid of a StepOne real-time PCR system (Applied Biosystems) using the following parameters: 10 minutes at 95°C, followed by 40 cycles of 15 seconds at 95°C and 1 minute at 60°C to 64°C. The real-time PCR mixture includes 7.5 µl Power SYBR Green PCR Master Mix, 0.5 + 0.5 µl forward and reverse primer respectively, 3.5 µl ddH_2O and 3.0µl of cDNA sample. The primer sets used in this study are shown in Table 1. In the real-time PCR, *L19* served as a control for variations in concentrations of mRNA and to ascertain reaction efficiency.

2.2.9 Collection and *in vitro* culture of granulosa cells

Six hrs after injecting immature mice (23 days old) with eCG, granulosa cells were collected from ovaries as described by Kawai *et al*. (2018). The cells were cultured in DMEM/F12 medium containing 1% (v/v) FCS in 5% (v/v) FCS-coated 96-well plates for 24 hrs at 37°C in an atmosphere of 5% CO_2 at maximum humidity. The medium described above was supplemented as follows: (a) no supplement (control), (b) 100 ng/mL FSH (National Institute of Diabetes and Digestive and Kidney Diseases, Torrance, CA), and 10 ng/ml testosterone (T), (c) FSH, T and 0.1 µg/ml LPS, and (d) FSH, T and 1 µg/ml LPS.

2.2.10 Immunohistochemistry

5 µm thick ovarian sections mounted on glass slides were deparaffinized and rehydration of the tissue sections was carried out by washing twice in xylene for 2 mins on both occasions followed by a chronological incubation in gradient concentration ethanol of (100, 95, 90, 80, and 70%) for 2 mins at each concentration followed by washing in PBS. Thereafter, the ovarian sections were incubated in 2% hydrogen peroxide and 80% methanol solution for 15 min to block endogenous peroxidase activity. Likewise, to prevent nonspecific binding the sections were incubated in 5% normal goat serum for 1 hr at room temperature.

Subsequently, the ovarian sections were treated overnight at 4°C with mouse anti-TLR4 monoclonal antibody (ab22048, Abcam USA) as the primary antibody at a dilution ratio of 1:500 in PBS containing 5% (w/v) BSA. On the following day, ovarian sections were washed with PBS including 0.3% (v/v) Triton X-100 followed by incubation with horse anti-rabbit IgG (1:200) (Sigma) as the secondary antibody. Thereafter, the binding of the primary antibody was visualized using diaminobenzidine (DAB) for 5 to 7 mins and ovarian sections were counterstained with hematoxylin, dehydrated, and mounted with DPX. The TLR4 labeling was observed under an optical microscope using BZ-II application software (Keyence, Tokyo, Japan).

2.2.11 Immunofluorescence staining

For immunofluorescence staining of ovarian sections using anti- Ki67 antibody (ab15580, Abcam USA), 5µm thick ovarian sections were deparaffinized using xylene followed by washing in PBS. Thereafter, the ovarian sections mounted on glass slides were deparaffinized and rehydration of the tissue sections was carried out by washing twice in xylene for 2 mins on both occasions. This

was followed by a chronological incubation in gradient concentration ethanol of (100, 95, 90, 80, and 70%) for 2 mins at each concentration, washed in PBS and boiled for 20 min in 10% citric acid (pH 6.0) for antigen activation. Thereafter, the sections were washed in PBS and nonspecific binding was blocked using 5% (w/v) BSA in MOM Immunodetection Kit or PBS (Vector Laboratories Inc, CA, USA). Furthermore, the ovarian sections were treated with Ki67 antibody (Abcam) with a dilution ratio of 1:200 as primary antibodies in 1% BSA (v/v) blocking solution at 4°C overnight. On the next day, the ovarian sections were washed in PBS containing 0.3% (v/v) Triton X-100, the staining was visualized with Cy3-conjugated goat anti-rabbit IgG (1:200) (Sigma) as a secondary antibody and counterstained using 4,6-diamidino-2-phenylindole (DAPI, Vector Laboratories Inc).

2.2.12 Morphological classification of follicles

The classification of follicles was performed as described by Umehera et al. (2017). 5 µm thick ovarian sections were cut from Paraffin-embedded blocks at intervals of 30 µm and mounted on glass slides, deparaffinized, rehydrated using ethanol followed by incubation in xylene and staining using hematoxylin-eosin to visualize the nuclei and cytoplasm was performed as described earlier for histological examination by light microscopy. The number of primary, secondary, and antral follicles in 12 sections per ovary was counted. Follicles with oocytes surrounded by a single layer of cuboidal granulosa cells were categorized as primary follicles, follicles with oocytes surrounded by two or more layers of granulosa cells with no visible antrum as secondary follicles while follicles with antrum within the granulosa cell layers enclosing the oocyte were counted as antral follicles. The analysis was carried out with an optical microscope using BZ-II application software (Keyence, Tokyo, Japan).

2.2.13 Genomic DNA extraction

Genomic DNA was obtained from mouse granulosa cells utilizing the QIAamp DNA Blood Mini Kit (Qiagen, Germantown, USA) based on the manufacturer's instructions. Granulosa cells collected from mouse ovaries were homogenized and treated step wisely with proteinase K and buffer AL. Thereafter, ethanol was added to the mixture and mixed properly by vortexing. The mixture was then transferred into a DNeasy Mini spin column and centrifuged at ≥ 6000 × g for 60 seconds and the flow-through in the 2 ml collection tube was discarded. Buffer AW1 was added to the column followed by centrifugation at ≥ 6000 × g for 1 minute and buffer and buffer AW2 was added followed by centrifugation at 20,000 × g for 3 minutes and the flow-through in the 2ml collection tube was discarded on both occasions. The DNA in the column was eluted by adding buffer AE to the column followed by centrifugation at 20,000 × g. The concentration of the DNA was calculated from the optical density at 260 nm with the assumption that the OD260 unit is equivalent to 50 ng/ml DNA. The purity of the DNA was estimated by measuring the absorbance ratio at 260/280nm.

2.2.14 Bisulfite sequence assay

Genomic DNA (1 mg) and 0.3 M NaOH (Nacalai) were added to the sodium bisulfite reaction mix from the EpiTect Bisulfite Kit (Qiagen), and then the mix was placed in a heating block set at 37°C for 20 minutes. Bisulfite DNA conversion of samples was carried out using the following parameters: 5 minutes at 95°C, 25 minutes at 60°C, 5 minutes at 95°C, 85 minutes at 60°C, 5 minutes at 95°C, 175 minutes at 60°C, 5 minutes at 95°C, and 120 minutes at 60°C. Thereafter, purification of bisulfite-converted DNA was performed as described by Kawai *et al*. (2018) using *Lhcgr* and Cyp19a1 (MeDip) primer sets as follows; forward, 5′-

GTGAGAGGGGAGGGTTGGAG-3′, and reverse, 5′-TTCAAGACCAACATTACCAA CACCA-3′; Forward- GGATTATTTGGATAATTATTATGGTTTT and Reverse- TAAAAATAAAATCCAATCTTCC, respectively.

2.2.15 Gel extraction and Gene Cloning

The PCR band containing the PCR product of the target gene was excised and extracted using Gel Extraction Kit (Qiagen, USA) according to manufacturer instructions. The extract was cloned into TOPO TA cloning vector (Invitrogen) and incubated at room temperature for 1 hr. Thereafter, the DNA and vector mixture was transferred to *E.coli* competent cells and incubated in ice for 30 mins at room temperature. For heat shock transformation of competent cells, the mixture was placed in a water bath at 42^{o}C for 40 secs and transferred to ice. In the recovery phase, SOC media was transferred into the mixture and placed in an incubator with a shaker for 1hr. This was followed by plating on Petri dishes containing LB agar with ampicillin and sprayed with X-gal. The petri dish was then incubated at 37^{o}C for 16 to 24 hr. Thereafter, white colonies were picked up and transferred individually to LB medium and placed in an incubator with a shaker at 37^{o}C for 24hr for amplification of colonies. After that, the cloudy LB medium was collected and purified using Qiagen Spin Miniprep Kit (Qiagen, USA) according to manufacturer instructions**.** Then EcoR1 enzyme and 10xH buffer were added to the extract and incubated at 37^{o}C for 1hr and the sample was loaded in 2% agarose gel to confirm the presence of the target gene. Thereafter, the extract is prepared for the sequence analysis.

2.2.16 DNA sequence analysis

The sequence analysis was performed using BigDye Terminator version 3.1/1.1 Cycle Sequencing Kit (Applied Biosystems). Sequence analysis was performed on more than five colonies for each

treatment. DNA nucleotide sequence was determined using the 3130/3130xl Genetic Analyzer (Applied Biosystems).

2.2.17 Statistical analysis

All data from three replicates were analyzed by either a Student's *t*-test or a one-way analysis of variance followed by a Tukey *post hoc* test (StatView; Abacus Concepts, Berkeley, CA). The percentage of methylation of CpG sites in the *LHCGR* promoter region was analyzed by the Quantification tool for Methylation Analysis (http://quma.cdb.riken.jp/).). In some studies, data obtained from three different cultures were analyzed by two-way ANOVA (Statview; Abacus Concepts, Inc.). All values are presented as the mean ± SEM. Treatments were considered significantly different from one another at $P < 0.05$.

2.3 Results

2.3.1 TLR4 expression and effect of LPS on ovarian morphology and health

To investigate the induction of TLR4 at different time points, we collected granulosa cells from the ovary of mice at 15 and 23 days as well as at 24 and 48 hr after eCG injection. There was a significant difference in the expression of TLR4 at 24 and 48 hr after eCG (Figure 2A), suggesting that TLR4 is highly expressed in larger follicles compared to smaller follicles found in immature mice. To determine the effect of endotoxin exposure on ovarian morphology, we first collected ovaries from mice treated with and without LPS before eCG injection; and mice injected with eCG- and/or LPS and carried out hematoxylin and eosin staining. Likewise, compact granulosa cells were observed in antral follicles of both the control and LPS-treated groups, and there was no damage to the follicles (Figure 3A). There was a significant difference between the secondary follicles, while there was no significant difference in the number of antral follicles in the control

and 1 µg/kg dosage LPS group (Figure 3B). However, in ovaries collected from mice before eCG injection, there was no significant difference in the number of follicles at each developmental stage (Figure 3A). To evaluate follicular atresia, immunohistochemistry-based TUNEL assay was carried out, and the number of observed atretic follicles in ovaries from mice treated with LPS and/or eCG injection were similar (Figure 4A).

2.3.2 Effect of LPS on ovarian morphology during the ovulatory phase.

When mice were injected with eCG and treated with hCG 48 hrs later, a higher number of corpus lutea was observed in the control group than in the LPS-treated group (Figure 5A). The total number of ovulated COCs in the oviduct of eCG-primed mice and the LPS-treated group (0.1 and 1 µg/kg) was significantly lower than the control group that was injected eCG without LPS (Figure 5B). In addition to preventing the release of preovulatory follicles during ovulation as shown in Figure 5A, LPS injection also results in a lower proportion of matured oocyte compared to the control group suggesting that oocyte maturation and development was disrupted by endotoxin action (Figure 5C).

2.3.3 The effect of LPS on the induction of EGF-like factors, progesterone receptor (PGR)-dependent events, and other targets of the LH-LH receptor (LHR)-dependent pathway

To analyze the induction of *Ptgs2, Nrg1, Cyp11a1 and Areg, Snap25* and *Star* mRNA in the granulosa cells of the ovary, granulosa cells were isolated from ovaries of eCG-primed mice at 48hr; 4 and 8hr after hCG injection (Figure 7). The expression of *Ptgs2* and *Star* were induced within 4hr after hCG. In the LPS treated groups *Ptgs2, Star,* and *Cyp11a1* were significantly reduced suggesting the role of LPS in regulating EGF-like factors, *Pgr*, and other LH-target genes involved in the ovulation process.

2.3.4 Effect of LPS on cell proliferation and development in the mouse ovary

The outcome of anti-Ki67 antibody immunoflourence staining in eCG-primed and LPS-treated mouse is shown in Figure 4B. The Ki67 positive cells were similar in both groups. We investigated the responsive ability of large and small follicles to TLR4 and observed positive TLR4 cells in antral follicles while TLR4 positive cells were undetected in smaller follicles of immature mice (Figure 2B).

2.3.5 Effect of LPS on the expression of genes in granulosa cells

To explore the effect of LPS on the expression of genes associated with follicle development *in vivo*, *Lhcgr, Cyp19a1, Ccnd2,* and *Fshr*, expression was significantly lower in granulosa cells (Figure 6A) from mouse ovaries in the LPS-treated groups than that in the control group. However, compared with the control group, there was no significant difference in the expression of Inhibin, *Ccnd2,* and *Fshr* (Figure 6A). In the *in vitro* data*, Lhcgr* and *Cyp19a1* expression in granulosa cells cultured with FSH+LPS were significantly lower than that of the control group (FSH alone), and there was no significant difference in the expression of *Ccnd2* (Figure 6B).

2.3.6 The effect of LPS on the induction of chemokines and cytokines

To analyze the induction of *Il6* and *Ccl5* mRNA in the granulosa cells of the ovary, granulosa cells were isolated from ovaries of eCG-primed mice at 48 hr, 4 and 8 hr after hCG injection (Fig 8). LPS stimulated the production of chemokines and cytokines such as *Ccl5* and *Il6* (Figure 8). In the LPS treated group there was a significant increase in the expression of *Il6* and *Ccl5* at the 4hr time point after hCG compared to the control group.

2.3.7 Effect of LPS action on the expression of *DNA (cytosine-5)-methyltransferase 1 in vivo* and *in vitro*

A significant reduction of *DNA (cytosine-5)-methyltransferase 1* (*Dnmt1*) was observed in granulosa cells of mice injected with eCG. The reduction was not observed in granulosa cells of LPS-treated mice, where the level of expression was similar to that of mice before eCG injection (Figure 9A). *In vitro* study also revealed that *Dnmt1* was significantly higher when granulosa cells were cultured in a medium containing 1 µg/ml LPS and FSH compared to the medium containing FSH (Figure 9B).

2.2.8 Epigenetic dynamics of LPS on DNA methylation at the *Lhcgr* and *Cyp19a1* gene promoter region

The injection of eCG to immature mice at a 48hr time point significantly resulted in the demethylation of the *Lhcgr* and *Cyp19a1* promoter region. Following the coinjection IP of eCG and LPS at the same time point, the decrease in the rate of methylation was not detected. Also, there was no significant difference observed in the methylation rate between the eCG and LPS coinjected group at 48 hr and the immature group (Fig 10A and B).

2.4 Discussion

An acute increase in LPS in the circulatory system causes serious systemic inflammation, which is known as sepsis, and sepsis triggers the release of proinflammatory cytokines. A chronic high-level increase in LPS also causes chronic inflammatory diseases such as inflammatory bowel disease and autoimmune and cardiovascular diseases (Suffredini *et al.,* 1989). LPS injection did not induce any negative changes to the phenotype of the ovary or morphology at each stage of the ovarian follicle. During the follicular development phase, the growth in diameter of small follicles

developing into antral follicles increases rapidly due to FSH stimulation (Matzuk and Lamb, 2002). It has also been reported that granulosa cell proliferation results in changes in the function of granulosa cells of the preovulatory follicle (Cuiling *et al.,* 2005). To this end, normal differentiation of granulosa cells was determined by incremental changes in the expression patterns of genes such as *Lhcgr* and *Cyp19a1.* However, following LPS treatment, our data demonstrated that the induction of *Lhcgr* and *Cyp19a1* was not observed. Granulosa cells that express a low level of *Lhcgr* do not acquire the ability to respond to ovulation stimulus, the endogenous LH surge, or exogenous hCG, which are required to induce ovulation (Kawai *et al*., 2016). In fact, the number of ovulated oocytes was significantly lower in LPS-treated mice than in control mice that were injected superovulation treatment. This condition mimics the follicular cyst, which is marked by a normal growth process from the primordial to the preovulatory follicle stage and is followed by the inability to release oocytes during the ovulatory phase (Garverick, 1997). This suggests that bacterial infection can cause follicular cyst in the ovary. While some studies have shown that endotoxin suppresses ovulation and reproductive performance (Erin *et al.,* 2008 and Suzuki *et al.,* 2001), there is little information about the mechanism that influences this occurrence. In contrast with smaller follicles, preovulatory follicles were highly impacted by the LPS-TLR4 pathway because the expression of TLR4 was significantly induced in granulosa cells at 24 and 48 hr after eCG injection.

While the expression of *Lhcgr* and *Cyp19a1* was suppressed by LPS, *Ccnd2* and *Fshr* levels were normal in granulosa cells, suggesting that selective activation of transcription factors occurred. Although these genes are induced by the PKA-dependent signal transduction pathway, their target transcription factors are different. *Ccnd2* transcription is directly regulated by CREB, while *Lhcgr* and *Cyp19a1* are activated by Sp1 and Sf-1 respectively. Moreover, it is known that the expression

of Sp1 is ubiquitous (Li *et al.,* 2004), suggesting that the downregulation of *Lhcgr* and *Cyp19a1* expression might be caused by the inability of Sp1 and Sf1 to access and bind to promoter sequences in both promoter regions. Our previous study reported that *Lhcgr* expression is highly associated with the demethylation of its promoter region in the granulosa cells of mouse ovaries (Kawai *et al.,* 2018). During embryonic cell division, the *de novo* methyltransferases DNMT3A and DNMT3B initiate CpG island methylation at regions of silent chromatin, and the replication of methylation patterns is maintained by DNMT1 and by other features within the DNA domain (Okano *et al.,* 1999). Strikingly, the expression level of *Dnmt1* was significantly decreased in granulosa cells from mouse ovaries injected eCG *in vivo* and those cultured with FSH *in vitro*. Likewise, the report that LPS influences epigenetic regulation during neuroinflammation in mice (Matt *et al.,* 2018) aligns with the result of our study, which shows that the coinjection of eCG and LPS and the inclusion of LPS in the culture medium upregulate *Dnmt1*. In concert with the data, the rate of DNA methylation in the *Lhcgr* promoter region was also affected by FSH and/or LPS. This suggests that in addition to the LPS-induced transient activation of inflammatory responses in both immune cells and granulosa cells, LPS is also capable of causing a long-lasting impact on gene expression patterns due to changes in DNA methylation status. This abnormal epigenetic regulation by LPS in granulosa cells causes follicular cysts, which dramatically decrease female fertility.

In conclusion, the present study demonstrated that the decrease in the induction of *Lhcgr* and *Cyp19a1* due to LPS is a result of the epigenetic regulatory action of LPS. The immunological response of the host to LPS or bacterial infection prevents the preovulatory follicles from responding to the LH surge, which is required for ovulation. Moreover, ovarian dysfunction and

polycystic ovaries, as well as other PIDs that are characterized by bacterial infection in humans and animals, are closely connected to the methylation of the *Lhcgr* promoter region.

Abstract

Lipopolysaccharide (LPS) is an endotoxin released by gram-negative bacteria, and it can pass through the protective physical barriers and tight junctions of the basement membrane. LPS has also been isolated from the genital tract of animals suffering from uterine damage and ovarian dysfunction. This study provides direct molecular evidence about the mechanism through which endotoxins cause reproductive disorders, such as follicular cysts and ovarian dysfunction. Granulosa cells and ovaries were collected from immature mice treated with eCG or with eCG and LPS injection intraperitoneal. Normal large antral follicles were observed in ovaries obtained from eCG and LPS coinjected mice, and the morphology of the ovaries was similar to that observed in the control group (eCG-injected mice). These antral follicles were not deemed atretic because few TUNEL-positive cells were observed. However, the granulosa cells of large antral follicles did not acquire the ability to respond to hCG stimulation. The number of ovulated oocytes was significantly lower in LPS-injected mice after superovulation compared to mice that were not exposed to LPS. The low reactivity was caused by the limited expression of the *Lhcgr*, which encodes the LH receptor in granulosa cells as well as an LPS-induced increase in the level of Dnmt1 expression both *in vivo* and *in vitro*. The methylation rate of the *Lhcgr* promoter region was significantly higher in granulosa cells obtained from the LPS treatment group compared with the control group. Together, these findings demonstrated that the decrease in the expression of *Lhcgr* due to LPS was a result of the epigenetic regulatory action of LPS. Our studies suggest that ovarian follicular cysts that is characterized by bacterial infection in humans and animals, is closely connected to the level of methylation of the *Lhcgr* promoter region.

Table 1. PCR primers used for profiling the expression of gene marker for GC's function

Gene	Forward Primer	Reverse Primer	Size (bp)
Lhcgr	5'-ACTGGTGTGGTTTCAGGAATT-3'	5'-CCTAAGGAAGGCATAGCCCAT-3'	244
Cyp19a1	5′-TTGCACCCAAATGAGGACAG-3′	5′-CTTCACTGGTCCCCAACACA-3′	290
Ccnd2	5′-TCACCACGTGTTCCCAAGAC-3′	5′-AGCGAATTCCCTCCATCAGA-3′	243
Nrg1	5' -AGAACCGGCTGTCTGCTTTT -3'	5' –TAGAGCTCCTCCGCTTCCAT -3'	373
Star	5' -GCAGCAGGCAACCTGGTG -3'	5' -TGATTGTCTTCGGCAGCC -3'	249
Ccl5	5'- ATATGGCTCGGACACCATA -3'	5'- GGGAAGGGTATACAGGGTCA -3'	242
Dnmt1	5'- GTGGCAAGAAGAAAGGCAAG -3'	5'- GCCCCCTTGTGAATAATCCT-3'	233
Il6	5'- CCGGAGAGGAGACTTCACAG -3'	5'- GGAAATTGGGGTAGGAAGGA -3'	421
Cyp11a1	5'-GGGAGACATGGCCAAGATGG-3'	5'-CAGCCAAAGCCCAAGTACCG-3'	279
Fshr	5′-TGGCCATTACTGGGAACACC-3′	5′-TGCCAAAGATGGGGAAGAGA-3′	261
Areg	5' -TTACTTTGGCGAACGGTGTG -3'	5' -TGTGCAGTCCCGTTTTCTTG -3'	231
Ptgs2	5' -TGTACAAGCAGTGGCAAAGG -3'	5' -GCTGTGGATCTTGCACATTG -3'	431
Snap25	5'- GAGATGCAGAGGAGGGCTGAC -3'	5'- GCTGGCCACTACTCCATCCTG -3'	309
L19	5'-GGCATAGGGAAGAGGAAGG-3'	5'-GGATGTGCTCCATGAGGATGC-3'	199
Inha	5'- TTGGAGGCAGACGCCTTATT -3'	5'- CGGTCTCTGCTGCTCCTTTT-3'	175

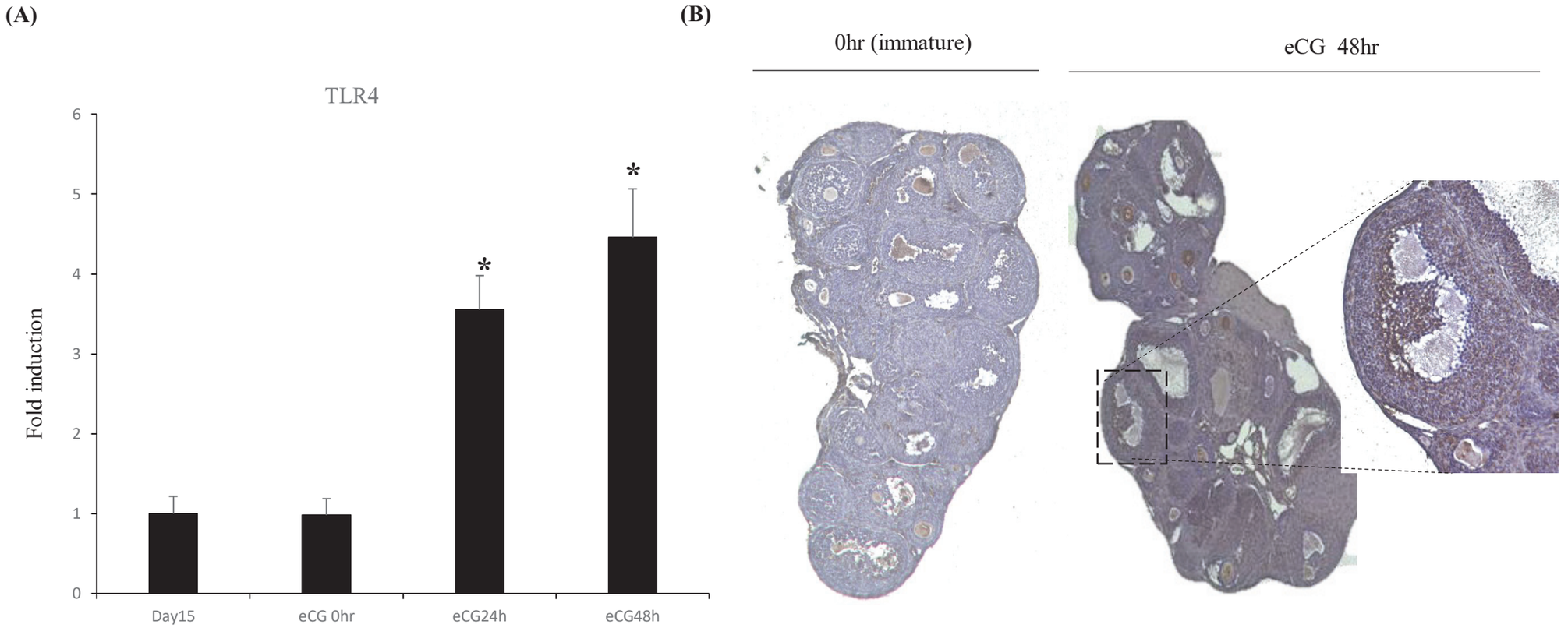

Figure 2. Expression of TLR4 (A) in granulosa cells of mice ovary at 15, 23 days and 24 and 48 hr after eCG, (B) Immunohistochemistry staining of the ovary during the immature and follicle development phase (eCG 48 hr). In (A) the value of granulosa cells from mice without eCG at 15 days was set as 1, and the data are presented as fold induction. Expression levels of TLR4 was normalized to those of *L19*. Values are given as mean ± standard error of the mean (SEM) of three replicates. If a significant difference was observed at each time points compared with the 15 days group the comparison analysis was performed by a Student's *t*-test, $*P < 0.05$. In (B) the ovaries were collected from immature mice and from mice injected with eCG after 48 hr. The ovarian sections were stained with anti-TLR7 antibody and digital images were captured using BZ-9000 microscope (Keyence).

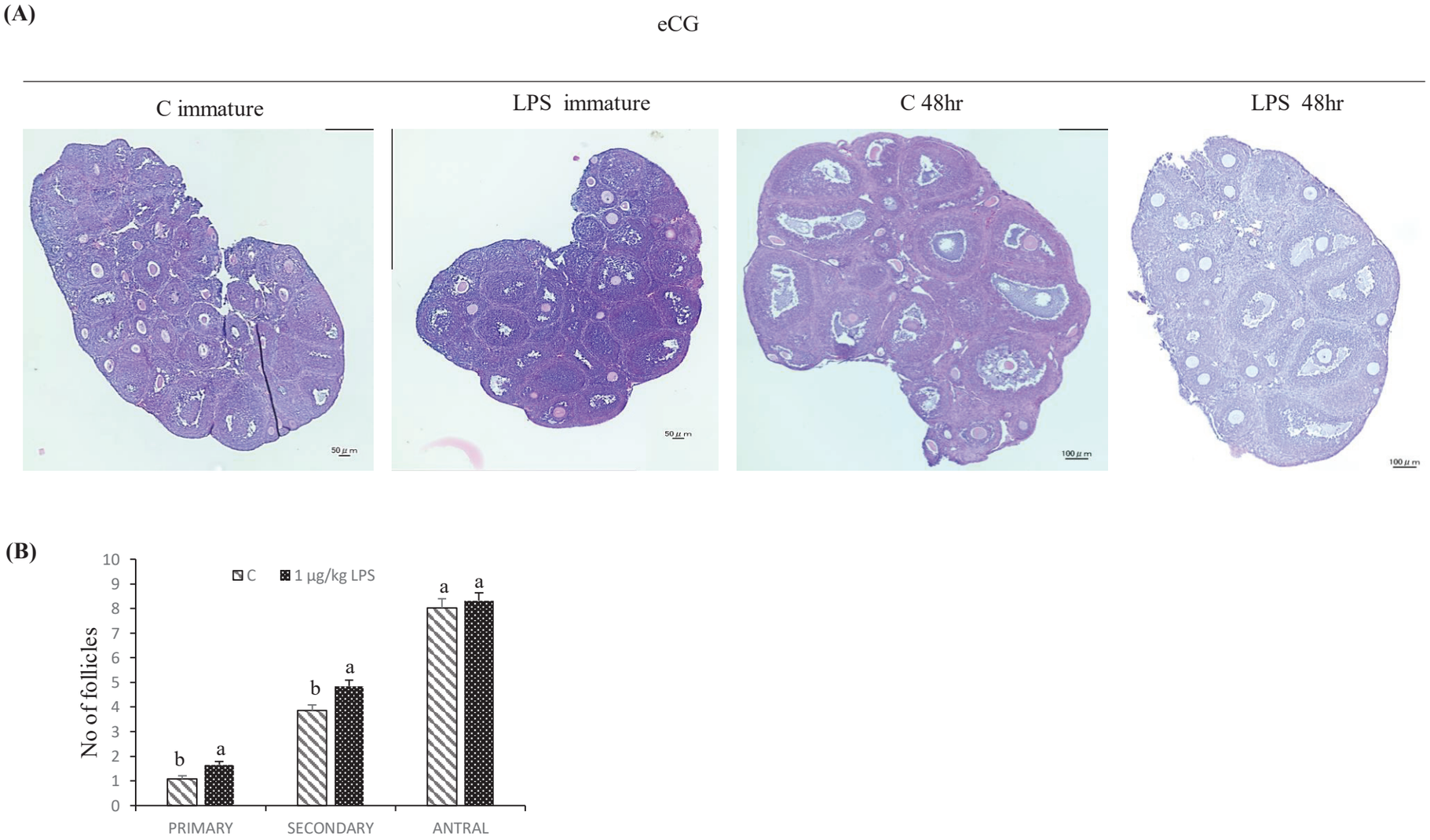

Figure 3. Ovarian morphology and follicular health (A) Hematoxylin-eosin staining during the follicular development. The ovaries were collected from immature mice and mice injected with or without eCG for 48 hr while the LPS group were injected with LPS intraperitoneally and digital images were captured using BZ-9000 microscope (Keyence). (B) The number of primary, secondary and antral follicles in mice ovary 48 hr after eCG and/or LPS injection and hematoxylin-eosin staining. The number of follicles were evaluated in 12 sections per ovary. Data are summarized as mean ± standard error of mean (SEM) of three mice for each group. Different alphabets (a and b) within the same graph differ significantly ($p < 0.05$)

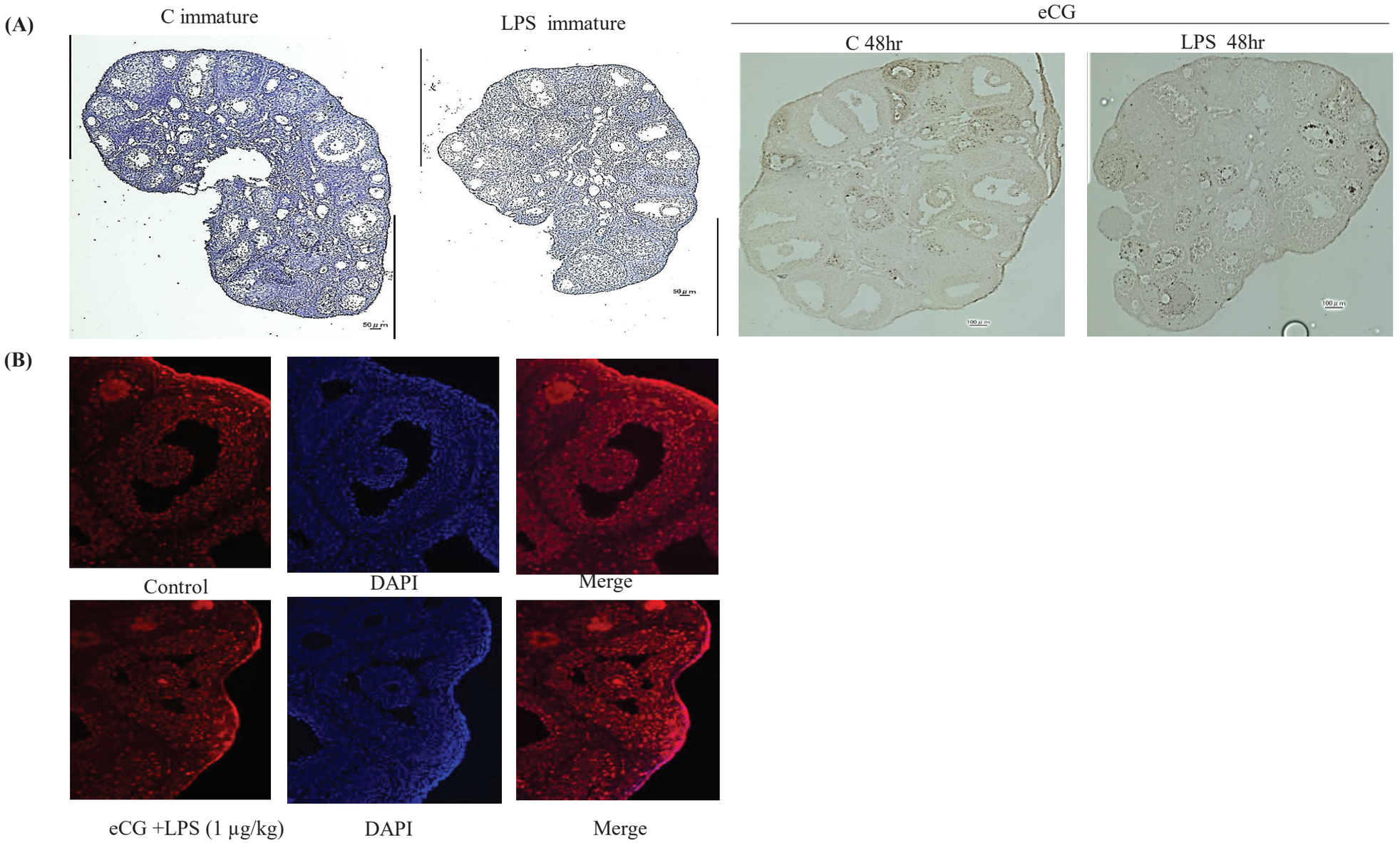

Figure 4. Follicular atresia and cell proliferation in ovarian follicles resulting from LPS action. (A) TUNEL staining of the ovary during the follicular development phase. The ovaries were collected from immature mice and injected with or without eCG and/or LPS for 48 hr. (B) Immunofluorescence staining of the ovary from mice injected with eCG with or without LPS at 48 hr using anti-Ki67 antibody. In (A) and (B) digital images were captured using BZ-9000 microscope (Keyence).

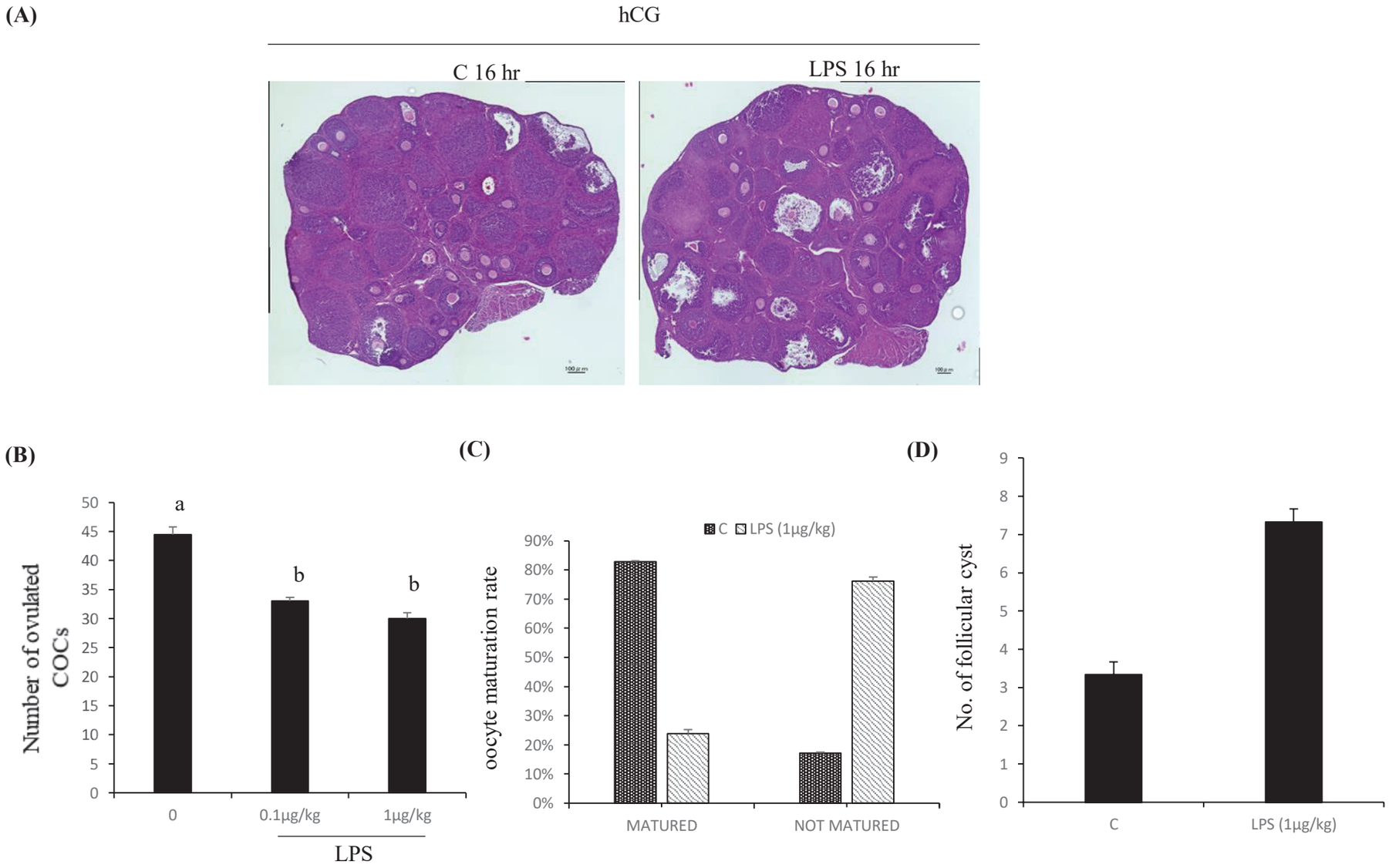

Figure 5. Ovarian morphology and follicular health (A) Hematoxylin-eosin staining of ovaries during the ovulation phase. The ovaries were collected from immature mice and injected with eCG and/or LPS followed by hCG injection and digital images were captured using BZ-9000 microscope (Keyence). (B) The average number of ovulated oocyte (C, 0.1, 1 μg/kg LPS). (C) the maturation rate (D) the average number of follicular cysts. Data are summarized as mean ± standard error of mean (SEM) of three mice for each group. Different alphabets (a and b) within the same graph differ significantly ($p < 0.05$).

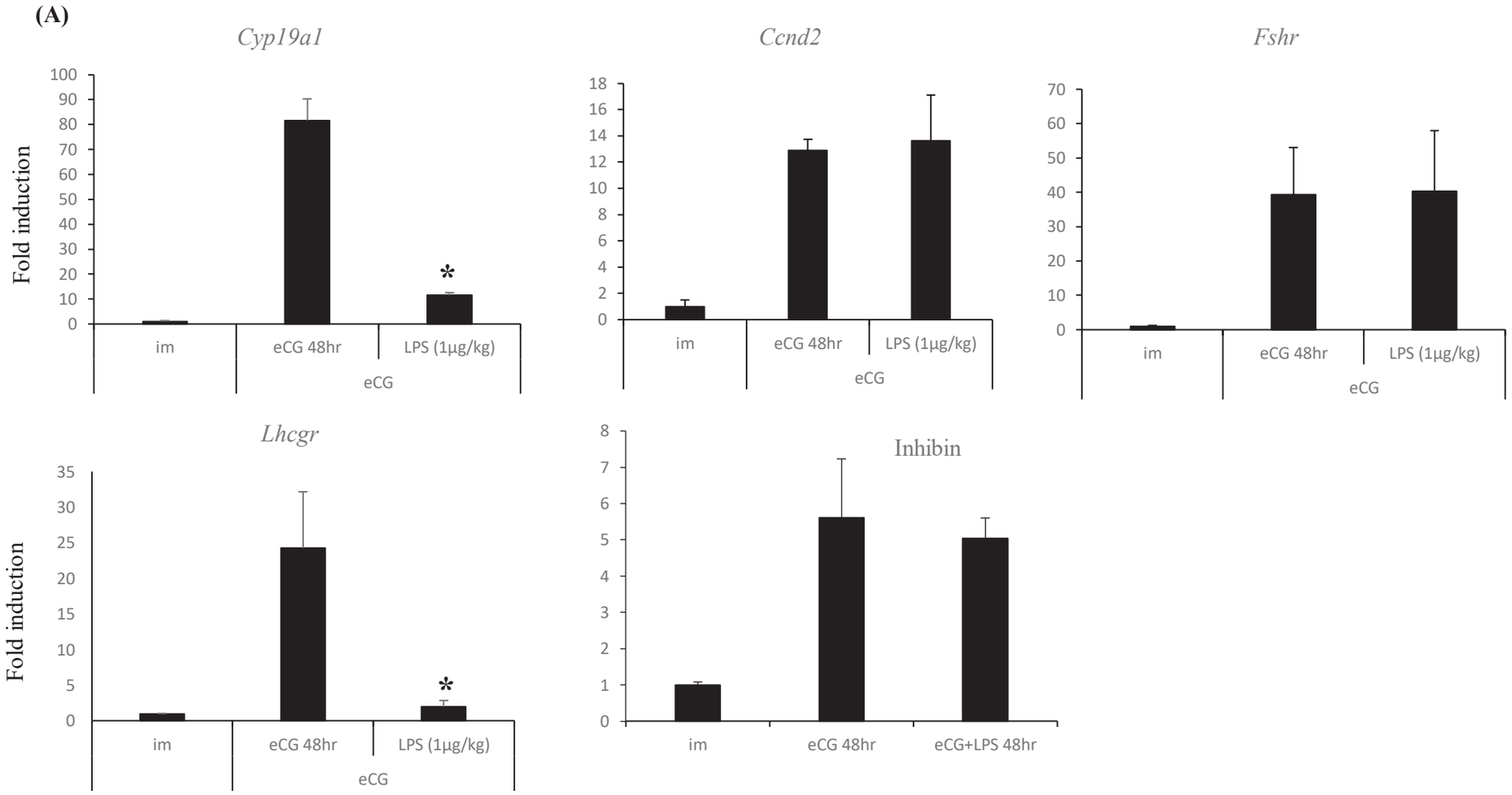

Figure 6A. The expression of *Cyp19a1, Ccnd2, Fshr, Lhcgr* and Inhibin in granulosa cells of mice at 23 days, and mice injected intraperitoneally with eCG and/or LPS for 48 hr. The value of granulosa cells from mice without eCG at 23 days was set as 1, and the data are presented as fold induction. Expression levels of the mRNA was normalized to those of *L19*. Values are given as mean ± standard error of the mean (SEM) of three replicates. If a significant difference was observed at each time points compared with the immature group the comparison analysis was performed by a Student's *t*-test, $*P < 0.05$.

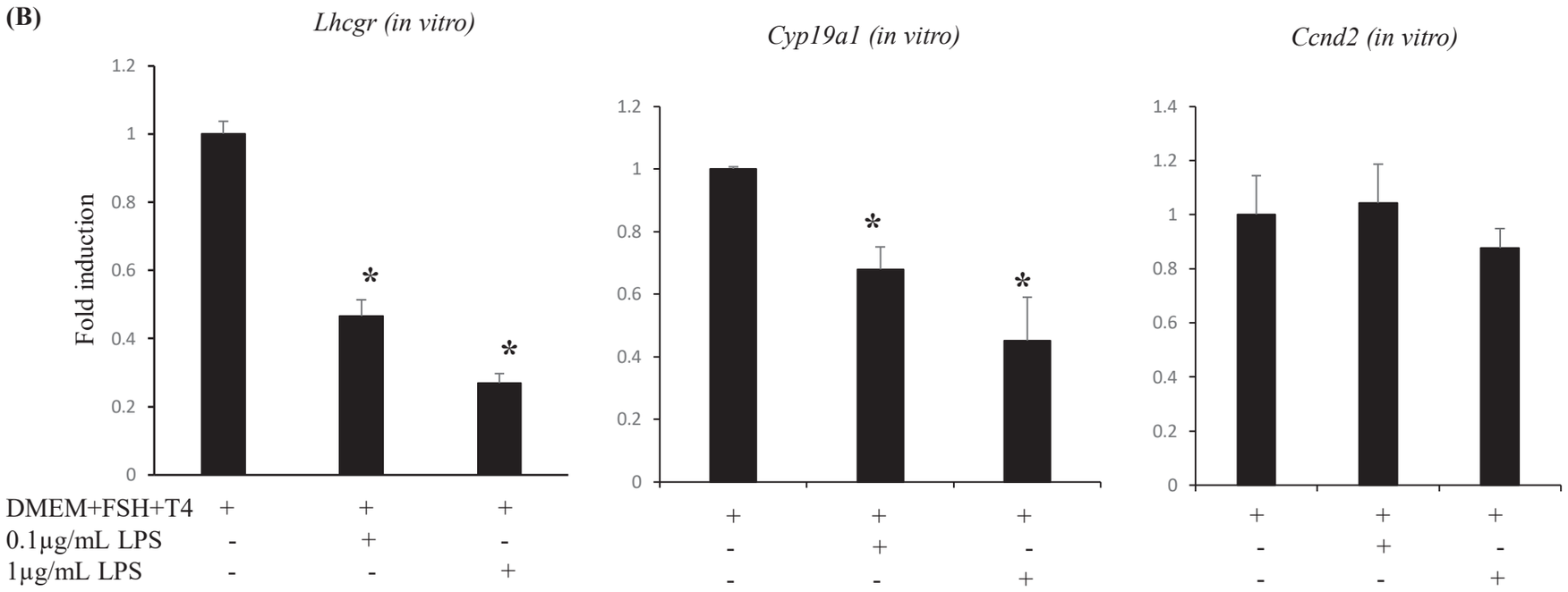

Figure 6B. The expression of *Lhcgr, Cyp19a1 and Ccnd2* in granulosa cells cultured *in vitro*. GC's were collected from 6h eCG primed mouse ovaries and cultured in 1% FCS supplemented DMEM/F12 media for 24 hr treated with or without FSH and Testosterone (T) and/or 0.1 and 1 µg/mL of LPS. The value of granulosa cells from mice without any treatment was set as 1, and the data are presented as fold induction. Expression levels of mRNAs were normalized to those of *L19*. Values are given as mean ± standard error of the mean (SEM) of three replicates. If a significant difference was observed at each time points compared with the immature group the comparison analysis was performed by a Student's *t*-test, $*P < 0.05$.

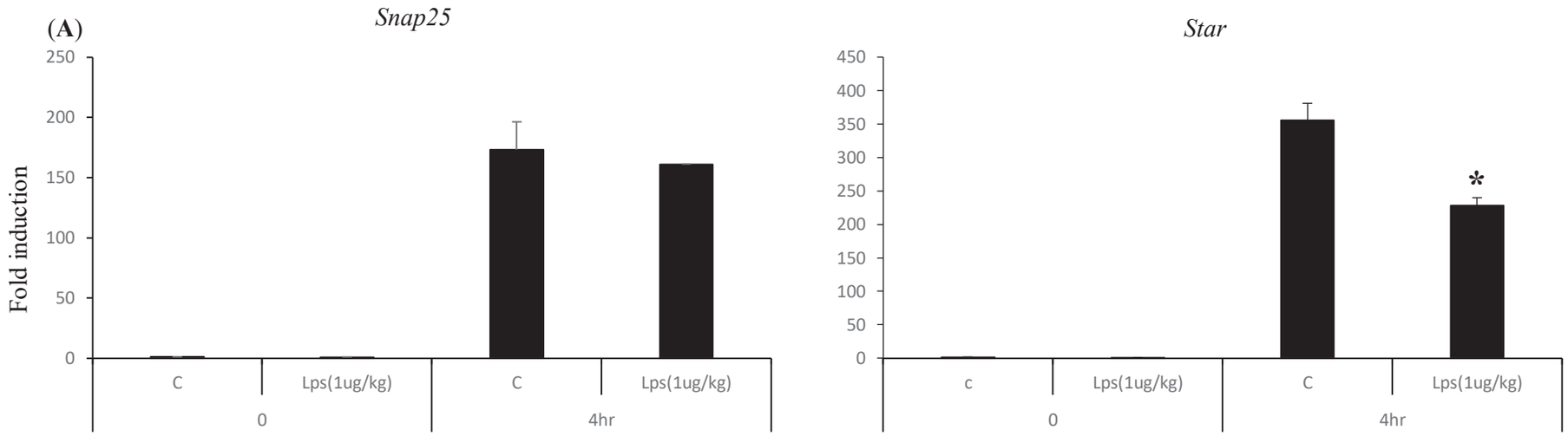

Figure 7A. The expression of *Snap25* and *Star* in granulosa cells of mice injected intraperitoneally with eCG, with or without hCG and/or LPS. The value of granulosa cells from mice injected with eCG only (0) was set as 1, and the data are presented as fold induction. Expression levels of the mRNA was normalized to those of *L19*. Values are given as mean ± standard error of the mean (SEM) of three replicates. If a significant difference was observed at each time points compared with the immature group the comparison analysis was performed by a Student's *t*-test, $*P < 0.05$.

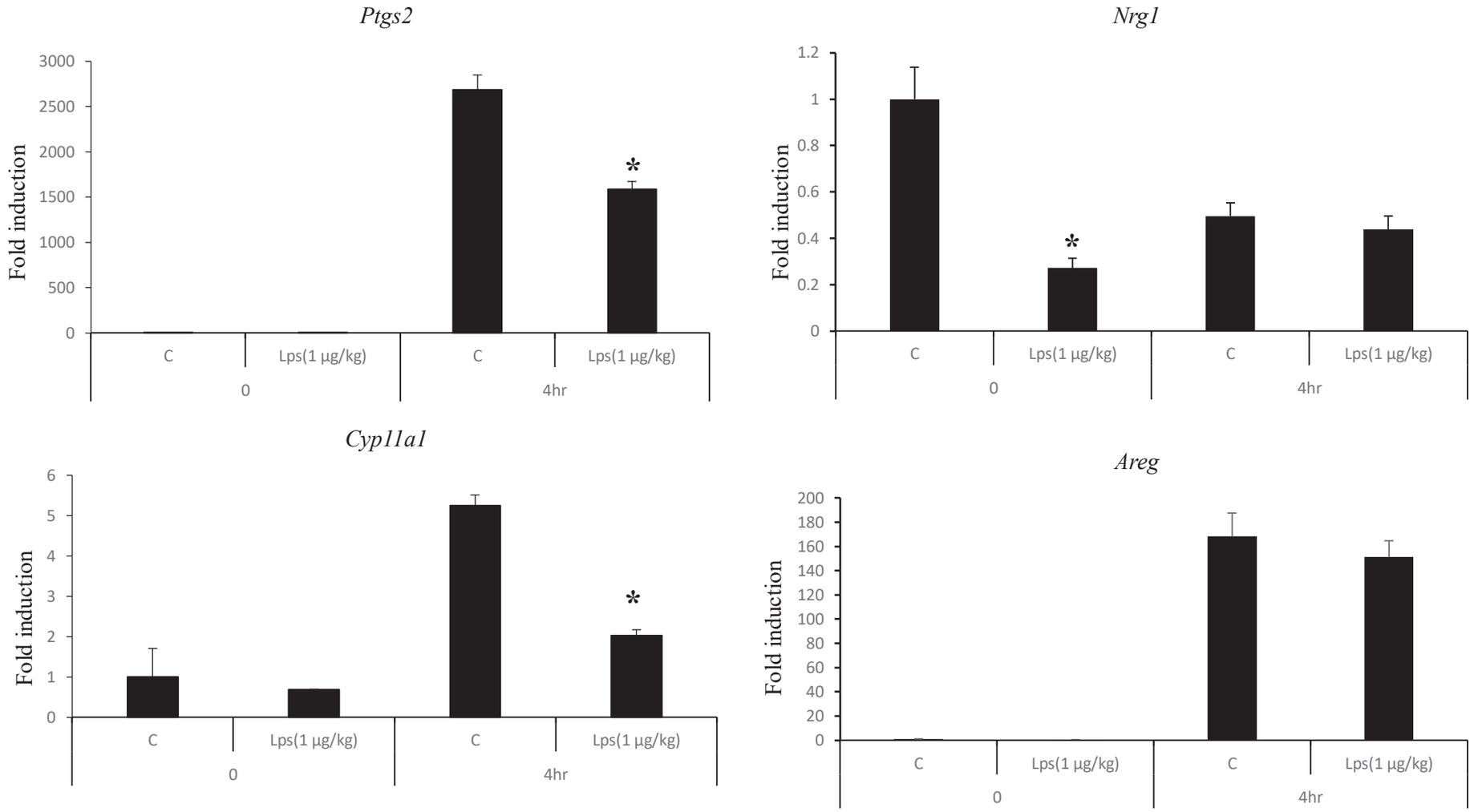

Figure 7B. The expression of *Ptgs2, Nrg1, Cyp11a1* and *Areg* in granulosa cells of mice at 23 days, and mice injected intraperitoneally with eCG with or without hCG and/or LPS. The value of granulosa cells from mice injected with eCG only (0) was set as 1, and the data are presented as fold induction. Expression levels of the mRNA was normalized to those of *L19*. Values are given as mean ± standard error of the mean (SEM) of three replicates. If a significant difference was observed at each time points compared with the immature group the comparison analysis was performed by a Student's *t*-test, $*P < 0.05$.

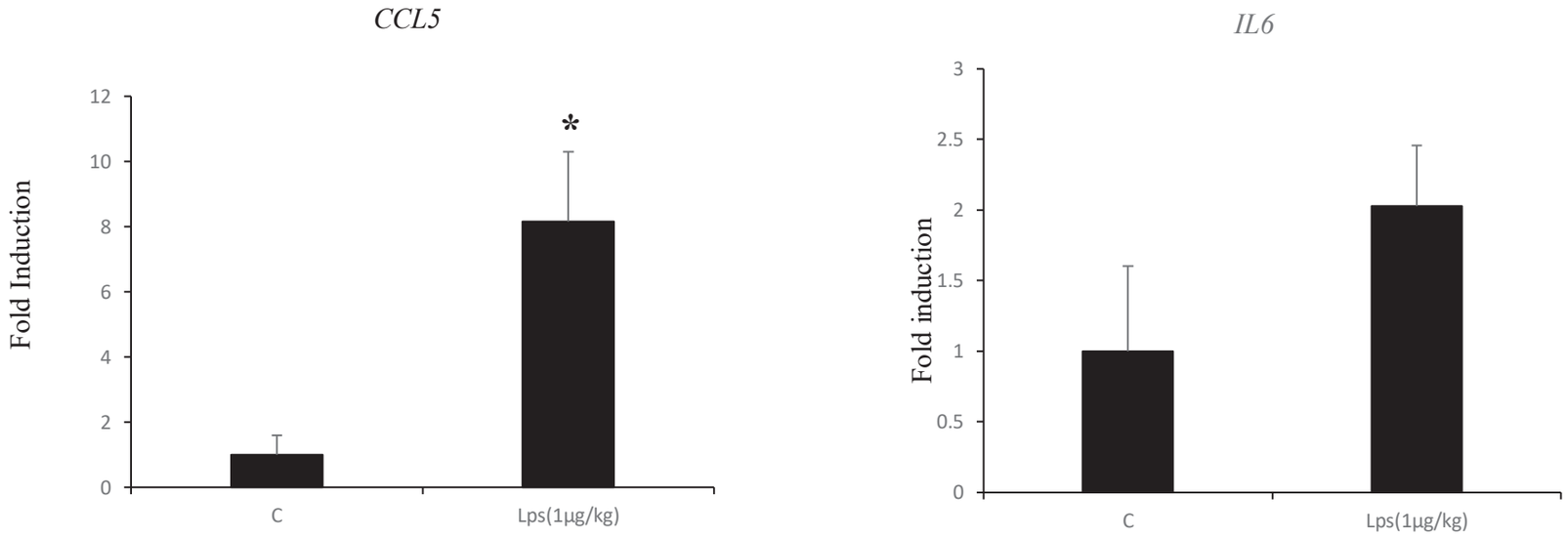

Figure 8. The expression of *chemokines and cytokines* in the granulosa cells of mice at 23 days, and mice injected intraperitoneally with eCG and/or LPS at 48 hr. The value of granulosa cells from mice injected with eCG only (0) was set as 1, and the data are presented as fold induction. Expression levels of the mRNA was normalized to those of *L19*. Values are given as mean ± standard error of the mean (SEM) of three replicates. If a significant difference was observed at each time points compared with the immature group the comparison analysis was performed by a Student's *t*-test, $*P < 0.05$.

(A)

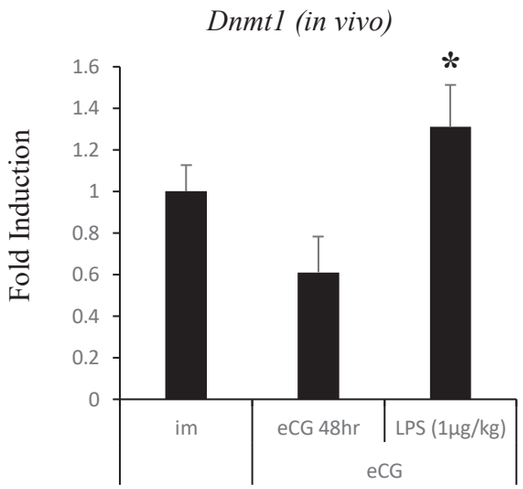

(B)

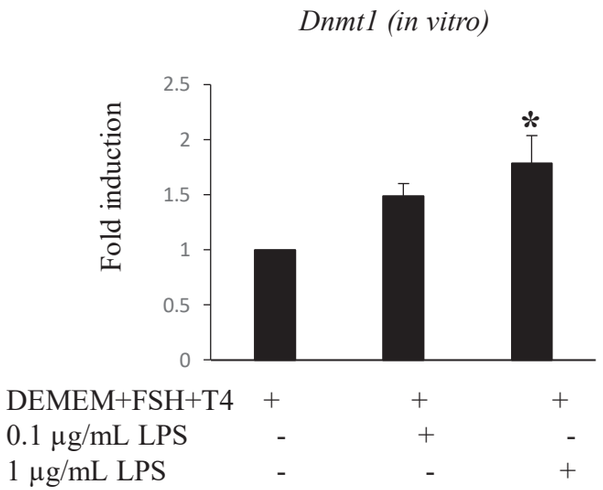

Figure 9. The expression of *Dnmt1* gene implicated in DNA methylation in **(A)** granulosa cells of immature mice and mice treated with eCG (control group) and co-administration of eCG and LPS (treatment group) for 48 hr (B) cultured granulosa cells after 6 hr of eCG injection in the presence of 1% FCS. The control group (FSH+T) and the treatment groups (FSH+T+ LPS (0.1 and 1 µg/ml). The value of granulosa cells from mice without eCG (immature) (A) and the value of granulosa cells cultured with FSH+T (B) were set as 1, and the data are presented as fold induction. Expression levels of genes were normalized to those of *L19*. Values are given as mean ± standard error of the mean (SEM) of three replicates ($P < 0.05$).

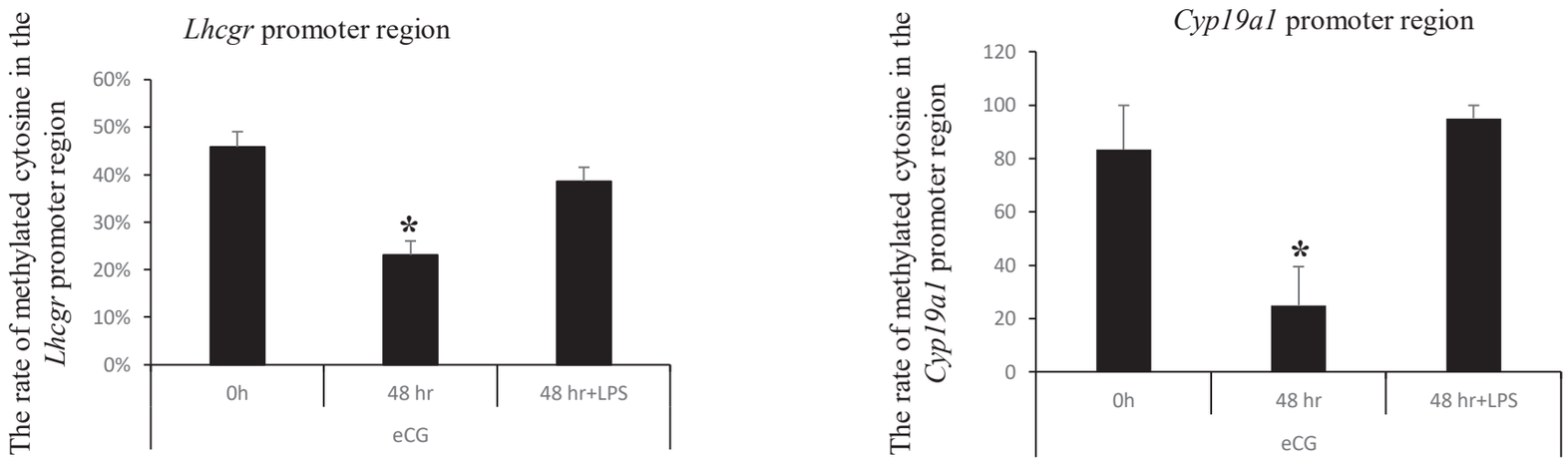

Figure 10. Kinetic changes of cytosine methylation in the *Lhcgr* promoter region in granulosa cells of mouse ovaries injected at eCG 0 hr and 48 hr time-point with and without LPS. Sequence analysis was carried out on over five colonies per treatment group. The studies were carried out in triplicate. Values are given a mean ± standard error of the mean (SEM). Significant changes were observed between eCG primed mice at 48 hr (*$P < 0.05$).

Experiment 2

Study on the roles of Toll-like receptor 7/8 in mouse ovary

Contents

	Topics	Page No
3.1	Introduction	46
3.2	Materials and Methods	47
3.3	Results	53
3.4	Discussion	57
	Abstract	60

3.1 Introduction

Infections of viral origin are notable causes of diseases of the reproductive system in both animal and human populations. The human papillomavirus (HPV), SARS-CoV-2, Hepatitis B&C virus, Porcine reproductive and respiratory syndrome (PRRS), and Mumps orthorubulavirus have been reported to cause abnormality in sex hormones and reduction in sperm quality, stillborns and overall low reproductive performances (Batiha *et al.,* 2020).

When entering a host cell membrane, the glycoprotein component on the virus surface binds with the virus-specific receptor, internalizes the virus (Hoffman et al., 2020; Wang et al., 2020) and allows the infection of the host cell. The fusion of the virus and target cell membrane, affords the virus the opportunity to release its genome and using the host cell organelles to replicate its RNA releasing new mature virion to other cells of interest (Boopathi et al., 2020). To ensure viral-cell fusion, host cell receptors which are specific to a particular organism are expressed in the cell infected by the virus (Griffiths *et al.,* 2020). Specific receptors that mediate the entry of SARS COV-2 and PRRS are angiotensin-converting enzyme 2 (ACE2) receptor and scavenger receptor CD163 respectively (Rahmandad *et al.,* 2020; Van Gorp et al., 2008).

Generally, viral particles of RNA virus can be recognized by both TLR7 and 8 in the infected cells. These receptors are localized on endoplasmic reticulum (ER) and trigger the activation of the signaling cascade and induce type 1 interferon (IFN) and pro-inflammatory cytokines (Jurk *et al.,* 2002; Pockros, 2002). TLR7 and TLR8 like other TLRs family, such as TLR2 and TLR4 contain Toll–interleukin 1 (IL-1) receptor (TIR) domain in their cytoplasmic region that associates with Myd88, an adapter molecule that plays a significant role in recruiting IL-1 receptor-associated kinase (IRAK) and tumor necrosis factor (TNF) receptor-associated factor 6 (TRAF6) to the TLRs (Akira *et al.,* 2001). Also, the Myd88 signaling pathway leads to the activation of NF-κB

transcription factors and c-Jun NH2 terminal kinase (Jnk) mitogen-activated protein kinases (MAPKs).

In chapter 2, TLR2 and TLR4 were expressed in ovarian granulosa cells and the activation suppressed *Lhcgr* expression. Since toll-like receptors 7/8 in the ovary can prompt an immune response in the presence of viral pathogens (Svingerud *et al.,* 2012; Welter, 2014), it was hypothesis that RNA viral infection in ovarian cells can directly damage reproductive performance. In addition, RNA viruses have been detected in reproductive organs or reproductive fluid and studies on TLR7/8 ligand (R848) have shown a strong suppression of oocyte fertilization (Pileri and Mateu, 2016; Batiha *et al.,* 2020; Umehara et al., 2020). Therefore, a time dependent expression of TLR7/8 and the mechanism by which TLR7/8 agonist (R848) affect the structure and function of the mouse ovary were examined.

3.2 Materials

The materials were described in Chapter 2 of Experiment 1. Additionally, Resiquimod (R848), horseradish peroxidase (HRP) labeled-progesterone and Standard solutions of progesterone was obtained from Sigma-Aldrich (St. Louis, MO). TLR7 antibody was obtained from Bioworld Technologies (Bloomington, MN).

3.2.1 Animals

Immature 3-week-old female C57BL/6 mice were obtained from Charles River Laboratories Japan (Yokohama, Japan). The animals were housed at the Experimental Animal Center, Hiroshima University, under a 12-hr light/12-hr dark schedule with food and water provided *ad libitum*. The animals were cared for in adherence to the National Institutes of Health *Guide for the Care and*

Use of Laboratory Animals, as approved by Hiroshima University's Animal Care and Use Committee (#C18-34).

3.2.3 Treatment of mice and collection of ovaries, cumulus cells, and granulosa cells

Twenty-three-day-old female mice were injected intraperitoneal (IP) with 4 IU of eCG to stimulate follicular growth. Thereafter, they were injected with 5 IU of hCG and/or R848 at 48 hr to stimulate ovulation and subsequent luteinization. Ovaries were collected at immature (0 hr), 24, 48 hr after eCG injection and 8 and 16 hr time points after hCG. Granulosa cells were collected at immature (0h), 24, 48 hr after eCG injection, and 8 and 16 hr time points after hCG.

3.2.4. Preparation of paraffin block and ovarian section staining

To prepare paraffin block for ovarian sectioning, the ovaries collected from three mice were fixed in 4% (w/v) paraformaldehyde (PFA) solution (Nacalai Chemical Co) overnight at 4°C, which was followed by dehydration and embedding in paraffin. The dehydration process involved a step-by-step incubation in 70, 80, 90, 95, and 100% ethanol solution for 2 hrs each, and the dehydrated ovaries were then incubated twice in xylene with each incubation period lasting for 2 hrs. Lastly, the ovaries were incubated for 2 hrs in paraffin liquid before they were appended in paraffin, and blocks were made by solidifying the liquid paraffin containing the ovaries. Thereafter, 5 μm thick sections were cut from the paraffin block by microtome and placed in water warmed up to 42ºC before they were mounted on slides and air-dried. Thereafter, the slide containing ovaries was deparaffinized by incubating in xylene twice for a period lasting 2 mins. The ovarian sections on the glass slide were then rehydrated using ethanol following a stepwise incubation in 100, 90, 80, and 70% ethanol for a period lasting 1 to 2 mins each. Thereafter, the sections were washed in distilled water and stained with eosin for 1 min followed by washing under running tap-water and

counterstaining with hematoxylin for 30 secs followed by washing under running tap water. The stained sections in the slides were then dehydrated by incubating step-wisely in 100, 90, 80, and 70% ethanol followed by incubating in xylene twice for a period lasting 2 mins. Thereafter, the ovarian sections are covered by a coverslip using the multi-mount DPX solution. The slides were airdried and visualized by an optical microscope using BZ-II application software (Keyence, Tokyo, Japan).

3.2.5 Immunofluorescence staining

For immunofluorescence staining of ovarian sections using anti-TLR7 antibody (Bioworld Technologies, Bloomington, MN), 5 μm thick ovarian sections were deparaffinized using xylene followed by washing in PBS. Thereafter, the ovarian sections mounted on glass slides were deparaffinized and rehydration of the tissue sections was carried out by washing twice in xylene for 2mins on both occasions followed by a chronological incubation in gradient concentration ethanol of (100, 95, 90, 80, and 70%) for 2 mins at each concentration then washed in PBS and boiled for 20 min in 10% citric acid (pH 6.0) for antigen activation. Thereafter, the sections were washed in PBS and nonspecific binding was blocked using 5% (w/v) BSA in MOM Immunodetection Kit or PBS (Vector Laboratories Inc, CA, USA). Furthermore, the ovarian sections were treated with TLR7 antibody with a dilution ratio of 1:200 as primary antibodies in 1% BSA (v/v) blocking solution at 4°C overnight. On the next day, the ovarian sections were washed in PBS containing 0.3% (v/v) Triton X-100, the staining was visualized with Cy3-conjugated goat anti-rabbit IgG (1:200) (Sigma) as a secondary antibody and counterstained using 4,6-diamidino-2-phenylindole (DAPI, Vector Laboratories Inc).

3.2.6 Extraction of protein and western blotting

For extraction of protein, the ovary was lysed using 1 mM EDTA solution containing complete phosphatase and protease inhibitors (Roche, Indianapolis, IN). Then sonication was done at >10 kHz ultrasonic frequencies, the lysates were centrifuged at 10000 × g for 10mins and the protein extracts were carefully collected as supernatant. The concentration of the protein collected was measured using the Bio-Rad protein assay kit (Bio-Rad Laboratories, Life Science Group, California, USA) based on the manufacturer's protocol at an absorbance of 750 nm in a spectrophotometer (Bio-Rad, California, USA). The concentration of the protein was determined by analyzing the standard curve which was standardized using Bio-Rad protein standard solution.

Western blotting was carried out as described by Kawai *et al.* (2016). Protein extracts were separated by 725 % SDS-PAGE run at 25 mA or 100 V using vertical electrophoresis for about 1hr 30mins. The protein in the gel was transferred to a nitrocellulose membrane (PVDF) (GE Bioscience, Newark, NJ, USA). 5% Bovine Serum Albumin dissolved in Tris-buffered saline (TBS) containing 0.05% (v/v) Tween-20 (TBST) to block non-specific binding sites. Thereafter, the membrane was incubated with primary antibodies (TLR7 or Beta-actin) diluted in 5% Bovine Serum Albumin at a concentration of 1:500 and 1:1000, v/v antibody respectively and stored overnight at 4ºC. After that, the membrane was washed in TBST for 2 hrs and the membrane was incubated in secondary antibody (HRP-conjugated anti-rabbit IgG antibody) (Cell Signaling Technology Catalogue number 7074) or HRP-conjugated anti-mouse IgG antibody for beta-actin at 1:5000, v/v antibody) (Cell Signaling Technology Catalogue number 70746). After repeated washing in TBST, enhanced chemiluminescence (ECL) detection was carried out using ECL kit (GE Bioscience) based on manufacturer's instructions, and the membrane was placed in (Bio-rad

ChemiDoc Touch Imaging System**)** to detect protein bands at appropriate exposure times. The detections were carried out in the three replicated samples and quantitative analysis was performed with the aid of ImageJ software (http://imageJ.nih.gov/ij/).

3.2.7 RNA extraction and RT-PCR

RNA extraction and RT-PCR analysis were carried out as described in Experiment 1 of Chapter 2.

3.2.8 Real-time PCR

The quantitative real-time PCR was carried out as described by Umehara et al. (2017). The procedure was explained in detail in Experiment 1 of Chapter 2. The primers used in this experiment were summarized in Table 3.

3.2.9 Collection of ovulated oocyte and in vitro fertilization

Twenty-five-day-old female mice were injected intraperitoneal (IP) with 4 IU of eCG to stimulate follicular growth. Thereafter, they were injected with 5 IU of hCG at 48 hr to stimulate ovulation and subsequent luteinization. Also, R848 was injected IP to mice at a dosage of 0.1μg/kg BW at 4h after hCG. At 16 hr after hCG injection, ovulated COCs were collected from the oviducts of three mice that were euthanized by needle puncture under the microscope and placed in 50μl of human tubal fluid (HTF) medium. One hr before the collection of the COCs, spermatozoa were collected from the cauda epididymis of an adult male mouse and placed in 500 μl of HTF medium to allow for capacitation in an incubator set at a temperature of 37^{o}C and atmospheric condition of 5% CO_2 at maximum humidity before the sperm was introduced to the HTF medium containing oocyte at a final concentration of 1,000 sperm cells per μl. Thereafter, the sperm-oocyte-containing

medium was incubated at 37ºC in an atmosphere of 5% CO_2 at maximum humidity for 8 hrs for fertilization to occur. After washing in HTF medium the oocytes are transferred to KSOM media and placed in the incubator at 37ºC and atmospheric condition of 5% CO_2 at maximum humidity for further development. The number of oocytes that were ovulated, matured, and fertilized was scored.

3.2.10 Collection and culture of granulosa cells

44 hrs after injecting immature mice (23 days old) with eCG, granulosa cells were collected from ovaries as described by Kawai *et al*. (2018). The cells were pre-cultured in DMEM/F12 medium containing 1% (v/v) FCS in 5% (v/v) FCS-coated 96-well plates for a preculture period of 4 hrs followed by a culture period of 4 hr at 37°C in an atmosphere of 5% CO_2 at maximum humidity. The medium described above was supplemented as follows: (a) no R848 (control), (b) 10 nM R848.

3.2.11 Measurement of progesterone

Media levels of progesterone was analyzed by a competitive enzyme immunoassay as described by Isobe and Nakao, (2003). 100 µl of secondary antibody in carbonate buffer (1:100 dilution) and incubate for 2 hrs at 20ºC and wash with PBS-T. Place 150 µl of assay buffer in each well and incubate for 30 mins at 20ºC for Blocking and wash twice with PBS-T. Also, 50 µl of sample which was extracted by ether method were placed in the ELISA plate. After the standard and samples have been placed in the ELISA plate, 50 µl of HRP-P4 (1:50,000) and 50 µl of P4-ab (1:100,000) was added to each well and incubated for 3 hrs at 20ºC. 150µl of TMB solution was added to each well and incubated for 30 mins at 20ºC and the reaction is stopped using 30 µl of 2N H_2SO_4. Thereafter the absorbance was read using the multilabel reader at 450 nm (2030

Multilabel Reader ARVO×4, Perking Elmer, Waltham, MA, USA). The level of progesterone was normalized through specific standard curve plotting against the standards.

3.2.12 Statistical analysis

All data from three replicates were analyzed by either Student's *t*-test or a one-way analysis of variance followed by a Tukey *post hoc* test (StatView; Abacus Concepts, Berkeley, CA). All values are presented as the mean ± SEM. Treatments were considered significantly different from one another at $P < 0.05$.

3.3 Results

3.3.1 Expression TLR7 and 8 in the mouse ovary

The presence of TLR7 and 8 were analyzed by immunofluorescence, RT-PCR, and western blotting. To detect the expression of TLR7 by immunofluorescence during the follicle development and ovulatory phase, ovaries were collected from eCG and hCG hormone-injected mice at immature, hCG (0 hr), 8 and 16 hr points. The result of Western blotting analysis of TLR7 is shown in Figure 11. The level of TLR7 in the ovary was highly expressed after hCG injection at 8h point (Figure 11B). These results indicate that viral pathogens have a dominant effect during the ovulatory phase. In Figure 12, the strong TLR7 positive signals were detected in mouse ovaries at hCG 0 and 8 hr compared to the immature and 16 hr groups. By RT-PCR, both *Tlr7* and *Tlr8* were expressed in spleen and were used as positive control (Figure 13B). More so, there was a time dependent difference in the expression of *Tlr7* and *Tlr8* in granulosa cells with 8h point having the highest level of expression (Figure 13B). However, *Tlr7* and *Tlr8* expression were detected in

cumulus cells but no time dependent difference in the level of expression was observed (Figure 13A).

3.3.2 Effect of Resiquimod (R848) on the expression of inflammation-associated genes

To assess the effect of R848 on the spleen organ, the expression of inflammation-associated genes was studied. Spleen was collected from mice injected eCG and hCG with or without R848 at 16 hr time point, and RNA was extracted from both the control and treatment group (0.1 μg/kg R848). It was observed that there was a significant increase in *Il6* and *Ifnγ* in the treatment group compared to the control group. However, a drastic reduction was observed in the *Ccl5* gene for the treatment group (Figure 14).

3.3.3 Effect of Resiquimod (R848) on ovarian morphology and maturation rate, number of ovulated oocytes, and fertilization rate

To evaluate the effect of TLR7- and TLR8-agonist (R848) on ovarian health, the ovaries were collected from mice injected eCG and hCG with or without R848 (injected 4 hr after hCG) at 16 hr time point and the ovarian morphology was checked after Hematoxylin-eosin staining. Luteinization of follicles can be observed in both the control and treatment groups (Figure 15A). The number of the ovulated oocyte in the control and R848 administered groups were similar (Figure 15B). However, the number of the matured ovulated oocytes in the R848 group decreased compared with the control group (Figure 15C). More so, the fertilization rate was significantly reduced in the treatment group compared to the control group (Figure 15D).

3.3.4 Effect of R848 on the induction of EGF-like factors, progesterone receptor (PGR)-dependent events, and other targets of the LH-LH receptor (LHR)-dependent pathway

To assess the effect of R848 on follicle development, ovulation, and steroid synthesis in granulosa cells, the expression of EGF-like factors, progesterone receptor (PGR)-dependent events, and genes associated with LH-LH receptor (LHR)-dependent pathway were studied. Granulosa cells were collected from mice injected with eCG and hCG with or without R848 and RNA was extracted from both the control and treatment groups (0.1 µg/kg R848). It was observed that the expression of *Ptgs2, Ereg, Areg, Pgr* were significantly increased at the 4hr point, whereas *Snap25, Star* were significantly increased at the 8 hr point and *Cyp11a1* was significantly increased at the 16 hr point (Figure 16A and B). However, *Nrg1* was not significantly different at all the time points. (Figure 16A). In the *in vitro* data, a dose-dependent increase was observed in the expression of *Cyp11a1, Star, HSD3β1, Adamts1, Snap25* and *Ptgs2* between the 1 and 10 nM R848 compared to the control group at 4hr point (Figure 16C).

3.3.5 Effect of R848 on the expression of Chemokine and cytokine

To evaluate the effect of Chemokine and cytokine in granulosa cells, the expression of *Il6* and *Ccl5* was studied**.** Granulosa cells were collected from mice injected with eCG and hCG with or without R848 and RNA was extracted from both the control and treatment groups (0.1 µg/kg R848). It was observed that the expression of *Il6* was significantly increased at the 4hr time point, whereas, in *Ccl5* no significant difference was observed (Figure 17).

3.3.6 R848 injection singularly induces luteinization of follicles

Since R848 can cause an over-secretion of epidermal growth factors and progesterone receptor target genes when coinjected with hCG (Figure 17), only R848 was injected at 48h point following eCG injection. Figure 18A shows that in the R848 treatment group ovulation of oocytes was observed but at an amount significantly lower than the control group. However, the possibility that ovulation was induced by endogenous GnRH cannot be ruled out. Therefore, GnRH-antagonist was injected every 24 hr to both groups. In this case, there was no ovulation of oocytes in the R848 and GnRH antagonist treatment groups unlike in the hCG and GnRH antagonist group where ovulation of oocytes were observed (Figure 18B). Hematoxylin-eosin staining of the ovary collected from the only R848 and GnRH antagonist group show that corpus luteum was formed and oocytes were trapped in the follicles (Fig 18C). Figure 18D confirms the supposition that R848 causes the luteinization of follicles, as the level of progesterone in the media increased in the group containing 10 nM R848.

3.3.7 Expression of ACE2 in mouse ovary

To detect SARS-CoV-2 receptors in the mouse ovary and granulosa cells respectively. cDNA was isolated from granulosa cells and mouse ovaries after 48hr of eCG injection. The receptors were detected by PCR amplification and visualized through gel electrophoresis. To evaluate the expression of the angiotensin-converting enzyme 2 (ACE2) receptor in granulosa cells, the granulosa cells were collected from mice injected eCG and hCG at 0, 4, 8, and 16 hr time points. ACE2 receptor expression was not significantly different at 0,4 and 16 hr time points except for 8h which had the highest level of expression (Figure 19).

3.4 Discussion

Infectious organisms of viral origin can circumvent the barriers of the cell membrane as they lack any unique foreign features that distinguish them from the host, however, TLRs have aptly developed strategies for recognizing viral particles (Gregory, 2007). More so, inherent in the host cells are receptors that bind with viral components and allow the uptake of viruses into host cells, where they replicate and cause degenerative outcomes (Zhou et al., 2018). In recent times, several viruses were reported to affect fertility and reproductive performance (Ljubojevic & Skerlev, 2014, Monavari *et al.,* 2013; Dondero *et al.* 1996; Xu *et al.,* 2006 and Ma *et al.,* 2020). Therefore, Experiment 2 was aimed to study the expression of TLR7/8 and specific endogenous receptors, and the mechanism by which R848 affect the structure and function of the mouse ovary.

The first phase of every viral infection is receptor recognition. In the result of the present experiment, Angiotensin-converting enzyme 2 (ACE2) receptors were detected in granulosa cells of mouse ovaries. This suggests that, since SARS-CoV-2 and its receptor ACE2 have a high binding affinity, there is a possibility that the virus transmissibility will be high in the host cell (Li *et al.,* 2005c). Likewise. the expression of TLR7 and 8 in the granulosa cell of mouse ovary shows that toll-like receptors are present on the cell membranes and can detect or recognize the presence of ssRNA viruses. More so, it also demonstrates its capacity to pose an inflammatory response to viral entry leading to the activation of NF-κB transcription factors through the MyD88 signaling pathway.

Although ACE2 receptor was expressed in the different time points, it was highest at 8h point after hCG injection. At the same time point, TLR7 expression was highest, demonstrating that viral pathogens have a dominant influence during the ovulatory phase.

Also, it was observed that TLR7/8 agonist (R848) induced an increase in the expression of immune genes such as IL6 and interferon-gamma which are related to the TLR7/8 signaling pathway. These results demonstrate that R848 induces immune responses in the spleen and ovaries of mice, suggesting that TLR7/8 signaling and the involvement of Myd88 may be responsible for the host immune response to viral invasion. Moreover, it has been reported that epidermal growth factors such as amphiregulin and epiregulin mediate the action of LH by activating the expression of EGF receptors which are present on granulosa cells and cumulus cells (Park *et al.,* 2004). It is the binding of the EGF domain with its receptor that activates the ERK1/2 pathway which results in COC expansion and oocyte maturation (Yamashita *et al.,* 2007). In this study, when R848 was co-injected with hCG, it led to the over-secretion of EGF-like factors and target genes involved in progesterone synthesis. Usually, the injection of hCG in superovulated mice prompts oocyte maturation, cumulus expansion, ovulation of matured oocyte, and luteinization while genes such as *Snap25, Pgr, Ereg, Areg*, *Ptgs2, Cyp11a1, Star,* and *Nrg1* were expressed at optimum levels. In the present study, the number of matured oocytes in the group co-injected with hCG and R848 led to the ovulation of mainly immature oocytes unlike the control group with a marked decrease in fertilization rate. This may be attributed to the impaired expression of the progesterone receptor gene and disruption of important mediators of LH actions in granulosa and cumulus cells leads to the impairs oocyte maturation (Breen *et al.,* 2013). Likewise, the induction of IL-6 has been reported to have a direct impact on the oocyte by causing negative effect on meiotic maturation (Bromfield and Sheldon, 2011).

In controlled ovarian stimulation, the injection of LH/hCG is required to initiate LH surge (Ron-El et al., 2000). LH stimulates cAMP formation and the activation of PKA signaling pathway

which initiates the expression of genes such as *Star* and progesterone receptor that facilitate the production of progesterone (Hickey et al., 1988). However, the action of R848 in inducing the terminal differentiation of GCs to luteal cells is not dependent on LH surge. Rather, R848 directly stimulate inflammatory reaction that leads to an increase in the induction of inflammation and luteinization associated genes. As in LH signaling, R848 induces *Snap25* via the progesterone pathway as well as other progesterone receptor target genes such as *Adamts1* and genes responsible for cholesterol synthesis leading to the production of progesterone necessary for luteinization. During this period there is a repression in *Cyp19a1* expression and a shift in granulosa cells steroidogenesis from the formation of estrogen to a progesterone producing cell by the increase in *Cyp11a1* and *Hsd3b1* (Fan et al., 2009).

Therefore, it was hypothesized that R848 can mimic the action of hCG hormone in prompting the ovulation and luteinization of follicles. To this end, only R848 was injected in superovulated mice to study its role in the ovulation process. It was observed that R848 afforded the development of follicles into Graafian follicles, induced luteinization and prompted a dose-dependent increase in progesterone secretion resulting in the formation of corpus luteum, however, it did not prompt ovulation of oocyte when co-injected with GnRH-antagonist to suppress endogenous LH increase (Diedrich *et al.,* 1994). It can be concluded that R848 suppresses oocyte maturation and fertilization and prompts the irreversible transition to a luteal cell phenotype without inducing ovulation by causing a decline in cell cycle activators and an increase in cell cycle inhibitors culminating in luteinization.

Abstract

Infections of viral origin are notable causes of diseases of the female reproductive system in both animal and human populations. The presence of receptors for these viruses allows for virus internalization in the host cell and an inflammatory response from the host to virus detected by toll-like receptors. This study highlights the presence of endogenous receptors for viruses of interest and mechanism by which TLR7/8 agonist, R848 cause low reproductive performance of the ovary. It was established that ACE2 and CD163 which are receptors for SARS-CoV-2 and PRRS are expressed in mouse ovaries. The expression of toll-like receptor 7 and ACE2 receptor was highest at 8h time point, indicating that viral pathogens greatly influence the ovulatory phase. It was also observed that R848 increased the production of cytokine and chemokines in the spleen and ovaries of mice. In mice treated with R848, the number of matured oocytes and fertilization rate was reduced. More so, R848 causes a dramatic increase in the expression of genes associated with progesterone receptor and epidermal growth factors. Although R848 did not induce ovulation, it retarded oocyte maturation and prompted the irreversible transition to a luteal cell phenotype by causing a decline in cell cycle activators and an increase in cell cycle inhibitors culminating in luteinization.

Table 2. PCR primers used for profiling the expression of SARS-COV2, TLRs and gene markers for GC's function

Genes	Forward Primer	Reverse Primer	Size (bp)
Adamts1	5'–CAGTACCAGACCAGACCTTGTGCAGACCTT-3'	5'–CACACCTCACTGCTTACTTACTGGTTTGA-3'	
HSD 3B1	5'–TGGGGAGAGAAGTCCATTCA-3'	5'–GGAGCCCCCATTCCTTACTA-3'	196
Nrg1	5' -AGAACCGGCTGTCTGCTTTT -3'	5' –TAGAGCTCCTCCGCTTCCAT -3'	373
StaR	5' -GCAGCAGGCAACCTGGTG -3'	5' -TGATTGTCTTCGGCAGCC -3'	249
CCL5	5'- ATATGGCTCGGACACCATA -3'	5'-GGGAAGGGTATACAGGGTCA-3'	242
Il6	5'- CCGGAGAGGAGACTTCACAG -3'	5'- GGAAATTGGGGTAGGAAGGA -3'	421
Cyp11a1	5'-GGGAGACATGGCCAAGATGG-3'	5'-CAGCCAAAGCCCAAGTACCG-3'	279
Areg	5' -TTACTTTGGCGAACGGTGTG -3'	5' -TGTGCAGTCCCGTTTTCTTG -3'	231
Ptgs2	5' -TGTACAAGCAGTGGCAAAGG -3'	5' -GCTGTGGATCTTGCACATTG -3'	431
Snap25	5'- GAGATGCAGAGGAGGGCTGAC -3'	5'- GCTGGCCACTACTCCATCCTG -3'	309
L19	5'-GGCATAGGGAAGAGGAAGG-3'	5'-GGATGTGCTCCATGAGGATGC-3'	199
Tlr7	5'-GGAAATTGCCCTCGATGTTA-3'	5'-CAAAAATTTGGCCTCCTCAA-3'	237
TLR8	5'- GAAGCATTTCGAGCATCTCC-3'	5'-GAAGACGATTTCGCCAAGAG-3'	188
ACE2	5'-CCTGTTCCGATCATCTGTTG-3'	5'-GACACATTTTGGGGTGAGGT-3'	153

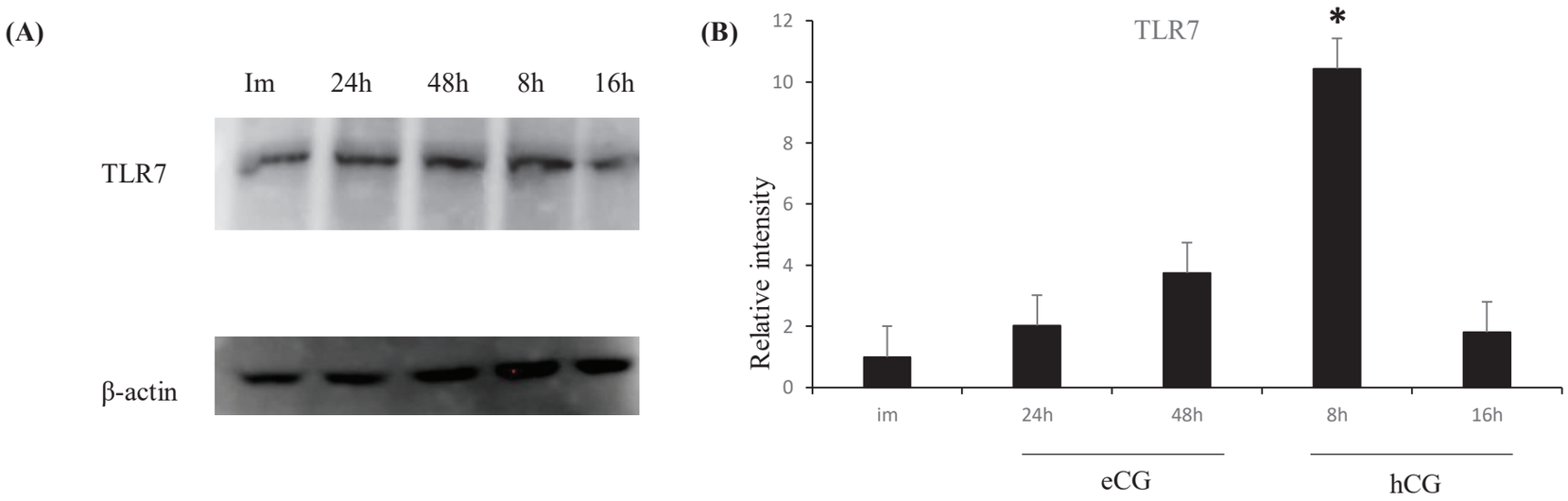

Figure 11. TLR7 expression in the ovary at immature, 24 and 48 hr after eCG injection and 8 and 16hr following hCG injection, (A) Expression of TLR7 through western blotting; where β-actin was used as control. (B) Quantitative expression of TLR7 over β-actin in the ovary. For reference, the data for the immature group was set as 1 and the data was expressed as relative intensity. Data are summarized as mean ± standard error of mean (SEM) of three mice for each group. Different alphabets (a, b and c) within the same graph differ significantly ($p < 0.05$).

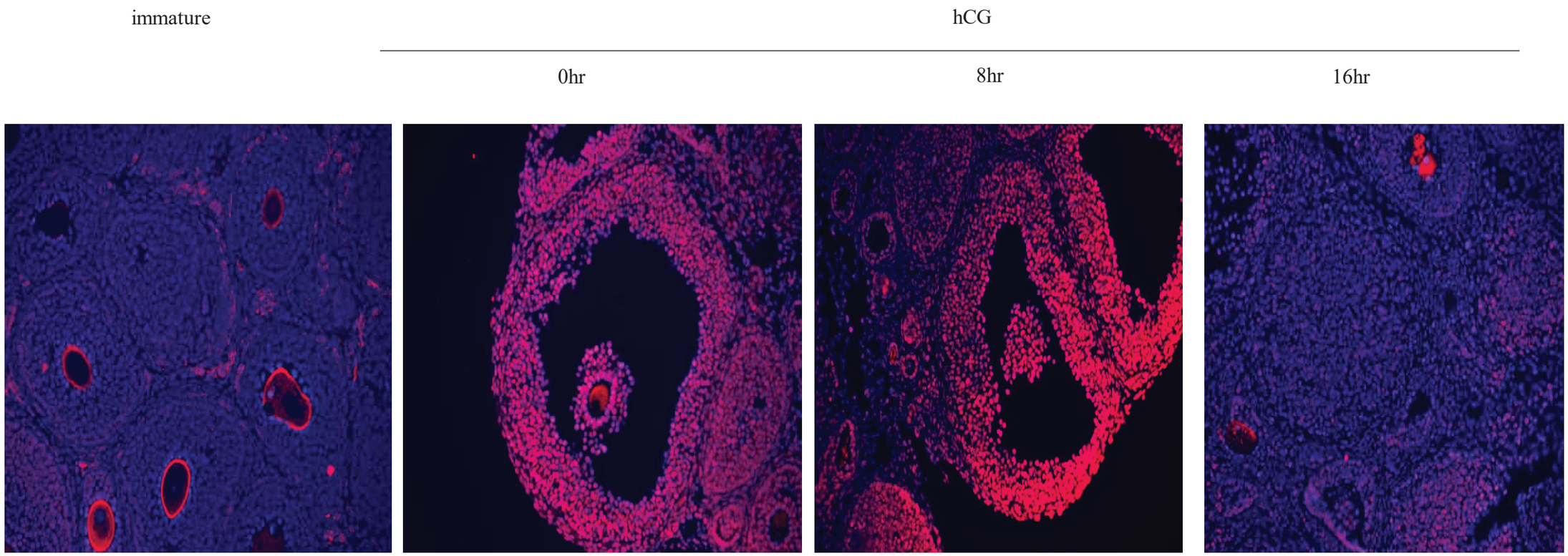

Figure 12. Immunofluorescence staining of the ovary during the immature, follicle development and ovulation phase. The ovaries were collected from immature mice and mice injected with or without eCG for 48 hr followed by hCG. The ovarian sections were stained with anti-TLR7 antibody and DAPI and digital images were captured using BZ-9000 microscope (Keyence).

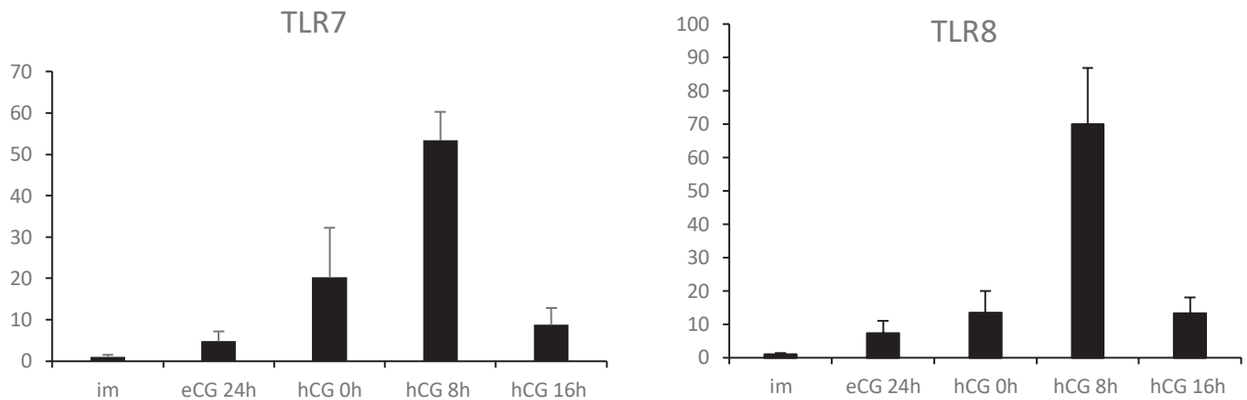

Figure 13. TLR7 and TLR8 expression in the ovary at immature, 24 and 48 hr after eCG injection and 8 and 16 hr following hCG injection, (A) Quantitative expression in the granulosa cells. For reference, the data for the immature group was set as 1 and the data was presented as fold induction. Data are summarized as mean ± standard error of mean (SEM) of three mice for each group. If a significant difference was observed at each time points compared with the immature group the comparison analysis was performed by a Student's *t*-test, $*P < 0.05$.

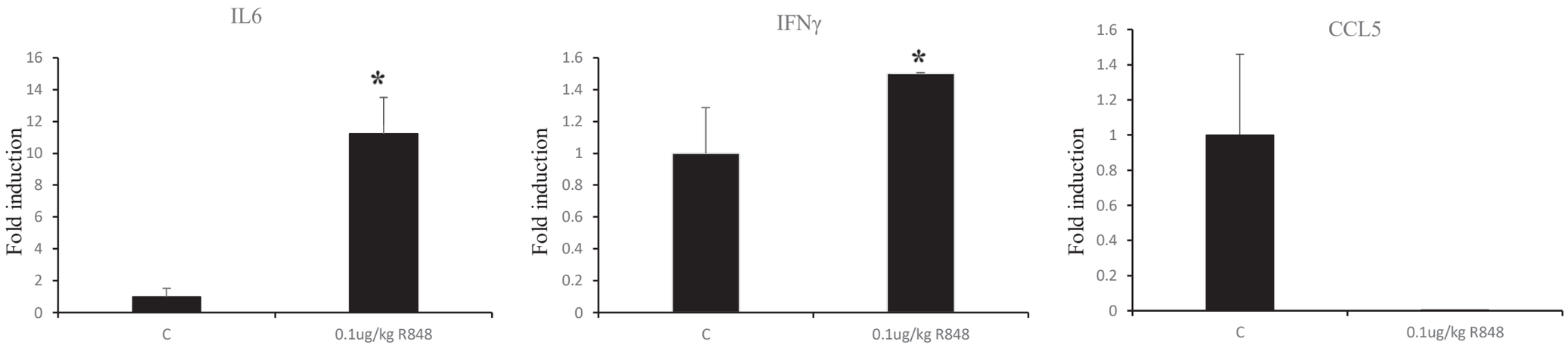

Figure 14. The expression of *IL6,* IFNγ and *CCL5* in the spleen of mice injected with Resiquimod (R848) at 16 hr after hCG. The value of mRNA from the control group was set as 1, and the data are presented as fold induction. Expression levels of the mRNAs was normalized to those of *L19*. Values are given as mean ± standard error of the mean (SEM) of three replicates. If a significant difference was observed between the control and treatment groups the comparison analysis was performed by a Student's *t*-test, $*P < 0.05$.

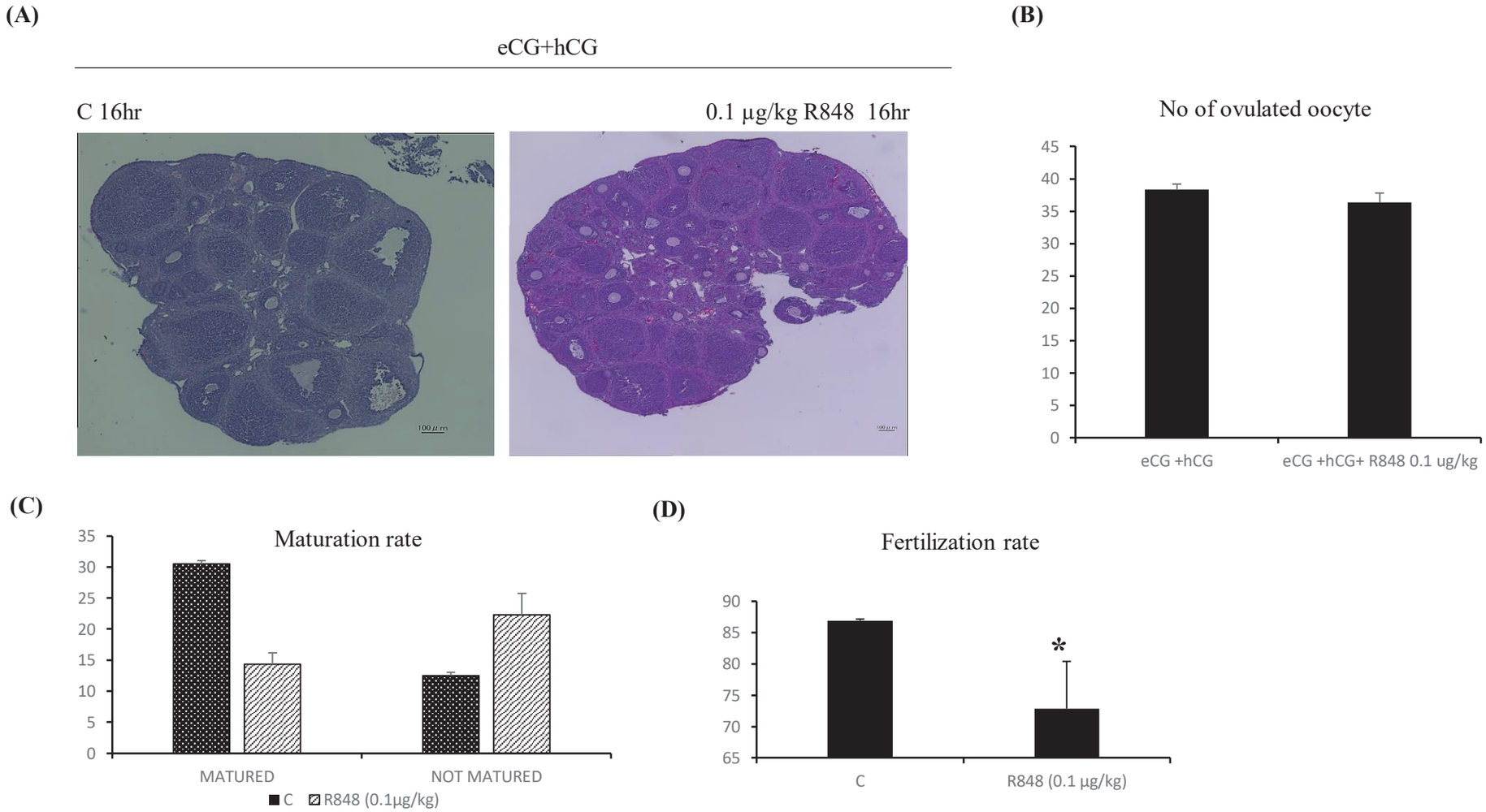

Figure 15. Ovarian morphology and follicular health (A) Hematoxylin-eosin staining of ovaries during the ovulation phase. The ovaries were collected from mice injected with eCG and/or Resiquimod (R848) followed by hCG injection and digital images were captured using BZ-9000 microscope (Keyence). (B) The average number of ovulated oocyte (0.1 µg/kg R848). (C) the maturation rate (D) fertilization rate. Data are summarized as mean ± standard error of mean (SEM) of three mice for each group. Different alphabets (a and b) within the same graph differ significantly ($p < 0.05$).

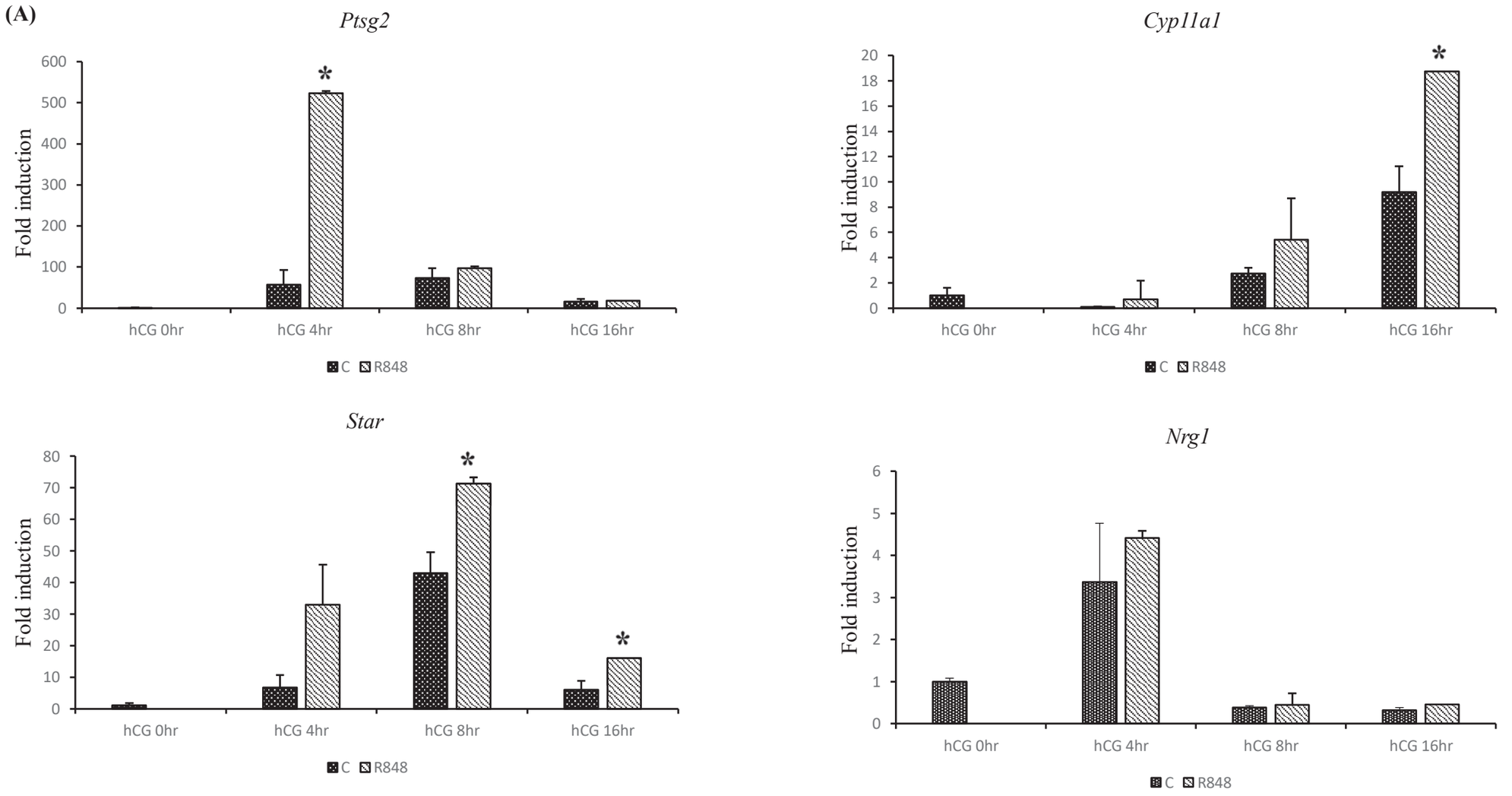

Figure 16A. The expression of *Ptgs2, Cyp11a1, Star* and *Nrg1* in granulosa cells of mice injected intraperitoneally with eCG with or without hCG and/or Resiquimod (R848). The value of granulosa cells from mice injected with eCG only (hCG 0 hr) was set as 1, and the data are presented as fold induction. Expression levels of the mRNA was normalized to those of *L19*. Values are given as mean ± standard error of the mean (SEM) of three replicates. If a significant difference was observed at each time points compared with the immature group the comparison analysis was performed by a Student's *t*-test, *$P < 0.05$.

(B)

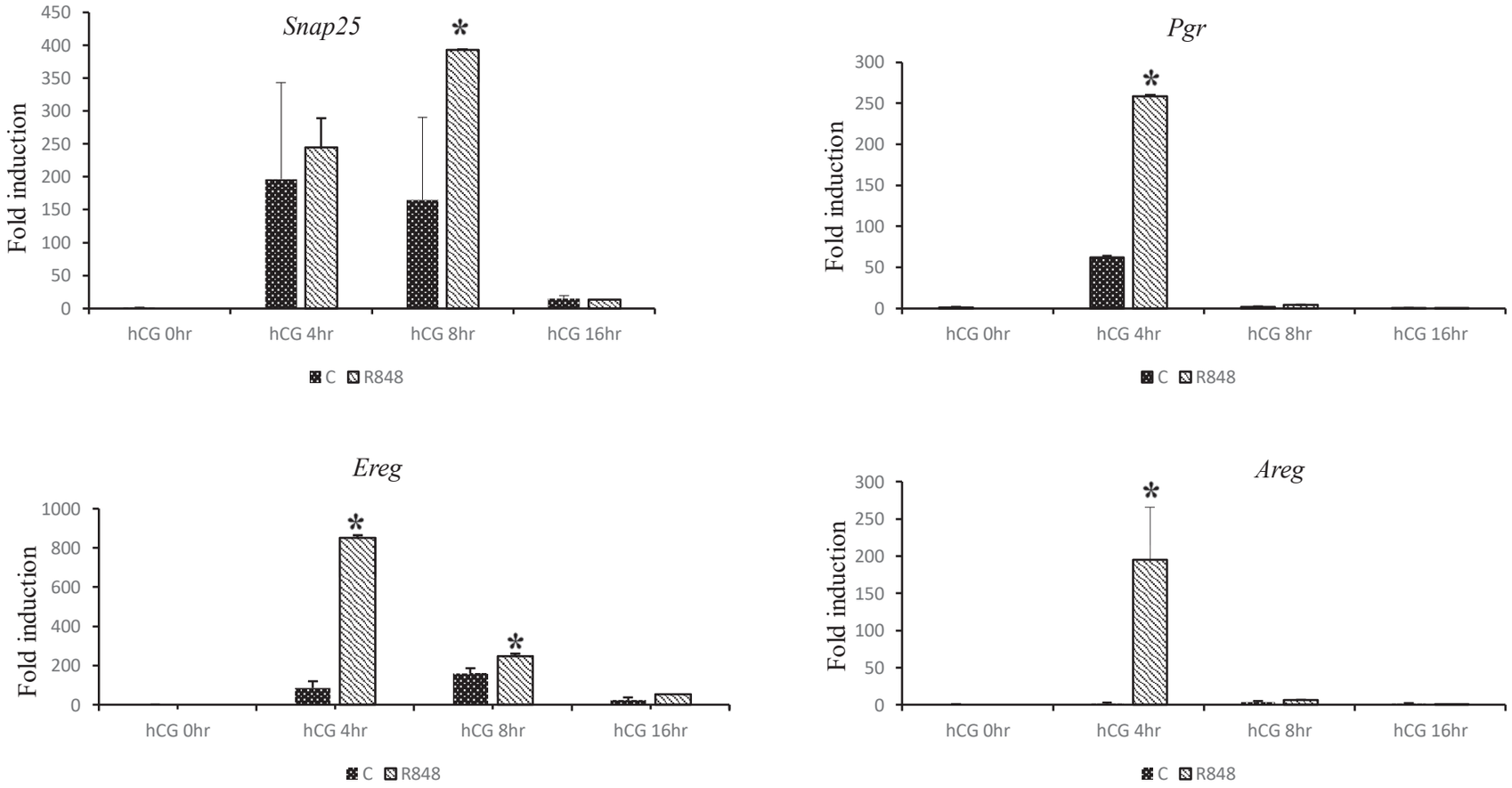

Figure 16B. The expression of *Snap25, Pgr, Ereg* and *Areg* in granulosa cells of mice injected intraperitoneally with eCG with or without hCG and/or R848. The value of granulosa cells from mice injected with eCG only (hCG 0 hr) was set as 1, and the data are presented as fold induction. Expression levels of the mRNA was normalized to those of *L19*. Values are given as mean ± standard error of the mean (SEM) of three replicates. If a significant difference was observed at each time points compared with the immature group the comparison analysis was performed by a Student's *t*-test, $*P < 0.05$.

(C)

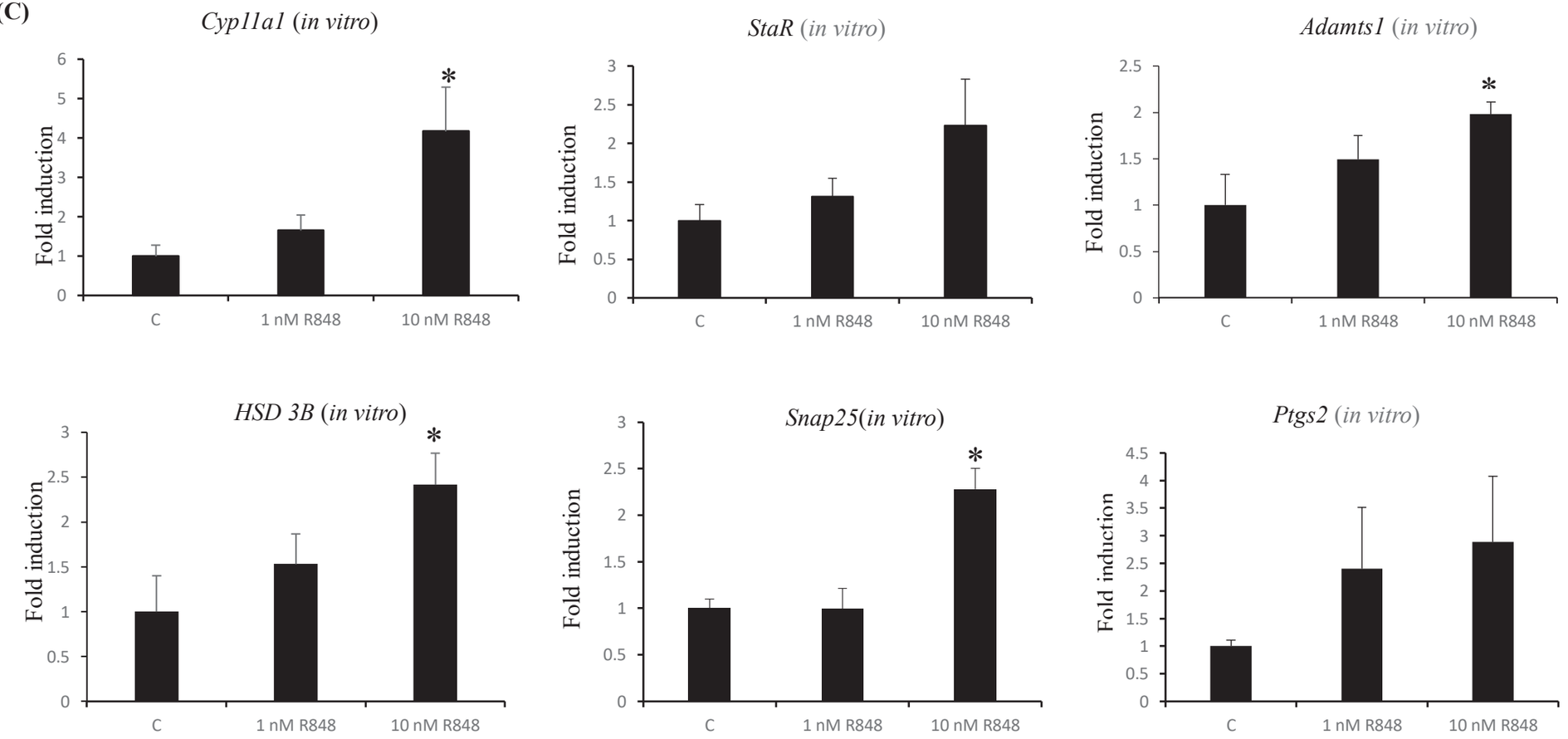

Figure 16C. Dose-dependent expression of *Snap25, Ptgs2, Cyp11a1, StaR, Adamts1* and *HSD3b1* in granulosa cells cultured *in vitro.* GC's were collected from 48 hr eCG primed mouse ovaries and cultured in 1% FCS supplemented DMEM/F12 media for 4h treated with or without R848 (1 and 10 nM). The value of granulosa cells cultured with DMEM/F12 were set as 1, and the data are presented as fold induction. Expression levels of genes were normalized to those of *L19*. Values are given as mean ± standard error of the mean (SEM) of three replicates. If a significant difference was observed at each time points compared with the DMEM/F12 or control group, the comparison analysis was performed by a Student's *t*-test, $*P < 0.05$.

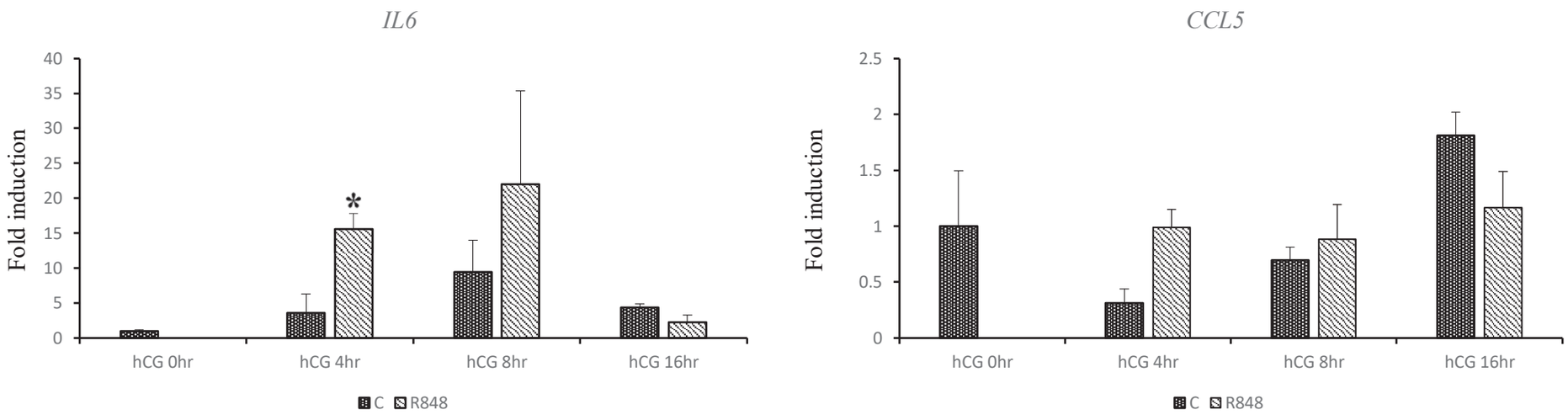

Figure 17. The expression of chemokines and cytokines in in granulosa cells of mice injected intraperitoneally with eCG with or without hCG and/or R848. The value of granulosa cells from mice injected with eCG only (hCG 0 hr) was set as 1, and the data are presented as fold induction. Expression levels of the mRNA was normalized to those of *L19*. Values are given as mean ± standard error of the mean (SEM) of three replicates. If a significant difference was observed at each time points compared with the immature group the comparison analysis was performed by a Student's *t*-test, $*P < 0.05$.

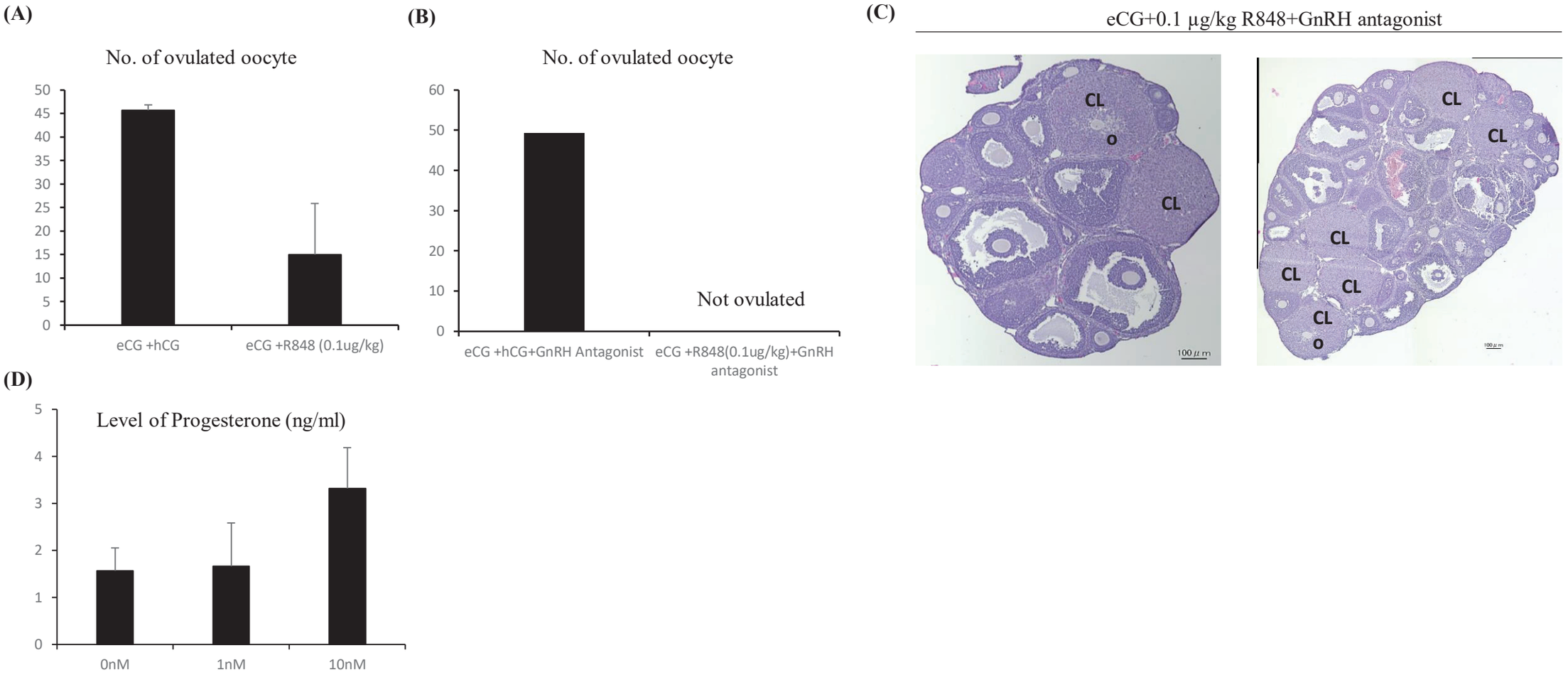

Figure 18. Ovarian morphology and follicular health (A) The average number of ovulated oocyte (eCG+hCG and eCG+R848 0.1 µg/kg). (B) The average number of ovulated oocyte (eCG+hCG+GnRH antagonist and eCG+R848 (0.1 µg/kg) +GnRH antagonist) (C) Hematoxylin-eosin staining of ovaries during the ovulation phase. (D) Levels of progesterone during lutea phase *in vitro*. The ovaries were collected from mice injected with eCG followed by R848 injection and digital images were captured using BZ-9000 microscope (Keyence) (CL- Corpus Luteum, O-oocyte). Progesterone level was measured using ELISA. Data are summarized as mean ± standard error of mean (SEM) of three mice for each group. If a significant difference was observed between the groups in each graph the comparison analysis was performed by a Student's *t*-test, $*P < 0.05$.

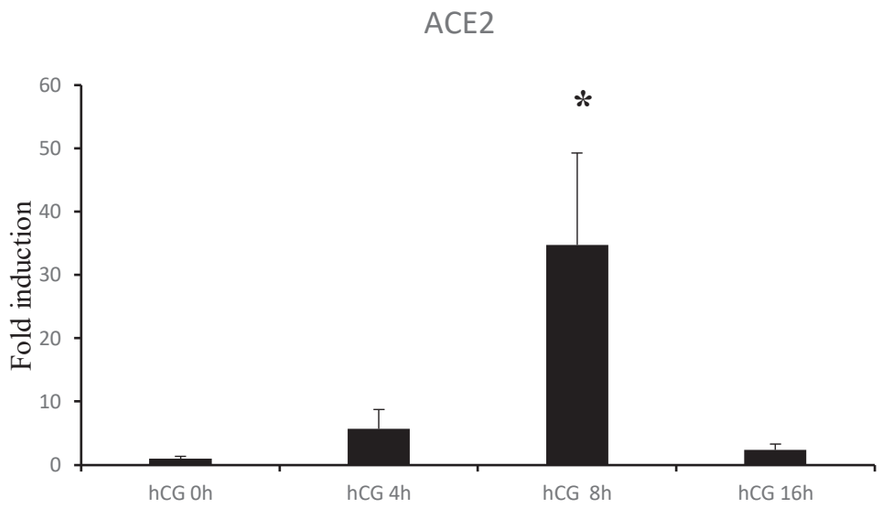

Figure 19. ACE2 receptor expression in the ovary at different time points

Chapter 4

General Discussion

(Pages 74 to 78)

Pelvic inflammatory disease describes the infection of the upper region of the female reproductive tract such as fallopian tubes, uterus, and ovaries by pathogenic microorganisms. When these microbes enter into the cervix, they alter the cervicovaginal environment and disrupt the normal microbiome of the vagina and in most cases, the overgrowing organism or the original pathogenic microbe ascend to the upper reproductive tracts (Westrom and Eschenbach, 1999). During this process they cause damage resulting from the inflammation of reproductive structures, leading to ovarian dysfunction and a sequelae to infertility (Brunham *et al.,* 2015).

A notable cause of abnormal reproductive outcomes is ovarian follicular cyst. In this condition, one or more mature follicles fail to ovulate following LH surge, however, the follicles further grow instead of undergoing atresia (Isobe, 2007). Follicular cysts have been associated with the inefficiencies of hypothalamus-pituitary function which regulate the occurrence and magnitude and timing of the LH surge (Garverick, 1997). However, the injection of hCG, a hormone with similar function as LH does not induce the ovulation process of all mature oocyte (Garverick, 1997), suggesting that not only the dysfunction of pituitary gland but the abnormal response ability to LH in granulosa cells of large antral follicles are factors required to induce follicular cyst. It has been known that infection with many kinds of bacteria including *Chlamydia trachomatis* and *N.* gono*rrhea* causes reproductive dysfunctioning (Scholes *et al.,* 2012). The presence or infusion of LPS have also been reported to cause ovulation anomalies and ovarian follicular cyst (Peter et al., 1989). In the present study, it was demonstrated that LPS interfered with the ovulation of matured Graafian follicle causing follicular cyst, indicating that bacterial infection is one of the factors to induce follicular cyst. Because LPS affects the whole body via the vascular system, follicular cyst results not only from the direct infection of the reproductive tract but from infections affecting

other organs. Therefore, infection of bacteria origin needs to be examined in the diagnosis of ovulation disorder not only in human infertility care but also in livestock animals.

The present study is the first study to understand the mechanisms by which LPS induces follicular cyst at the molecular level. The study shows that the induction of follicular cyst is associated with abnormal epigenetic regulation in granulosa cells of preovulatory follicles. DNA methylation, 5-methylcytosine content of DNA, is an epigenetic mechanism that plays a fundamental role in the regulation of gene expression, especially during differentiation (Reik, 2007). Methylation can inhibit gene expression by inhibiting transcription factor binding to promoter region of genes. Therefore, the demethylation in the promoter region is involved in the transcription of the genes. In granulosa cells, LPS did not change the morphology, proliferation, and cell survivability; however, FSH-induced cell differentiation to express *Lhcgr* was selectively suppressed by LPS. The DNA methylation status in *Lhcgr* promoter region was maintained at higher level in granulosa cells even when eCG was injected with LPS. In other reports, the role of LPS in inhibiting osteoblastic differentiation of fibroblasts derived from human periodontal ligament by inducing DNA hypermethylation of RUNX2 have also been established (Uehara, et al., 2014). However, the present study for the first time demonstrates that LPS downregulated the expression level of DNMT1, an enzyme that copy DNA methylation pattern from parent DNA strand to daughter strand in FSH-stimulated granulosa cells. Thus, the LPS-induced abnormal epigenetic regulation may be observed in not only *Lhcgr* promoter region but also other genes, which impacts on large scale gene expression patterns not only in granulosa cells, but in other cell types infected with bacteria or stimulated by LPS.

Bacterial infections are recognized by TLR2 and TLR4 while viral infections are detected by other TLRs family. However, in most cases the TLRs family adhere to the same downstream pathway.

Additionally, infections resulting in ovarian dysfunction, poor pregnancy outcomes, and neonatal health are not only caused by pathogenic microbes of bacteria origin but also by viruses (Coyne and Lazear, 2016; Racicot and Mor, 2017). In recent times, the role of viruses in the disruption of male and female reproductive health has become the front burner ((Racicot and Mor, 2017). Many families of viruses have a strong tropism for the male reproductive system, especially the testis, and about thirty different species can affect semen quality (Osburn, 1994; Salam and Horby, 2017). In addition, some of these viruses can impair fertility and can be sexually transmitted (Gimenes, 2014). Regarding the male reproductive health, viral infections reach the testis through the bloodstream, causing damage by direct harmful effects on target organs or indirectly through pro-inflammatory cytokines (Guazzone, 2009). The contamination of male reproductive organs and spermatozoa leads to male sub-fertility or infertility resulting from signaling deficiencies in testicular cells that may be aggravated by pro-inflammatory mediators. In the female, these inflammatory genes play a role in steroidogenesis and interfere with LH action during the process of oocyte maturation, ovulation and luteinization (Bornstein, 2004). However, there is no report to show that the viral infections are found in the reproductive organs and that viral infections directly causes damages to the reproductive performances of both male and female. The present study is the first to show that TLR7 and TLR8, receptors for RNA virus were expressed in granulosa cells after LH surge and the stimulation induced ovulation process in part; however, TLR7 and TLR8 pathway strongly suppressed oocyte maturation.

More so, it is known that LH surge is required for ovulation and luteinization of follicles. However, there are other processes such as gonadotropin-induced ovulation that mimic the action of LH. This is due to a specific degree of homology between both hormones (Ma et al., 2015). In experiment 2, R848, a ligand for TLR7 and TLR8 prompts the expression of inflammatory genes,

epidermal growth factors and progesterone receptor target genes that are involved in cumulus expansion, ovulation and luteinization. However, its inability to induce oocyte maturation and completion of the ovulation process leading to the release of oocyte may be attributed to the timing of R848-induced progesterone synthesis which represses *Cyp19a1* expression and causes a shift in granulosa cell orientation. Thus, it is one possibility that RNA virus infection would induce luteinization process before LH surge with follicle rapture, but without oocyte maturation. The occurrence of premature luteinization of granulosa cells before LH surge causes poor ovarian response to controlled ovarian hyperstimulation and an impaired receptivity of the endometrium leading to reduced pregnancy rates (Fanchin et al., 1993; 1997). In conditions where *Cyp11a1* are upregulated with an abrupt repression in *Cyp19a1* there will be a decline in natural and IVF pregnancy outcome because of the impairment of the normal growth and maturation of the oocyte which is a direct reflection of the physiological status of granulosa cells. Overall, the findings of this study will be useful in understanding that women and livestock exposed to bacterial and viral infections not only stand the risk of developing follicular cyst conditions but also highly susceptible to premature luteinization. The different phenotypes between virus infection and bacterial infection are possibly explained by the different timing of TLRs expression in granulosa cells. The downstream pathway of the TLRs involved in detecting bacterial and viral pathogens are mostly common, suggesting that epigenetic abnormality in granulosa cells of preovulatory and periovulatory follicles in pathogen-infected female would induce different transcription pattern. The abnormal transcriptome might suppress successful ovulation process. The new information reinforces the need to implement livestock management practices that prevent exposure of animals to microbes. Furthermore, this understanding regarding luteinization of follicles resulting from

viral infection is believed to be useful in the diagnosis of reproductive diseases and improving pregnancy outcomes in both livestock and human.

In conclusion, this study suggests that LPS induces the methylation of the CpG island in the *Cyp19a1* and *Lhcgr* promoter regions. More so, pathogenic microbes of viral origin have a similar effect as their bacteria counterpart and can cause infertility. TLR7/8 agonist R848 mimics LH action by induces luteinization of follicles resulting in the formation of corpus luteum. Attention has been drawn to care of the female gender during the ovulatory phase in a bid to facilitate conception due to the susceptibility to viral infections at that time point. Over the years, many bacteria and viruses have consistently caused economic losses to farmers and many women have tried conceiving but to no avail. However, with the presence of host-cell receptors that allow the entry of viruses, there is the possibility of the use of the mouse model approach to study these microbes and the impact of inflammatory responses posed by immune cells on reproductive functioning. Furthermore, given that bacterial and viral pathogens can cause failure of the female reproductive organ, research focused on improving the efficacy and safety of ART and natural pregnancy outcomes should explore the impact of ssRNA viruses.

Chapter 5

Summary

(Pages 80 to 83)

Summary

Infertility is a major cause for concern especially in parts of the world that place a high value on childbearing. Besides, sub-fertility or infertility often causes heavy losses to breeders and dairy farmers as they require the animals to get pregnant for milk production and herd expansion. Infectious diseases of bacteria or viral origin induces inflammatory responses from the host, however, the mechanism by which they impact negatively on reproductive health is unknown. These studies aim to determine the deleterious effect of infectious diseases on ovarian functioning at a cellular and molecular level using the mouse model approach.

1. **Study on the effect of LPS on overall ovarian health and Epigenetic dynamics of the *Lhcgr* and *Cyp19a1* gene promoter region**

Lipopolysaccharide (LPS) is an endotoxin and a component of the cell membrane of gram-negative bacteria, and it can pass through the protective physical barriers and tight junctions of the basement membrane. Apart from having been isolated from the genital tract of animals suffering from uterine damage and ovarian dysfunction, LPS action affects the epigenetic signature of genes regulating and inducing a cycle of methylation in the DNA around the promoter region. In Experiment 1, it was hypothesized that bacterial infection changes the DNA methylation status of the *Lhcgr* and *Cyp19a1* promoter regions. To clear this hypothesis, granulosa cells and ovaries were collected from immature mice treated with eCG or with eCG and LPS injection intraperitoneal. More so, granulosa cells were cultured in DMEM/F12 with or without supplement and the addition of LPS (0.1 and 1 µg/ml LPS). Likewise, the expression of DNMT1 in granulosa cells of mice treated with LPS was investigated (*in vivo* and *in vitro*) and the epigenetic dynamics of LPS on DNA methylation was studied. In the results, Normal large antral follicles were observed in ovaries obtained from eCG and LPS coinjected mice, and the morphology of the ovaries was similar to

that observed in the control group (eCG-injected mice). These antral follicles were not deemed atretic because few TUNEL-positive cells were observed. However, the granulosa cells of large antral follicles did not acquire the ability to respond to hCG stimulation. Also. the number of ovulated oocytes was significantly lower in LPS-injected mice after superovulation compared to mice that were not exposed to LPS. It was also observed that the low reactivity was caused by the limited expression of the *LHCGR* gene, which encodes the LH receptor in granulosa cells as well as an LPS-induced increase in the level of Dnmt1 expression both *in vivo* and *in vitro*. The methylation rate of the *LHCGR* promoter region was significantly higher in granulosa cells obtained from the LPS treatment group compared with the control group. Together, for the first time these findings demonstrated that the decrease in the expression of *Lhcgr* and Cyp19a1 as well as the induction of chemokines is due to bacterial infection/LPS which leads to ovarian follicular cysts in humans and animals. More so, the decrease in the induction of *Lhcgr* and *Cyp19a1* due to LPS exposure is a result of the epigenetic regulatory action of LPS.

2. Study on the roles of Toll-like receptor 7/8 in mouse ovary

Viral particles and TLR7/8 agonists (Resiquimod) are detected by the host through Pattern Recognition Receptors (PPRs) and they induce type 1 interferon (IFN) and pro-inflammatory cytokines. The presence of receptors for specific pathogen allows for entry and transfer of elements across the host plasma membrane. In experiment 2, it was hypothesized that TLR7/8 are expressed in mouse ovaries and TLR7/8 agonist (R848) causes a negative impact on the structure and functioning of the ovary. To clear this hypothesis, the mechanism by which TLR7/8 causes ovarian dysfunction was studied by injecting TLR7/8 agonist (R848) to eCG-superovulated immature mice and culturing granulosa cells in DMEM/F12 medium with and without R848 (1 and 10nM dosage). It was observed that R848 increased the production of cytokine and chemokines in the spleen of

mice. Also, in mice treated with R848, the number of matured oocytes and fertilization rate was reduced. More so, R848 causes a dramatic increase in genes associated with progesterone receptor and epidermal growth factors such as *Areg, Ereg*, *Cyp11a1*, *Star*, *PgR*, *Snap25* in both *in vivo* and *in vivo* studies. For the first time, R848 was reported to prompt the luteinization of follicles. It was also established that *ACE2* and *CD163* which are receptors for SARS-CoV-2 and PRRS are expressed in mouse ovaries. Although TLR7/8 and ACE2 receptor was expressed in the different time points, it was highest at 8h point which demonstrates that the influence of viruses is highest during the ovulatory phase. In addition, for the first time this study shows that the injection of only R848 to superovulated mice caused the luteinization of follicles and a dose-dependent increase in progesterone synthesis when granulosa cells were cultured *in vitro*. These suggests that R848 prompts the irreversible transition to a luteal cell phenotype without inducing ovulation by causing a decline in cell cycle activators and an increase in cell cycle inhibitors culminating in luteinization. Also, the presence of receptors for SARS-CoV-2 virus and PRRS in mouse also provides novel opportunities for understanding the mechanism of action of these viruses.

3. Conclusion

In conclusion, the present study demonstrated that the decrease in the induction of *Lhcgr* and *Cyp19a1* due to LPS is a result of the epigenetic regulatory action of LPS. The immunological response of the host to LPS or bacterial infection prevents the preovulatory follicles from responding to the LH surge, which is required for ovulation. Moreover, ovarian dysfunction and polycystic ovaries, as well as other PIDs that are characterized by bacterial infection in humans and animals, are closely connected to the methylation of the *Lhcgr* promoter region. In addition, R848 suppresses oocyte maturation and fertilization and prompts the irreversible transition to a

luteal cell phenotype without inducing ovulation by causing a decline in cell cycle activators and an increase in cell cycle inhibitors culminating in luteinization. This study provides a novel contribution to the field of mammalian ovarian biology. It is also essential to understanding the etiology of reproductive diseases and the mechanism of action of infectious diseases in a bid to improve the efficacy and safety of ART in animal management systems and in developing therapeutic treatment.

REFERENCES

Aaltonen J, Laitinen MP, Vuojolainen K, Jaatinen R,Horelli-Kuitunen N, Seppa L, Louhio H, Tuuri T, Sjoberg J, Butzon R, Hovatta O., Dale L. & Ritvos O. (1999). Human growth differentiation factor 9 (GDF-9) and its novel homolog GDF-9B are expressed inoocytes during early folliculogenesis. *Journal Clinical Endocrinology and Metabolism*. 84:2744-2750

Akashi S, Saitoh S, Wakabayashi Y, Kikuchi T, Takamura N, Nagai Y, Kusumoto Y, Fukase K, Kusumoto S, Adachi Y, Kosugi A, Miyake K. (2003). Lipopolysaccharide interaction with cell surface Toll-like receptor 4-MD-2: higher affinity than that with MD-2 or CD14. *Journal of Experimental Medicine.* 198(7):1035-42.

Akira S, Takeda K, Kaisho T. (2001). Toll-like receptors: critical proteins linking innate and acquired immunity. *Nature Immunology*. 2:675–80.

Akira S, Uematsu S, Takeuchi O. (2006). Pathogen recognition and innate immunity. *Cell.* 124: 783–801.

Akira, S., & Takeda, K. (2004). Toll-like receptor signaling. In *Nature Reviews Immunology*. 4: 499–511.

Akira, S., Hemmi, H., (2003). Recognition of pathogen-associated molecular patterns by TLR family. *Immunology Letters.* 85: 85–95.

Akira, S., Takeda, K. & Kaisho, T. (2001). Toll-like receptors: critical proteins linking innate and acquired immunity. *Nature Immunology.* 2: 675–680

Akira, S., Uematsu, S., & Takeuchi, O. (2006). Pathogen recognition and innate immunity. In *Cell,* 124, 783–801.

Akira, S.,Takeda, K. & Kaisho, (2001). Toll-like receptors: critical proteins linking innate and acquired immunity. *Nature Immunology.* 2: 675–680

Bakaysa, S.L., J.A. Potter, M. Hoang, C.S. Han, S. Guller, E.R. Norwitz, V.M. Abrahams, (2014). Single- and double-stranded viral RNA generate distinct cytokine and antiviral responses in human fetal membranes, *Molecular Human Reproduction*, 20: 701–708.

Balla, A., Danilovich, N., Yang, Y., and Sarian, M. R. (2003). Dynamics of ovarian development in the FORKO immature mouse: Structural and functional implications for ovarian reserve. *Biology of Reproduction*. 69:1281-1293.

Barros, C.M., Ereno RL, Simoes RA, Fernandes P, Buratini J, Nogueira MF. (2010). Use of knowledge regarding LH receptors to improve super-stimulatory treatments in cattle. *Reproduction Fertility and Development*. 22:132-137.

Batiha, O, Al-Deeb, T, Al-zoubi, E, Alsharu, E. (2020). Impact of COVID-19 and other viruses on reproductive health. *Andrologia*. 52(9):e13791.

Baumgarten, S. C., & Stocco, C. (2018). Granulosa Cells. In M. K. Skinner (Ed.), *Encyclopedia of Reproduction.* 2: 8–13.

Bernard D, Woodruff TK (2001). Glycoprotein hormones: transgenic mice as tools to study regulation and function. Totowa, NJ:Humana Press.

Blank S.K., C.R. McCartney, J.C. Marshall (2006). The origins and sequelae of abnormal neuroendocrine function in polycystic ovary syndrome. *Human Reproduction Update.* 12(4):351-361

Bornstein SR, Rutkowski H, Vrezas I. (2004). Cytokines and steroidogenesis. Molecular Cell *Endocrinology*. 215(1-2):135-41

Breen SM, Andric N, Ping T, Xie F, Offermans S, Gossen JA, Ascoli M. (2013). Ovulation involves the luteinization hormone-dependent activation of G(q/11) in granulosa cells. *Molecular Endocrinology*. 27:1483–1491.

Bromfield, J.J., Sheldon, I.M., (2011). Lipopolysaccharide initiates inflammation in bovine granulosa cells via the TLR4 pathway and perturbs oocyte meiotic progression in vitro. *Endocrinology* 152: 5029–5040.

Brunham RC, Gottlieb SL, Paavonen J. (2015). Pelvic inflammatory disease. *New England Journal of Medicine*. 372:2039-48.

Brunham RC. (2015). A Chlamydia vaccine on the horizon. Science. *Immunology.* 348:1322-3

Buccione R,Vanderhyden BC, Caron PJ, Eppig JJ (1990). FSH-induced expansion of the mouse cumulus oophorus in vitro is dependent upon a specific factor (s) secreted by the oocyte. *Developmental Biology.* 138:16–25.

Byskov AG (1986). Differentiation of mammalian embryonic gonad. *Physiological Reviews* 66, 71–117.

Carabatsos MJ, Elvin J, Matzuk MM, Albertini DF (1998). Characterization of oocyte and follicle development in growth differentiation factor-9-deficient mice. *Developmental Biology.* 204:373–384.

Cattanach BM, Iddon CA, Charlton, HM, Chiappa SA, Fink G (1977). Gonadotrophin-releasing hormone deficiency in a mutant mouse with hypogonadism. *Nature* 269: 338–340

Cavanaugh D. Nidovirales: a new order compromising coronavaridae and arteriviridae. *Archives of Virology*. 142:629-633.

Chen N, Zhou M, Dong X, Qu J, Gong F, Han Y, Qiu Y, Wang J, Liu Y, Wei Y, Xia J, Yu T, Zhang X, Zhang L. (2020). Epidemiological and clinical characteristics of 99 cases of 2019 novel coronavirus pneumonia in Wuhan, China: a descriptive study. *Lancet.* 395 507–513.

Chiron D, Bekerediian-Ding I, Pellat-Deceunvnck C, Bataille R, Jego G (2008). Toll-like receptors: lessons to learn from normal and malignant human B cells. *Blood*. 112: 2205–13.

Cloeckaert, A., M. Grayon, O. Grepinet, and K. S. Boumedine. (2003). Classification of Brucella strains isolated from marine mammals by infrequent restriction site-PCR and development of specific PCR identification tests. *Microbes and Infections*.5**:**593-602.

Cuiling, L, Wei Y, Zhaoyuan H, & Yixun L. (2005). Granulosa cell proliferation differentiation and its role in follicular development. *Chinese Science Bulletin* 50: 2665.

Deb, K, Chaturvedi MM, Jaiswal YK. (2004). Comprehending the role of LPS in Gram-negative bacterial vaginosis: ogling into the causes of unfulfilled child-wish. *Archives of Gynecology and Obstetrics*. 270: 133–146.

Diaz FJ, Wigglesworth K, Eppig JJ (2007). Oocytes are required for the preantral granulosa cell to cumulus cell transition in mice. *Developmental Biology.* 305:300–311.

Dondero, F., Rossi, T., D'Offizi, G., Mazzilli, F., Rosso, R., Sarandrea, N., Aiuti, F. (1996). Semen analysis in HTV seropositive men and in subjects at high risk for HTV infection. *Human Reproduction*, *11*(4), 765–768.

Dong J, Albertini DF, Nishimori K, Kumar TR, Lu N & Matzuk MM (1996). Growth differentiation factor-9 is required during early ovarian folliculogenesis. *Nature.* 383 531-535.

Edson, M. A., Nagaraja, A., and Matzuk, M. M. (2009). The mammalian ovary from genesis to revelation. *Endocrine Reviews.* 30: 624-712.

Ekman, A.K., Adner, M., Cardell, L.O., (2011). Toll-like receptor 7 activation reduces the contractile response of airway smooth muscle. *European Journal of Pharmacology*. 652: 145–151.

Eppig JJ, Wigglesworth K, Pendola F, Hirao Y. (1997). Murine oocytes suppress expression of luteinizing hormone receptor messenger ribonucleic acid by granulosa cells. *Biology of Reproduction*. 56(4):976–98

Eppig JJ, Wigglesworth, K, Pendola FL (2002). The mammalian oocyte orchestrates the rate of ovarian follicular development. *Proceedings of National Academy of Science USA.* 99:2890–2894

Espey, L.L., Lipner, H. (1994). Ovulation. In: Knobil, E., Neill, J.D., (Eds.), *The Physiology of Reproduction*, 2nd ed. Raven Press, New York, pp. 725–780.

Fahrner, J. A., S. Eguchi, J. G. Herman, and S. B. Baylin. (2002). Dependence of histone modifications and gene expression on DNA hypermethylation in cancer. *Cancer Resolutions*. 62**:**7213-7218.

Fan HY, Liu Z, Shimada M, Sterneck E, Johnson PF, Hedrick SM, Richards JS (2009). MAPK3/1 (ERK1/2) in ovarian granulosa cells are essential for female fertility. *Science.*324:938–941.

Fanchin R, de Ziegler D, Taieb J, Hazout A, Frydman R. (1993). Premature elevation of plasma progesterone alters pregnancy rates of in vitro fertilization and embryo transfer. Fertility and Sterility. 59:1090-4.

Fanchin R, Righini C, Olivennes F, Ferreira AL, Ziegler D, FrydmanR. (1997). Consequences of premature progesterone elevation on the outcome of in vitro fertilization: insights into a controversy. Fertility and Sterility. 68:799-805,

Fitzgerald KA, Palsson-McDermott EM, Bowie AG, Jefferies C,Mansell AS, Brady G, Brint E, Dunne A, Gray P, Harte TM, McMurray D, Smith DE, Sims JE, Bird TA, O'Neill LA. (2001). Mal (MyD88-adaptor-like) is required for Toll-like receptor-4 signal transduction. *Nature.* 413:78–83.

Fitzgerald, Katherine & Rowe, Daniel & Barnes, Betsy & Caffrey, Daniel & Visintin, Alberto & Latz, Eicke & Monks, Brian & Pitha, Paula & Golenbock, Douglas. (2003). LPS-Tlr4 signaling to IRF-3/7 and NF-kappaB involves the toll adapters TRAM and TRIF. *The Journal of experimental medicine*. 198. 1043-55.

Fitzpatrick SL, Carlone DL, Robker RL, Richards JS. (1997). Expression of aromatase in the ovary: down-regulation of mRNA by the ovulatory luteinizing hormone surge. *Steroids*. 62(1):197-206.

Fortune J. and R. Cushman and C. M. Wahl and S. Kito (2000). The primordial to primary follicle transition. *Molecular and cellular endocrinology*. 163:53-60.

Garverick, H.A. (1997). Ovarian Follicular Cysts in Dairy Cows1. *Journal of Dairy Science*. 80:995–1004.

Gimenes F, Souza RP, Bento JC, Teixeira JJ, Maria-Engler SS, et al. (2014).Male infertility: a public health issue caused by sexually transmitted pathogens. Nature Reviews Urology. 11: 672–87.

Gorospe, W.C., Hughes Jr F.M., Spangelo, B.L. (1992). Interleukin-6: on and production by rat granulosa cells in vitro. *Endocrinology.* 130:1750-1752

Gottschall, P.E., Uehara A, Hoffmann ST, Arimura A (1987). Interleukin-1 inhibits follicle stimulating hormone-induced differentiation in rat granulosa cells in vitro. *Biochemical and Biophysical Research Communications.* 149: 502–509.

Griffiths, C.D., Bilawchuk, L.M., McDonough, J.E. et al. (2020). IGF1R is an entry receptor for respiratory syncytial virus. *Nature*. 583, 615–619

Guazzone VA, Jacobo P, Theas MS, Lustig L. (2009). Cytokines and chemokines in testicular inflammation: a brief review. *Microscopy Research and Technique*. 72: 620–8

Hamon MA, Cossart P (2008). Histone modifications and chromatin remodeling during bacterial infections. *Cell Host Microbe*. 4(2):100–109.

Haziak, K., Herman AP, Zaremba DT. (2014). Effects of central injection of anti-LPS antibody and blockade of TLR4 on GnRH/LH secretion during immunological stress in anestrous ewes. *Mediators of Inflammation*. 2014:867170.

Hernandez-Gonzalez I, Gonzalez-Robayna I, Shimada M, Wayne CM, Ochsner SA, White L, Richards JS (2006). Gene expression profiles of cumulus cell oocyte complexes during ovulation reveal cumulus cells express neuronal and immune-related genes: does this expand their role in the ovulation process? *Mol Endocrinology.* 20:1300–1321

Hernandez-Gonzalez, I. Gonzalez-Robayna, I., Shimada M, Wayne CM, Ochsner SA, White L, Richards JS. (2006). Gene expression profiles of cumulus cell oocyte complexes (COCs) during ovulation reveal cumulus cells express neuronal and immune-related genes: does this expand their role in the ovulation process? *Molecular Endocrinology.* 20: 1300-1321.

Hickey GJ, Chen SA, Besman MJ, Shively JE, Hall PF, GaddyKurten D & Richards JS. (1988). Hormonal regulation, tissue distribution, and content of aromatase cytochrome p450 messenger ribonucleic acid and enzyme in rat ovarian follicles and corpora lutea: relationship to estradiol biosynthesis. Endocrinology. 122 1426–1436.

Hoque, S.A.M, Kawai, T, Zhu Z, Shimada M. (2019). Mitochondrial Protein Turnover Is Critical for Granulosa Cell Proliferation and Differentiation in Antral Follicles, *Journal of the Endocrine Society*. 3:324–339.

Horng T, Barton GM, Medzhitov R. (2001). TIRAP: an adapter molecule in the Toll signaling pathway. *Nature Immunology*. 2:835–41.

Hoshino, K. etl. (1999). Cutting edge: Toll-like receptor 4 (TLR4)-deficient mice are hyporesponsive to lipopolysaccharide: evidence for TLR4 as the *Lps* gene product. *Journal of Immunology.* 162, 3749–3752

Hsueh AJ, Billig H, Tsafriri A (1994). Ovarian follicle atresia: a hormonally controlled apoptotic process. *Endocrine Reviews* 15, 707–724.

Hunzicker-Dunn, M.E., Lopez-Biladeau B, Law NC, Fiedler SE, Carr DW, Maizels ET. (2012). PKA and GAB2 play central roles in the FSH signaling pathway to PI3K and AKT in ovarian

granulosa cells. *Proceedings from the National Academy of Science USA*. 109: E2979–E2988.

Iguchi-Ariga, S. M. M., and W. Schaffner. (1989). CpG methylation of the cAMP-responsive enhancer/promoter sequence TGACGTCA abolishes specific factor binding as well as transcriptional activation. *Genes and Development*. 3:612-619.

Ihle J.N. (1996). Stats: signal transducers and activators of transcription. *Cell.* 84:331-334.

Isobe N. and Nakao T. (2003). Direct enzyme immunoassay of progesterone in bovine plasma. *Animal Science Journal.* 74, 369–373.

Isobe, N. 2007. Follicular cysts in dairy cows. *Animal Science Journal.* 78: 1–6

Jiang, S., Hillyer, C., & Du, L. (2020). Neutralizing antibodies against SARS-CoV-2 and other human coronaviruses. *Trends in Immunology*, 41(5), 355– 359.

Jo M., Curry Jr T.E. (2006). Luteinizing hormone-induced RUNX1 regulates the expression of genes in granulosa cells of rat preovulatory follicles. *Molecular Endocrinology.* 20:2156-72.

Julie A. Potter, Mancy Tong, Paulomi Aldo, Ja Young Kwon, Mary Pitruzzello, Gil Mor, Vikki Abrahams M. (2020). Viral infection dampens human fetal membrane type I interferon responses triggered by bacterial LPS, *Journal of Reproductive Immunology.* 140:103126,

Jurk, M. Heil, F. Vollmer, J. Schetter, C. Krieg, AM. Wagner, H. Lipford, G. Bauer S. (2002). Human TLR7 or TLR8 independently confer responsiveness to the antiviral compound R-848. *Nature Immunology.* 3:499

Kan, B., Wang, M., Jing, H., Xu, H., Jiang, X., Yan, M., Liang, W., Zheng, H., Wan, K., Liu, Q., et al. (2005). Molecular evolution analysis and geographic investigation of severe acute respiratory syndrome coronavirus-like virus in palm civets at an animal market and on farms. *Journal of Virology*.79: 11892–11900

Kawai, T. (2012). Endogenous acetaldehyde toxicity during antral follicular development in the mouse ovary. *Reproductive Toxicology*. 33(3):322–330.

Kawai, T., Adachi, O., Ogawa, T., Akira, S. (1999). Unresponsiveness of MyD88-deficient mice to endotoxin. *Immunity.* 11:115–122.

Kawai, T., Yanaka, N., Richards JS., Shimada, M. (2016). De novo-synthesized retinoic acid in ovarian antral follicles enhances FSH-mediated ovarian follicular cell differentiation and female fertility. *Endocrinology.* 157(5):2160–2172.

Kawai, T., Richards JS., Shimada, M. (2018). The Cell Type–Specific Expression of *LHCGR* in Mouse Ovarian Cells: Evidence for a DNA-Demethylation–Dependent Mechanism. *Endocrinology.* 159(5): 2062–2074.

Kliebenstein J, Neumann E, Holtkamp DJ. et al. (2013). Assessment of the economic impact of porcine reproductive and respiratory syndrome virus on United States pork producers. *Journal of Swine Health and Production*. 21(2):72-84.

Knight PG & Glister C 2001 Potential local regulatory functions of inhibins, activins and follistatin in the ovary. *Reproduction*. 121:503-512.

Kreisel, K., Torrone E., Bernstein K., Hong J., Gorwitz R. (2017). Prevalence of Pelvic Inflammatory Disease in Sexually Experienced Women of Reproductive Age-United States, 2013–2014. *Morbidity and Mortality Weekly Report.* 66:80–83.

Law, N.C., Kyriss B., Nilson, JH., Hunzicker-Dunn, M. (2013). *LHCGR* expression in granulosa cells: roles for PKA-phosphorylated β-catenin, TCF3, and FOXO1. *Molecular Endocrinology*. 27(8):1295–1310.

Lei ZM, Mishra S, Zou W, Xu B, Foltz M, Li X, Rao CV. (2001). Targeted disruption of luteinizing hormone/human chorionic gonadotropin receptor gene. *Molecular Endocrinology.* 15:184–200.

Li, L, He S., Sun J. (2004). Gene regulation by Sp1 and Sp3. *Biochemistry and Cell Biology*, 82, 460-471.

Li, W., Greenough, T.C., Moore, M.J., Vasilieva, N., Somasundaran, M., Sullivan, J.L., Farzan, M., and Choe, H. (2004). Efficient replication of severe acute respiratory syndrome coronavirus in mouse cells is limited by murine angiotensin-converting enzyme 2. *Journal of. Virology*. 78: 11429–11433.

Li, W., Zhang, C., Sui, J., Kuhn, J.H., Moore, M.J., Luo, S., Wong, S.K., Huang, I.C., Xu, K., Vasilieva, N., et al. (2005c). Receptor and viral determinants of SARS-coronavirus adaptation to human ACE2. *The EMBO Journal*. 24, 1634–1643.

Ljubojevic, S., & Skerlev, M. (2014). HPV-associated diseases. *Clinics in Dermatology*, *32*(2), 227–234.

Lock, L. F., N. Takagi, and G. R. Martin. (1987). Methylation of the Hprt gene on the inactive X occurs after chromosome inactivation. Cell 48:39-46.

Lohrer, P., *et al.,* 2000. Lipopolysaccharide directly stimulates the intrapituitary interleukin-6 production by folliculostellate cells via specific receptors and the p38α mitogen-activated protein kinase/nuclear factor-κB pathway. *Endocrinology*, 141: 4457–4465.

Ma, M., Wang, J., Xu, L., Zhang, Q., Du, B., Jiang, X., Shi, Q., Zhou, L., Li, B., Saito, H. & Kurachi, H. (2015). Effects of two human chorionic gonadotropin doses administered to the ovarian states during the in vitro fertilization and embryo transfer program. *Biomedical Reports*. 3, 215–219.

Marshak-Rothstein A. (2006). Toll-like receptors in systemic autoimmune disease. *Nature Reviews Immunology. 6: 823–35.*

Matsuyama S, Nagata N, Shirato K, Kawase M, Takeda M & Taguchi F 2010 Efficient activation of the severe acute respiratory syndrome coronavirus spike protein by the transmembrane protease TMPRSS2. *Journal of Virology* 84 12658–12664.

Matt, S.M, Zimmerman JD., Lawson MA, Bustamante AC., Uddin M., Johnson RW. (2018). Inhibition of DNA Methylation with Zebularine Alters Lipopolysaccharide-Induced Sickness Behavior and Neuroinflammation in Mice. *Frontiers in Neuroscience*. 12:636.

Matzuk, M.M., Lamb, D.J., (2002). Genetic dissection of mammalian fertility pathways. *Nature Cell Biology*. 4:41–9

McGee EA., Hsueh AJ (2000). Initial and cyclic recruitment of ovarian follicles. *Endocrinology Reviews.* 21:200 – 214

Medzhitov R. (2008). Origin and physiological roles of inflammation. *Nature. 454:428–35.*

Medzhitov, R. Kagan, J.C. (2006). Phosphoinositide-mediated adaptor recruitment controls toll-like receptor signaling. *Cell.* 125: 943-955

Miller, R. L., Gerster, J. F., Owens, M. L., Slade, H. B. & Tomai, M. A. (1999). Imiquimod applied topically: a novel immune response modifier and new class of drug. *Int. J. Immunopharmacology.* 21, 1–14.

Minegishi T, Nakamura K, Takakura Y, Miyamoto K, Hasegawa Y, Ibuki Y, Igarashi M. (1990). Cloning and sequencing of human LH/hCG receptor cDNA. *Biochemical Biophysical Research Communications.* 172:1049–1054.

Monavari, S. H., Vaziri, M. S., Khalili, M., Shamsi-Shahrabadi, M., Keyvani, H., Mollaei, H., & Fazlalipour, M. (2013). Asymptomatic seminal infection of herpes simplex virus: Impact on male infertility. *Journal of Biomedical Research*, *27*(1), 56–61.

Mutskov, V., and G. Felsenfeld. 2004. Silencing of transgene transcription precedes methylation of promoter DNA and histone H3 lysine 9. *The EMBO Journal*. 23**:**138-149.

Okano, M., Bell, DW, Haber, DA., Li, E. (1999). DNA methyltransferases Dnmt3a and Dnmt3b are essential for de novo methylation and mammalian development. *Cell.* 99:247–257.

Park JY, Su YQ, Ariga M, Law E, Jin SL, Conti M. (2004). EGF-like growth factors as mediators of LH action in the ovulatory follicle. *Science.* 303:682–684

Park JY, Su YQ, Ariga M, Law E, Jin SL, Conti M. (2004). EGF-like growth factors as mediators of LH action in the ovulatory follicle. *Science*. 303:682–684.

Park, J.Y., Su, Y.Q., Ariga, M., Law, E., Jin, S.L. C., Conti, M. (2004). **EGF-like growth factors as mediators of LH action in the ovulatory follicle.** *Science.* 303: 682-684.

Peter, A. T., Bosu, W. T. and DeDecker, R. J. 1989. Suppression of preovulatory luteinizing hormone surges in heifers after intrauterine infusions of Escherichia coli endotoxin. *American Journal of Veterinary Resolution*. 50: 368–373

Pileri, E., Mateu, E. (2016). Review on the transmission porcine reproductive and respiratory syndrome virus between pigs and farms and impact on vaccination. *Veterinary Resolutions.* 47, 108.

Pockros, P.J. Guyader D, Patton, H, Tong MJ., et al. (2007) Oral resiquimod in chronic HCV infection: safety and efficacy in 2 placebo-controlled, double-blind phase IIa studies. J. Hepatol. 47, 174–182

Pollanen R, Sillat T, Pajarinen J, Levon J., Silat T. (2009*).* Microbial antigens mediate HLA-B27 diseases via TLRs. *Journal of Autoimmunity.; 32:172–7.*

Portela VM, Goncalves PBD, Veiga AM, Nicola E, Buratini J Jr & Price CA (2008). Regulation of angiotensin type 2 receptor in bovine granulosa cells. *Endocrinology*. 149:5004–5011.

Potter, J.A., et al. (2015). Viral single stranded RNA induces a trophoblast pro-inflammatory and prognosis in preterm labor. *American Journal of Reproductive Immunology*. 75: 112–125.

Purcell, M.K., Smith, K.D., Hood, L., Winton, J.R., Roach, J.C., 2006. Conservation of Toll-Like receptor signaling pathways in teleost fish. *Comparative Biochemistry and Physiology. Part D Genomics Proteomics.* 1: 77–88.

R.J. Norman, M. Brannstrom (1994). White cells and the ovary-incidental invaders or essential effectors? *Journal of Endocrinology.* 140:333-336.

Rakoff-Nahoum S, Medzhitov R. (2009). Toll-like receptors and cancer. *Nature Reviews Cancer. 9: 57–63.*

Reik W. (2007). Stability and flexibility of epigenetic gene regulation in mammalian development. *Nature*.447:425–432.

Richards JS (2007). Genetics of ovulation. *Seminars in Reproductive Medicine.* 25:235–242

Richards JS, Liu Z, Shimada M (2008). Immune-like mechanisms in ovulation. *Trends Endocrinol Metab.* 19:191–196.

Richards JS. (1994). Hormonal control of gene expression in the ovary. *Endocrine Reviews*. 15:725-751.

Richards, J.S. (2007). Genetics of ovulation. *Seminars in Reproductive Medicine.* 25: 235-242

Rietschel, E.T., Schade, FU., Kirikae, T., Mamat U. (1994). Bacterial endotoxin: molecular relationships of structure to activity and function. *FASEB Journal.* 8.:217–225.

Rifkin IR, Leadbetter EA, Busconi L, et al. (2005). Toll-like receptors, endogenous ligands, and systemic autoimmune disease. *Immunology Reviews.; 204: 27–42.*

Robker, R.L., Richards, J.S., (1998a). Hormone-induced proliferation and differentiation of granulosa cells: a coordinated balance of the cell cycle regulators cyclin D2 and $p27^{KIP1}$, *Molecular Endocrinology*. 12: 924–940.

Robker, R.L., Richards, J.S., (1998b). Hormonal control of the cell cycle in ovarian cells: proliferation versus differentiation, *Biology of Reproduction*. 5: 476–482.

Ron-El R, Raziel A, Schachter M, Strassburger D, Kasterstein E, Friedler S. (2000). Induction of ovulation after gnRH antagonists. *Human Reproduction Update.* 6:318-21.

Ross, J.D., 2002. An updated on pelvic inflammatory disease. *Sexually Transmitted Infections*. 78:18–19.

Saatcioglu, H. D., Cuevas, I., & Castrillon, D. H. (2016). Control of oocyte reawakening by kit. *PLoS Genetics*, 12, e1006215.

Salam AP, Horby PW. (2017). The breadth of viruses in human semen. *Emerging Infectious Disease.* 23:1922–4

Scholes D, Satterwhite CL, Yu O, Fine D, Weinstock H, Berman S. (2012). Long-term trends in *Chlamydia trachomatis* infections and related outcomes in a U.S. managed care population. *Sexually Transmitted Diseases*. 39:81-8.

Selig, J.I., (2013). Impact of DNA methylation on the regulation of the luteinizing hormone/choriogonadotropin receptor expression. Exp Clin Endocrinol Diabetes.121(3)

Seong SY, Matzinger P. (2004) Hydrophobicity: an ancient damage-associated molecular pattern that initiates innate immune responses. *Nature Reviews Immunology.* 4:469–78.

Sheldon, I.M., Dobson, H., (2004). Postpartum uterine health in cattle. *Animal Reproduction Science*. 82–83 295–306.

Shimada, M. (2007). Induced expression of pattern recognition receptors (PRRs) in cumulus oocyte complexes (COCs): novel evidence for innate immune-like cells functions during ovulation. 20:3228-39

Shimada, M., Hernandez-Gonzalez I., Gonzalez-Robanya I., Richards JS. (2007). Induced expression of pattern recognition receptors in cumulus oocyte complexes: novel evidence for innate immune-like functions during ovulation. *Molecular Endocrinology.* 20: 3228–3239.

Shimada, M., Yanai Y., Okazaki, T., Noma N., Kawashima, I., Mori T., Richards JS. (2008). Hyaluronan fragments generated by sperm-secreted hyaluronidase stimulate cytokine/chemokine production via the TLR2 and TLR4 pathway in cumulus cells of ovulated COCs, which may enhance fertilization. *Development*. 135: 2001-11

Shimazu, R. Akashi-Takamura S., Ogata H., Nagai Y. (1999). MD-2, a molecule that confers lipopolysaccharide responsiveness on Toll-like receptor 4. *Journal of. Experimental Medicine.* 189, 1777–1782.

Shimizu, A., Kato, M., Ishikawa, O., (2014). Bowenoid papulosis successfully treated with imiquimod 5% cream. *Journal of Dermatology*. 41:545–546.

Stephen F., Helen M., Debbie W., (2000). Follicular dynamics in the polycystic ovary syndrome. *Molecular and Cellular Endocrinology*. 163: 49-52,

Su YQ, Wigglesworth K, Pendola FL, O'Brien MJ, Eppig JJ (2002). Mitogen-activated protein kinase activity in cumulus cells is essential for gonadotropin-induced oocyte meiotic resumption and cumulus expansion in the mouse. *Endocrinology* 143:2221–2232.

Suffredini, A.F., Fromm, RE., Margaret, M., Parker MD., et al. (1989). The cardiovascular response of normal humans to the administration of endotoxin. *The New England Journal of Medicine*. 321:280–7.

Suzuki, C., Yoshioka, K., Iwamura, S., Hirose, H. (2001) Endotoxin induces delayed ovulation following endocrine aberration during the proe-strous phase in Holstein heifers. *Domestic Animal Endocrinology.* 20,267–278.

Svingerud, T., Solstad, T., Sun, B., Nyrud, M.L., Kileng, O., Greiner-Tollersrud, L., *et al.* (2012). Atlantic salmon type I IFN subtypes show differences in antiviral activity and cell-dependent expression: evidence for high IFNb/IFNc-producing cells in fish lymphoid tissues. Journal of Immunology. 189: 5912–5923.

Tamura, K., Kawaguchi T., Hara T., Takatoshi S., et al. (2000). Interleukin-6 decreases estrogen production and messenger ribonucleic acid expression encoding aromatase during in vitro cytodifferentiation of rat granulosa cell. *Molecular Cell Endocrinology*. 170:103–111.

Tamura, K., Kawaguchi T., Kogo H. (2001). Interleukin-6 inhibits the expression of luteinizing hormone receptor mRNA during the maturation of cultured rat granulosa cells. *Journal of Endocrinology.* 170:121–127

Temperley, N.D., Berlin, S., Paton, I.R., Griffin, D.K., Burt, D.W. (2008). Evolution of the chicken Toll-like receptor gene family: a story of gene gain and gene loss. *BMC Genomics*. 9: 62.

Tingen, C., Kim, A. and Woodruff, T.K. (2009). The primordial pool of follicles and nest breakdown in mammalian ovaries. *Molecular Human Reproduction.* 15: 795-803.

Tsan MF, Gao B. (2004). Endogenous ligands of toll-like receptors. *Journal of Leukocyte Biology. 76:514–9.*

Tuomanen, E., Liu H, Hengstler B, Zak O, Tomasz A. (1985). The induction of meningeal inflammation by components of the pneumococcal cell wall. *Journal of Infectious Diseases*. 151:859–868.

Tuomanen, E.I., Tomasz A, Hengstler B, Zak O. (1985). The relative role of bacterial cell wall and capsule in the induction of inflammation in pneumococcal meningitis *Journal of Infectious Diseases.* 151:535–540.

Uehara O, Abiko Y, Saitoh M, Miyakawa H, Nakazawa F. (2014). Lipopolysaccharide extracted from Porphyromonas gingivalis induces DNA hypermethylation of runt-related transcription

factor 2 in human periodontal fibroblasts. *Journal of Microbiology, Immunology, and Infection*. 47: 176-181.

Umehara, T., Kawai T., Kawashima I., Tanaka K., et al. (2017). The acceleration of reproductive aging in Nrg1flox/flox;Cyp19-Cre female mice. *Aging Cell*. 16:1288–1299

Umehara, T., Kawashima I., Kawai T., Hoshino Y., et al. (2016). Neuregulin 1 Regulates Proliferation of Leydig Cells to Support Spermatogenesis and Sexual Behavior in Adult Mice. *Endocrinology.* 157:4899–4913.

Van Gorp H, Van Breedam W, Delputte PL, Nauwynck HJ. (2008). Sialoadhesin and CD163 join forces during entry of the porcine reproductive and respiratory syndrome virus. *Journal of General Virology.* 89(Pt 12):2943-2953.

Verweij SP, Karimi O, Pleijster J, Lyons JM, de Vries HJC, Land JA, et al. (2016). TLR2, TLR4 and TLR9 genotypes and haplotypes in the susceptibility to and clinical course of Chlamydia trachomatis infections in Dutch women. *Pathogens and Disease*. 74:ftv107.

Wagner, T.L., Ahonen, C.L., Couture, A.M., Gibson, S.J., Miller, R.L., Smith, R.M., *et al.* (1999). Modulation of TH1 and TH2 cytokine production with the immune response modifiers, R-848 and imiquimod. *Cellular Immunology*. 191: 10–19.

Webb R, Campbell BK, Garverick HA, Gong JG, Gutierrez CG & Armstrong DG (1999). Molecular mechanisms regulating follicular recruitment and selection. *Journal of Reproduction and Fertility Supplement*. 54:33-48

Webb R, Nicholas B, Gong JG, Campbell BK, Gutierrez CG, Gaverick HA & Armstrong DG (2003). Mechanism regulating follicular development and selection of the dominant follicle. *Reproduction Supplement.* 61:71-90.

Welter H, Huber A, Lauf S, Einwang D, Mayer C, Schwarzer JU, Kohn FM & Mayerhofer A (2014). Angiotensin II regulates testicular peritubular cell function via AT1 receptor: a specific situation in male infertility. *Molecular and Cellular Endocrinology* 393 171–178.

Weström L, Eschenbach D. Pelvic inflammatory disease. In: Holmes K K, Sparling P E, Mårdh P, et al, (1999). Sexually Transmitted Diseases. 3rd edn. New York: McGraw Hill, 783–809.

Williams, E.J., Fischer, D.P. Noakes, D.E. England, G.C.W. Rycroft, A. Dobson, H. Sheldon, I.M. (2007). The relationship between uterine pathogen growth density and ovarian function in the postpartum dairy cow. *Theriogenology.* 68: 549–559.

Xiao F, Tang M, Zheng X, Liu Y, Li X & Shan H (2020). Evidence for gastrointestinal infection of SARS-CoV-2. *Gastroenterology.* 158:1831–1833.

Xu, J., Qi, L., Chi, X., Yang, J., Wei, X., Gong, E., Gu, J et al.. (2006). Orchitis:A complication of Severe Acute Respiratory Syndrome (SARS)1. *Biology of Reproduction*, *74:* 410–416.

Yamashita Y, Kawashima I, Yanai Y, Nishibori M, Richards JS, Shimada M. (2007). Hormone-induced expression of tumor necrosis factor-converting enzyme/A disintegrin and metalloprotease-17 impacts porcine cumulus cell oocyte complex expansion and meiotic maturation via ligand activation of the epidermal growth factor receptor. *Endocrinology*.148:6164–6175.

Yoneda N, Yoneda S, Niimi H, Ueno T, Hayashi S, Ito M, Shiozaki A, Urushiyama D, Hata K, Suda W, Hattori M, Kigawa M, Kitajima I, Saito S. (2016). Polymicrobial Amniotic Fluid Infection with Mycoplasma/Ureaplasma and Other Bacteria Induces Severe Intra-Amniotic Inflammation Associated with Poor Perinatal Prognosis in Preterm Labor. *American Journal of Reproductive Immunology*. 75:112-25.

Zhang L, Liu J, Bai J, Wang X, Li Y, Jiang P. (2013). Comparative expression of Toll-like receptors and inflammatory cytokines in pigs infected with different virulent porcine reproductive and respiratory syndrome virus isolates. *Virology Journal.*10:135.

Zheng YY, Ma YT, Zhang JY & Xie X (2020). COVID-19 and the cardiovascular system. *Nature Reviews: Cardiology* 17 259–260.

Zhou QH, Deng CZ, Li ZS, et al. (2018). Molecular characterization and integrative genomic analysis of a panel of newly established penile cancer cell lines. Cell Death and Disease. 9:684.

Zou, X., Chen, K., Zou, J., Han, P., Hao, J., & Han, Z. (2020). Single-cell RNA-seq data analysis on the receptor ACE2 expression reveals the potential risk of different human organs vulnerable to 2019-nCoV infection. *Frontiers of Medicine*, 14: 185– 192